TECHNISCHE
UNIVERSITÄT
WIEN

DISSERTATION

Analytic and Numerical Study of a Cross-Diffusion Model for Ion Transport

ausgeführt zum Zwecke der Erlangung des akademischen Grades
einer Doktorin der technischen Wissenschaften unter der Leitung von

Ansgar Jüngel

E101 – Institut für Analysis und Scientific Computing, TU Wien

eingereicht an der Technischen Universität Wien
Fakultät für Mathematik und Geoinformation

von

Anita Gerstenmayer

Matrikelnummer: 00926858

Hasenstraße 23

3430 Tulln

Diese Dissertation haben begutachtet:

1. **Prof. Dr. Claire Chainais-Hillairet**
   Univ. Lille, CNRS, UMR8524, Inria - Laboratoire Paul Peinlevé, F-59000 Lille, Frankreich

2. **Dr.rer.nat.habil. Annegret Glitzky**
   Weierstraß-Institut für Angewandte Analysis und Stochastik, Berlin, Deutschland

3. **Prof. Dr. Ansgar Jüngel**
   Institut für Analysis und Scientific Computing, Technische Universität Wien, Österreich

Wien, am ...

Kurzfassung

Der Transport von Ionen durch biologische Kanäle kann auf makroskopischer Ebene durch partielle Differentialgleichungen für die Evolution der Ionenkonzentrationen beschrieben werden. Bezieht man bei der Modellierung Füllungseffekte mit ein, die durch den beschränkten Raum in den engen Ionenkanälen hervorgerufen werden, so führt dies zu Kreuzdiffusionstermen in den Gleichungen. Das resultierende Modell für die Ionenkonzentrationen besteht aus einem stark gekoppelten System nichtlinearer parabolischer Diffusionsgleichungen, die zusätzlich einen Driftterm beinhalten. Dieser Term verhält sich proportional zum Gradienten des elektrischen Potentials, welches über eine Poisson-Gleichung mit den Ionenkonzentrationen gekoppelt ist. Das Ziel dieser Arbeit ist die mathematische Analyse des vorliegenden Modells, sowie die Entwicklung zuverlässiger numerischer Verfahren für die approximative Lösung der Gleichungen.

Die starke Kopplung der Gleichungen durch die Kreuzdiffusionsterme stellt eine große Herausforderung für die Existenzanalysis dar, da sie den Einsatz klassischer Methoden wie Maximumsprinzipien verhindert. Außerdem sorgt eine Degeneriertheit der Diffusionsmatrix für schwächere a priori Abschätzungen. Diese Schwierigkeiten können durch Ausnützung der Entropiestruktur des Systems und Transformation der Gleichungen in Entropievariablen überwunden werden. Im ersten Teil dieser Dissertation wird die Existenz von schwachen Lösungen für alle Zeit bewiesen, sowie die Eindeutigkeit der schwachen Lösung unter zusätzlichen Annahmen an die Parameter und die Regularität der Lösung. Der Existenzbeweis basiert auf einer Entropiemethode, die für diese Arbeit erweitert wird um die inhomogenen gemischten Randbedingungen und den Driftterm behandeln zu können. Die Degeneriertheit wird dabei durch die Anwendung eines speziellen Aubin–Lions Kompaktheitslemma überwunden. Der Beweis der Eindeutigkeit schwacher Lösungen beruht auf der Methode von Gajewski.

Für ein numerisches Approximationsverfahren ist es von zentraler Bedeutung, strukturelle Eigenschaften wie die Nichtnegativität der Lösung oder die Entropiestruktur der Gleichungen auf der diskreten Ebene zu erhalten. In der vorliegenden Arbeit werden zwei neue Verfahren für das Kreuzdiffusionsmodell präsentiert und analysiert, welche die Struktur des Systems auf verschiedene Weise approximieren.

Das erste Verfahren kombiniert eine implizite Eulerdiskretisierung der Zeitableitung mit einem Finite-Volumen-Schema für die Diskretisierung der Ortsvariablen. Das Schema nützt die Drift-Diffusionsstruktur der Gleichungen, welche mit doppeltem Upwind-Verfahren diskretisiert werden. Zunächst wird die Existenz diskreter Lösungen gezeigt. Um jedoch eine diskrete Entropieungleichung, Eindeutigkeit und Konvergenz der numerischen Approximation zu beweisen, müssen vereinfachende Annahmen getroffen werden, unter anderem die Vernachlässigung des elektrischen Potentials. Als Hilfsmittel für den Konvergenzbeweis wird eine neue diskrete Variante des Aubin–Lions Lemma für den vorliegenden degenerierten Fall gezeigt.

Das zweite Verfahren basiert wiederum auf einem impliziten Eulerschema in der Zeit, jedoch kombiniert mit einer Finite-Elemente-Methode für die Ortsdiskretisierung. Hierbei werden die Gleichungen nicht in der ursprünglichen Form, sondern die in Entropievariablen formulierte Variante als Ausgangspunkt verwendet. Dadurch kann die Analyse des Verfahrens im Wesentlichen analog zu jener der kontinuierlichen Gleichungen durchgeführt werden. Um die Existenz diskreter Lösungen zu garantieren, muss allerdings ein Regularisierungsterm hinzugefügt werden. Die Erhaltung der Entropiestruktur und die Konvergenz des Verfahrens wird bewiesen, in diesem Fall ohne zusätzliche Einschränkungen für die Modellparameter.

Beide numerische Verfahren werden anhand von anwendungsorientierten Testsimulationen getestet und verglichen. Das erste numerische Experiment simuliert einen Calciumkanal, das zweite einen bipolaren Ionenkanal, jeweils in zwei Ortsdimensionen. Das Langzeitverhalten der Lösungen, insbesondere der Abfall der Entropie, sowie experimentelle Konvergenzraten werden untersucht.

Abstract

The transport of ions through biological channels, on a macroscopic level, can be described with a system of partial differential equations (PDEs) for the evolution of the ion concentrations. If one considers additional size exclusion effects, occurring in narrow pores, cross-diffusion terms appear in the system. The ion concentrations then solve strongly coupled diffusion equations with a drift term involving the electric potential which is coupled to the concentrations through a Poisson equation. The aim of this thesis is to close gaps in the analysis of this cross-diffusion model and provide reliable numerical approximations that capture the behavior of its solutions.

The main challenge for the analysis of the model lies in the cross-diffusion terms, which prevent the use of standard PDE tools such as maximum principles. Additionally, the system possesses a formal gradient-flow structure revealing nonstandard degeneracies that lead to further considerable difficulties. The first part of the thesis consists of showing that bounded weak solutions to the system exist globally in time, and, under certain conditions on the coefficients of the system, are unique. The proofs are based on the boundedness-by-entropy method, extended to nonhomogeneous boundary conditions and the coupled potential, and the uniqueness technique of Gajewski. The degeneracy is overcome by the use of a special Aubin–Lions compactness lemma.

For the design of a numerical scheme it is crucial to preserve important properties such as the nonnegativity of the solutions or the entropy structure of the equations on a discrete level. In the second part of the thesis, two new numerical schemes for the cross-diffusion model are presented and analyzed. Each scheme preserves and uses the structure of the system differently.

The first scheme is a combination of an implicit Euler approximation for the time derivative and a finite-volume method in the spatial variables. The latter is based on the drift-diffusion structure of the equations, using two-point flux approximations with "double" upwind mobilities. The existence of solutions to the fully discrete scheme is proved. When the particles are not distinguishable and the dynamics is driven by cross diffusion only, it is shown that the scheme preserves the structure of the equations like nonnegativity, upper bounds, and entropy dissipation. The degeneracy is overcome by proving a new fully discrete version of an Aubin–Lions lemma of "degenerate" type.

The second scheme is again based on an implicit Euler method in time, together with a finite-element method for the space discretization. This scheme does not build up on the original equations, but rather on the system transformed to entropy variables. Therefore, the analysis of the scheme can be carried out in a similar way as in the continuous case. In order to guarantee the existence of discrete solutions, a regularization has to be added. A discrete version of the entropy inequality and the convergence of the scheme is proven, without any additional assumptions on the model parameters.

In the last part of the thesis we show how our newly developed schemes can be used in

two test cases which are inspired from biological applications. The first example we explore is the simulation of calcium selective channels, and the second example is that of a bipolar ion channel. These examples are considered in two spatial dimensions. We investigate the large time behavior of the solutions - in particular the decay of the entropy and the experimental convergence rates.

Danksagung

Eidesstattliche Erklärung

Ich erkläre an Eides statt, dass ich die vorliegende Dissertation selbstständig und ohne fremde Hilfe verfasst, andere als die angegebenen Quellen und Hilfsmittel nicht benutzt bzw. die wörtlich oder sinngemäß entnommenen Stellen als solche kenntlich gemacht habe.

Wien, am ...   _____

Contents

Contents

1 Introduction

The aim of this thesis is to provide a rigorous theoretical analysis and reliable numerical schemes for a degenerate parabolic cross-diffusion system that models the flow of ions and the electric potential in an open ion channel. In this introductory chapter we will establish the background on the modeling of ion channels, consider in detail the mathematical model which is the focus of our work and review known mathematical techniques to deal with cross-diffusion systems. We will conclude the chapter with the description of our own contributions, and the structure of the thesis.

1.1 Mathematical Models for Ion Transport through Channels

In simple terms, an ion channel is just a protein with a hole down its middle. As such, it forms a continuous pathway for ions across the otherwise impermeable wall of a cell. Ion channels are present in all living cells and regulate many essential biological functions, such as electric signaling in the nervous system or muscle contractions.

Naturally, there is more to ion channels than simply forming a hole. In fact, all ion channels have some basic characteristics in common [44]:

- They are excitable molecules that respond to certain stimuli (e.g. electric signals or neurotransmitters) by gating, which means the opening and closing of the pore.

- They only allow certain types of ions to pass through. This selective permeability is achieved by a selectivity filter.

- Ions are conducted passively down their electrochemical gradient, no metabolic energy is consumed.

- The rate of passage of ions is very high, often more than 10^6 ions per second pass through the open channel.

Ever since the pioneering works of Hodgkin and Huxley in the 1950s [45], mathematical and computational models for ion flow through channels have been a subject of intensive research in the mathematical community. Modeling approaches range from detailed descriptions of the channel proteins and atoms on a microscopic level to macroscopic continuum models that are formulated in terms of averaged densities instead of individual ions. An overview on some of the most commonly used models can be found for example in the review paper [54].

In the literature, there is some controversy on which type of model is most suitable for capturing the characteristic properties of ion channels mentioned above. All-atom molecular dynamics, which entail an explicit description of the involved atoms, are considered to

be the most accurate, but also the most computationally expensive approach, making them unfeasible in some cases. Employing continuum descriptions for the ion concentrations, on the other hand, leads to partial differential equation models which are less detailed but still often capture the essential features of the problem. These models do not only facilitate a deeper understanding of ion transport mechanisms, but also pose interesting mathematical problems, and therefore are the focus of this work.

The probably most popular macroscopic model for describing ion transport is the Poisson–Nernst–Planck (PNP) equations. The roots of this model date back to the 19th century and the formulation of the basic equations of electro-diffusion by Nernst and Planck [58]. In the context of ion channels, the equations can be derived as a mean-field limit from microscopic particle models [56], leading to diffusion equations for the concentrations u_i of n different species of ions:

$$\partial_t u_i = \operatorname{div} \mathcal{F}_i, \quad \mathcal{F}_i = D_i\big(\nabla u_i + c_i \mu_i e z_i \nabla \Phi\big), \quad i = 1, \dots, n, \tag{1.1}$$

where D_i are the diffusion constants, μ_i mobility constants, e the elementary charge, z_i the valence and Φ the electric potential. The fluxes satisfy Fick's law of diffusion, which states that the diffusive flux is proportional to the concentration gradient. The continuity equations for the concentrations are supplied with a self-consistent Poisson equation for the electric potential. The resulting system has been successfully applied to many problems, not only for biological models for ion channels [30] but also in the context of semiconductors, where it is often referred to as drift-diffusion system [74].

Although widely used, some shortcomings of the classical PNP model put its adequacy for the description of ion channels into question. One of the main issues is dealing with size exclusion effects that naturally occur in ion channels, as the space inside the selectivity filters is small even compared to the ion diameters. In [23] it is demonstrated via comparison with Brownian dynamics simulations that the mean-field approximation in the PNP theory breaks down in narrow channels with radii smaller than the Debye length. Therefore, while the PNP model provides quite accurate results for large channels or low ion concentrations, a different model is needed to capture phenomena occurring in crowded channels, such as current saturation.

Numerous efforts were made in order to overcome the deficiencies of the PNP model with respect to size exclusion effects. We will mention here a few of them. One possible extension of the classical equations was achieved by using density functional theory. In this approach, hard-sphere interactions between ions are artificially included via excess chemical potentials [41]. A different starting point with similar end result was presented in [29]. In this work, the authors use an energetic variational approach, where a repulsive potential energy is added to the total energy functional. The resulting equations include convolution integrals which are often simplified by localization of the nonlocal size effects to reduce computational effort [46]. A different strategy consists in the modification of mobilities of the ions due to size exclusion. This was done independently in [71] and [16] leading to a modification of the PNP system that includes cross-diffusion terms, which we describe in detail in the next section. Compared to the other approaches, it has the advantages of being computationally tractable and without any nonlocal effects. Although not formulated in the context of ion channels, we also want to mention the approach of [27].

Here, an electrolyte model with thermodynamically consistent coupling between mechanics and diffusion is proposed, leading to cross-diffusion equations for the ion concentrations coupled to momentum balance equations.

1.2 The Model Equations

In the modified Poisson–Nernst–Planck model proposed by Burger et al. [16], the evolution of the concentrations $u_i = u_i(x,t)$ of $i = 1, \ldots, n$ different species of ions that are moving through a single open channel is given by the parabolic equations

$$\partial_t u_i = \operatorname{div} \mathcal{F}_i, \quad \mathcal{F}_i = D_i\big(u_0 \nabla u_i - u_i \nabla u_0 + u_0 u_i (e z_i \mu_i \nabla \Phi + \nabla W_i)\big), \qquad (1.2)$$

where $D_i > 0$ denote the diffusion constants, z_i the ion charges, e the elementary charge, $\mu_i > 0$ the mobility parameters, $\Phi = \Phi(x,t)$ the electric potential, $W_i = W_i(x)$ some external potentials and $u_0 = u_0(x,t)$ the solvent concentration. We assume to have volume filling, which means that there is a maximal possible (constant) volume density $\tilde{u}$ that is achieved everywhere, as all space that is not occupied by ions is immediately filled by the electrically neutral solvent, $\tilde{u} = \sum_{i=0}^n u_i$. Note that it is assumed here that all ions have the same size. Incorporating different ion radii into the model is possible, but leads to some more mathematical difficulties, see [65, chapter 5]. Formally, equations (1.2) can be derived from a microscopic lattice-based model, see [16, Section 3.1]. The classic PNP model (1.1) can be recovered by just setting the solvent concentration $u_0 \equiv 1$.

The electric potential Φ is coupled to the concentrations u_i, $i = 1, \ldots, n$ via the Poisson equation

$$-\epsilon_0 \epsilon_r \Delta \Phi = e \left(\sum_{i=1}^n z_i u_i + f \right), \qquad (1.3)$$

where ϵ_0 and ϵ_r are the vacuum and relative permittivity and $f = f(x)$ is a permanent charge density. Both equations (1.2) and (1.3) are solved for $(x,t) \in \Omega \times (0, \infty)$ with a bounded domain $\Omega \subset \mathbb{R}^d$, $d \geq 1$.

The above equations can be written in a dimensionless form using the scaling

$$x = \tilde{L} x_s, \quad \Phi = \tilde{\Phi} \Phi_s, \quad u_i = \tilde{u} u_{is}, \quad f = \tilde{u} f_s, \quad D_i = \tilde{D} D_{is}, \quad t = \tilde{t} t_s, \qquad (1.4)$$

where $\tilde{L}$, $\tilde{\Phi}$, $\tilde{u}$, $\tilde{D}$ and $\tilde{t}$ are the typical length, voltage, concentration, diffusion and time, respectively. If we set $\tilde{t} = \tilde{L}^2 / \tilde{D}$, equations (1.2) and (1.3) are transformed to

$$\partial_t u_{is} = \operatorname{div} D_{is}\big(u_{0s} \nabla u_{is} - u_{is} \nabla u_{0s} + u_{0s} u_{is} (\beta_i z_i \nabla \Phi_s + \nabla W_{is})\big),$$

$$-\lambda^2 \Delta \Phi_s = \sum_{i=1}^n z_i u_{is} + f_s,$$

with an appropriately scaled external potential W_{is}, $1 = \sum_{i=0}^n u_{is}$, and the effective parameters

$$\lambda^2 = \frac{\epsilon_0 \epsilon_r \tilde{\Phi}}{e \tilde{L}^2 \tilde{u}}, \quad \text{and} \quad \beta_i = e \tilde{\Phi} \mu_i. \qquad (1.5)$$

3

For the remainder of this work we need to make the assumption that $\beta_i = \beta$ (or equivalently $\mu_i = \mu$) for all species. While this seems restrictive, there is a physical justification for this simplification. The actual electrical mobility constant for the ith species is given by $\eta_i = D_i \mu_i e z_i$ in equation (1.2). The Einstein relation tells us that diffusion and mobility are connected via $\eta_i = e z_i D_i / (k_B \theta)$, where k_B is the Boltzmann constant and θ is the temperature that is assumed to be constant. Therefore, it follows that $\mu_i = 1/(k_B \theta) =: \mu$ for $i = 1, \ldots, n$, which is closely related to the inverse thermal voltage $e/(k_B \theta)$.

For a full description of our system, we need to provide initial and boundary conditions for the above set of equations. From a modeling view point, it is reasonable to require that the boundary conditions should match the setup of the standard experiments that use the patch-clamp method. This technique was developed by Neher and Sakmann in the 1970s and makes it possible to measure the current through a single ion channel [57]. Mathematically speaking, there is a part of the boundary (Γ_N) that is impermeable, since ions cannot go through the channel walls. However, as the system is not closed, there must also be a part of the boundary (Γ_D) that is in contact with external reservoirs where the concentrations are prescribed, leading to mixed Dirichlet–Neumann boundary conditions. Similarly, for the electric potential, the channel walls should be insulated, but it is influenced by the voltage applied at two electrodes (Γ_E). We assume for simplicity that the Dirichlet boundaries of the potential and concentrations coincide, i.e. that $\Gamma_D = \Gamma_E$.

Omitting the subscript s for the scaled quantities from this point onward, we can now state the full problem that will be the focus of this thesis:

$$\partial_t u_i = \operatorname{div} \mathcal{F}_i, \quad \mathcal{F}_i = D_i\big(u_0 \nabla u_i - u_i \nabla u_0 + u_0 u_i(\beta z_i \nabla \Phi + \nabla W_i)\big), \quad i = 1, \ldots, n, \quad (1.6)$$

$$-\lambda^2 \Delta \Phi = \sum_{i=1}^{n} z_i u_i + f, \quad (1.7)$$

in $\Omega \times (0, \infty)$, with $u_0 = 1 - \sum_{i=1}^{n} u_i$, equipped with the boundary conditions

$$\mathcal{F}_i \cdot \nu = 0 \text{ on } \Gamma_N, \quad u_i = \overline{u}_i \text{ on } \Gamma_D, \quad i = 1, \ldots, n, \quad (1.8)$$

$$\nabla \Phi \cdot \nu = 0 \text{ on } \Gamma_N, \quad \Phi = \overline{\Phi} \text{ on } \Gamma_D, \quad (1.9)$$

and the initial condition

$$u_i(\cdot, 0) = u_i^I \quad \text{in } \Omega, \ i = 1, \ldots, n. \quad (1.10)$$

As we will elaborate in the next section, the above formulation of the ion transport problem is not necessarily the most suitable for the analysis or numerical simulations. Therefore, we introduce a different formulation that relies on the entropy (or free energy) of the model. For simplicity, we disregard for the moment the mixed boundary conditions (they will be treated in chapter 2). In that case, a natural entropy (or free energy) of the system (1.6)-(1.7) is given by the functional $\mathcal{H}(u) = \int_\Omega h(u)\,dx$ with

$$h(u) = \sum_{i=0}^{n} \big(u_i(\log u_i - 1) + 1\big) + \sum_{i=1}^{n} u_i(\beta z_i \Phi + W_i). \quad (1.11)$$

Introducing a new set of variables $w_i = \partial h(u)/\partial u_i = \log(u_i/u_0) + \beta z_i \Phi + W_i$, as in [16], we can rewrite the evolution equation (1.6) as

$$\partial_t u_i = \operatorname{div}(D_i u_i u_0 \nabla w_i). \quad (1.12)$$

1.3 Mathematical Challenges and State of the Art

1.3.1 Analysis

The evolution equations (1.6) for the ion concentrations can be written as the system

$$\partial_t u_i = \operatorname{div}\left(\sum_{j=1}^{n} A_{ij}(u)\nabla u_j + D_i u_0 u_i \nabla V_i \right), \quad i = 1,\ldots,n, \tag{1.13}$$

where $V_i = \beta z_i \Phi + W_i$ is the effective potential and the diffusion matrix $(A_{ij}(u))$ is defined by

$$A_{ii}(u) = D_i u_i, \quad A_{ij}(u) = D_i(u_0 + u_i), \quad j \neq i.$$

We easily observe from equations (1.13) that the concentration gradient of each species of ions influences the flux of the other species. This phenomenon is called cross-diffusion and has sparked an active field of research in mathematical analysis, but also in other natural sciences (see e.g. [75] for a summary of experiments highlighting the effects of cross-diffusion phenomena). Numerous applications in biology, chemistry and physics can be described by reaction-diffusion systems that include cross-diffusion. One of the most prominent examples is the population dynamics model of Shigesada et al. [69]. Other examples include the modeling of avascular tumor growth [47], multicomponent fluid mixtures described with Maxwell-Stefan equations [10], and the evolution of bacterial biofilms [64]. In the ion transport model, cross-diffusion occurs due to the excluded-volume effects. This observation has also been made in [14], where a cross-diffusion model is derived from discrete stochastic equations.

The analysis of cross-diffusion models is in general rather delicate, as the strong coupling between the equations usually prevents the use of classical tools such as maximum principles and parabolic regularity. More specifically, looking at the diffusion matrix of the ion transport system defined in (1.13), we clearly observe that $(A_{ij}(u))$ is not symmetric and generally also not positive semidefinite. Therefore, even the local-in-time existence of weak solutions is not trivial. While a minimum principle can be used to show the nonnegativity of u_i, $i = 1,\ldots,n$, there is no maximum principle available for this system of equations. Even though we expect the solution to be bounded by 1 due to the volume filling, it is not immediately clear how to prove the nonnegativity of $u_0 = 1 - \sum_{i=1}^{n} u_i$.

In addition to these difficulties that are typical for most cross-diffusion models, the ion transport problem (1.6)-(1.10) poses some more mathematical challenges. A severe problem for the analysis arises due to the degenerate structure hidden in the equations when the solvent concentration u_0 vanishes. This degeneracy becomes more evident in the alternative formulation (1.12). Furthermore, we also have to deal with the drift term induced by the electric potential and the coupled Poisson equation, as well as the mixed boundary conditions.

The key ingredient to show the existence of solutions for many cross-diffusion systems is the fact that they often possess an entropy. Mathematically speaking, this means that there exists a functional $\mathcal{H}(u) = \int_\Omega h(u)\,dx$, where h is a convex nonnegative function usually known as the entropy density, that is non-increasing along solutions to the system

(note that the physical entropy has the opposite sign and is non-decreasing). The basic assumption is that the system can be written as a formal gradient-flow

$$\partial_t u = \mathrm{div}\left(B\nabla\frac{\delta\mathcal{H}}{\delta u}\right), \tag{1.14}$$

where $\delta\mathcal{H}/\delta u$ is the variational derivative of the entropy with respect to u and B is a positive semidefinite and, in our particular case, even diagonal diffusion matrix (see equation (1.12)). The variational derivative can be identified with its Riesz representative $Dh(u) := w$ which is used as a new set of variables. These new variables are called entropy variables and are closely related to the notion of chemical potentials.

The gradient-flow formulation has two important advantages. Firstly, along the flow of the equation the entropy functional formally satisfies a functional inequality of the form

$$\frac{d\mathcal{H}(u)}{dt} + \mathcal{I}(u) \leq 0, \tag{1.15}$$

which we will refer to as entropy production inequality. The term

$$\mathcal{I}(u) = \int_\Omega \nabla w : B\nabla w \, dx,$$

where the symbol ":" denotes the Frobenius matrix product, is called entropy production and is nonnegative since B is positive semidefinite. From this relation, a priori estimates on the solution can be derived.

The second advantage of using the gradient-flow formulation is that if we assume that the derivative of the entropy density $Dh : \mathcal{D} \to \mathbb{R}^n$ is invertible on a bounded set $\mathcal{D}$, boundedness of the solution in the original variables is achieved via $u = (Dh)^{-1}(w)$ without the use of a maximum principle.

The idea of using the entropy variable transformation for the mathematical analysis of cross-diffusion systems goes back to [24]. The first result using this method for the ion transport model was achieved by Burger et al. [15], which also seems to be the first result for a cross-diffusion model with volume filling. In this work, a reduced version of the model is studied, with only two species of ions, a given electric potential and homogeneous Neumann boundary conditions. The entropy functional for the system is introduced and the global existence of weak solutions is shown by first solving an approximate problem in entropy variables. Later, this approach was formalized and refined as "boundedness-by-entropy method" in [49], the name referring to the fact that the transformation from entropy variables back to the original ones guarantees the boundedness of solutions. In [76], the existence of solutions for an arbitrary number of species and slightly more general equations was proven, still without the coupled potential and with homogeneous Neumann boundary conditions. The stationary version of (1.6)-(1.9) was investigated in [16]. Related models were discussed recently for example in [7, 13], however their results cannot be directly applied to our problem.

Several of the above mentioned papers also address the question of uniqueness of solutions. In general, there seem to be very few results on the uniqueness of weak solutions to cross-diffusion systems, and those that exist are based on the rather restrictive assumption

that the diffusion coefficients of all species are equal. A uniqueness result for a reduced version of the ion transport model (without the electric potential) is given in [50, Theorem 4.4], which was later generalized in [76]. The proof is based on the method of Gajewski [36]. In [7], uniqueness is proved for a nonlocal cross-diffusion model using Banach's fixed point theorem, still under the assumption of equal diffusion constants. For the stationary version of the ion transport problem well-posedness is proven in [16] under some simplifying assumptions.

1.3.2 Numerics

In the previous section we have tried to motivate how the entropy structure of the ion transport model is crucial for its analysis. Therefore, when designing a numerical scheme for the approximate computation of solutions, one should pay attention to preserve this kind of structural property on a discrete level. In order to obtain a stable algorithm, features of the continuous solution such as nonnegativity, boundedness and gradient estimates need to be true for the discrete solution as well. Unfortunately, there is no standard procedure on how to obtain such structure preserving schemes for nonlinear PDE systems.

Due to its immense popularity, there exist numerous numerical schemes for approximating the classical PNP system. Some of these schemes are formulated and tested in the context of ion channels, e.g. [53, 77], whereas others focus more on convergence analysis in a general setting [20, 62].

For the modified PNP model considered in this work, the situation is quite different. While some simulations of the stationary equations were done in [16], to our knowledge, no numerical analysis or simulation was done to date for the full ion transport problem (1.6)-(1.10). However, some efforts were made regarding the discretization of other cross-diffusion systems. We will mention some of them in the following.

The equations considered in this thesis are parabolic, hence we need to discretize both in the time and space variables. There is a huge variety of different methods for these discretizations. Most commonly, the implicit Euler method is used for the time discretization, as it is relatively simple yet yields good stability properties. It is worth mentioning that there are also efforts to obtain higher order schemes that still preserve entropy structures, see e.g. [52]. Regarding the space discretization, finite-volume and finite-element methods seem to be the most popular choices for obtaining numerical schemes for cross-diffusion systems, although there exist also other possibilities, e.g. finite-difference schemes as applied in [21]. In the following, we briefly introduce the concepts of finite-volume and finite-element methods and discuss some literature related to cross-diffusion systems.

Finite-volume (FV) methods are a type of discretization that is usually applied for the approximation of PDEs that express conservation laws. We explain the method by means of a general parabolic equation

$$\partial_t u - \operatorname{div} \mathcal{F}(u, \nabla u) = 0 \text{ on } \Omega \times (0, T). \tag{1.16}$$

Rather than on the actual PDE, finite-volume schemes are based on local balance equations. These equations are obtained by partitioning the spatial domain Ω into a family $\mathcal{T}$ of so-called control volumes, and then integrating the PDE over each such volume $K \in \mathcal{T}$ with

7

the help of the divergence theorem:

$$\int_K \partial_t u \, dx + \int_{\partial K} \mathcal{F}(u, \nabla u) \cdot \nu_K \, ds = 0,$$

where ν_K is the outward pointing unit normal vector to ∂K. The set of balance equations is subsequently discretized with respect to a set of discrete unknowns u_K. These unknowns can be interpreted as approximations of the mean values of the continuous quantities over the control volumes,

$$u_K \approx \frac{1}{\mathrm{m}(K)} \int_K u(x) \, dx,$$

where $\mathrm{m}(K)$ stands for the Lebesgue measure of the control volume. In combination with an implicit Euler method with uniform time step $\triangle t$ for the time derivative, this leads to

$$\mathrm{m}(K) \frac{u_{i,K}^k - u_{i,K}^{k-1}}{\triangle t} + \sum_{\sigma \in \mathcal{E}_K} \int_\sigma \mathcal{F}(u, \nabla u) \cdot \nu_\sigma \, ds = 0,$$

where $\mathcal{E}_K$ is the set of edges (or faces) of the cell K. The main challenge for the design of a FV scheme is to find a suitable discretization $\mathcal{F}_{K,\sigma} \approx \int_\sigma \mathcal{F}(u, \nabla u) \cdot \nu_\sigma \, ds$ of the fluxes at the volume boundaries. The flux approximations should be conservative (the flux entering a control volume from its neighbor is exactly the opposite of the flux entering the neighbor from the control volume) and consistent (the numerical flux tends to the continuous one as the mesh gets finer), however there is no systematic way to derive such a scheme.

For a simple diffusive flux, $\mathcal{F} = -\nabla u$, the two-point flux approximation scheme is widely used. In this case, the flux over the face σ between two control volumes K and L is approximated by

$$\mathcal{F}_{K,\sigma} = \frac{\mathrm{m}(\sigma)(u_K - u_L)}{\mathrm{d}(x_K, x_L)},$$

where u_K and u_L are approximations of the function u on the control volumes and $\mathrm{d}(x_K, x_L)$ is the distance between their centers. If the mesh satisfies the orthogonality assumption that the strait line between the centers x_K and x_L is orthogonal to σ, then this approximation is conservative and consistent [33]. For more general fluxes this property is not clear anymore, especially in our case of a nonlinear and strongly coupled system.

In recent literature, finite-volume schemes have been used for the discretization of many cross-diffusion systems. An upwind two-point flux approximation was recently used in [60] for a seawater intrusion cross-diffusion model. A two-point flux approximation with a nonlinear positivity-preserving approximation of the cross-diffusion coefficients, modeling the segregation of a two-species population, was suggested in [3], assuming positive definiteness of the diffusion matrix. The Laplacian structure of the population model (still for positive definite matrices) was exploited in [55] to design a convergent linear finite-volume scheme, which avoids fully implicit approximations. A semi-implicit finite-volume discretization for a biofilm model with a nonlocal time integrator was proposed in [63]. Finite-volume schemes for cross-diffusion systems with nonlocal (in space) terms were also analyzed; see, for instance, [2] for a food chain model and [1] for an epidemic model. A structure-preserving FV discretization for another cross-diffusion system with nonlocal interactions was recently

investigated in [19]. Moreover, a finite-volume scheme for a Keller–Segel system with additional cross diffusion and discrete entropy dissipation property was investigated in [9]. All these models, however, do not include volume filling and do not possess the degenerate structure explained before.

Finite-element (FE) methods are without a doubt the most popular tool for the numerical analysis of PDEs. In contrast to finite-volume methods, their starting point is the weak formulation of the equations. In the case of the parabolic equation (1.16), a weak solution to the equation is a function u in a suitable Hilbert space V such that

$$\int_\Omega \partial_t u \, \phi \, dx + \int_\Omega \mathcal{F}(u, \nabla u) \cdot \nabla \phi \, dx = 0 \text{ for all } \phi \in V. \tag{1.17}$$

The discretization method is a special kind of Galerkin method, where the (infinite dimensional) space V for the solution and the test functions is replaced by a finite dimensional subspace V_h. This subspace is again based on a partition of the domain Ω into cells, and the subscript h is a discretization parameter that is usually a measure of the mesh size. If the solution is expected to be in $H^1(\Omega)$, a common choice for V_h is the space of continuous functions that are linear on each cell. A basis for this space is formed by the "hat functions" χ_j that are equal to one on the jth node and equal to zero on all other nodes. The approximate solution can then be expressed as a linear combination of the basis functions and the discrete unknowns are the corresponding coefficients.

Finite-element methods have been applied successfully for the discretization of some cross-diffusion models. In [6] a convergent finite-element scheme for a cross-diffusion population model was presented. The approximation is not based on entropy variables, but a regularization of the entropy itself that is used to define a regularized system. The same technique was also employed in [38]. A lumped FE method was used in [35] for a reaction-cross-diffusion equation on a stationary surface with positive definite diffusion matrix, and optimal convergence rates were shown. In [51], an implicit Euler Galerkin approximation in entropy variables for a Poisson-Maxwell-Stefan system was shown to converge. Recently, an abstract framework for the numerical approximation of evolution problems with entropy structure was proposed in [28]. The discretization presented in this work is based on a discontinuous Galerkin method in time and a Galerkin approximation in space. When applied to cross-diffusion systems, this approach leads to an approximation in entropy variables that preserves the entropy dissipation. However, the existence of discrete solutions or convergence of the scheme is not discussed.

1.4 Main Results and Structure of the Thesis

Chapter 2 is devoted to the analysis of the cross-diffusion system, focusing on the questions of existence and uniqueness of weak solutions. The main results shown in this chapter are:

- We prove the global-in-time existence of weak solutions to the ion transport model (1.6)-(1.10) (Theorem 2.1). The proof is based on the "boundedness-by-entropy method" [49]. The main novelties of this result compared to the work done in [49, 76] are the extension of the method to mixed Dirichlet-Neumann boundary conditions

and the inclusion of the electric potential. This also entails the definition of a relative entropy that takes the boundary data into account, and a formal computation of the corresponding entropy variables (see Appendix A).

- Assuming equal diffusion constants and ion charges (i.e. $D_i = D$ and $z_i = z$ for $i = 1, \ldots, n$) and some additional regularity, we prove the uniqueness of weak solutions (Theorem 2.3). For this, we use the entropy method of Gajewski [36].

The work presented in this chapter is based on a research cooperation with A. Jüngel (TU Wien), which was published under the title *Analysis of a degenerate parabolic cross-diffusion system for ion transport* in the *Journal of Mathematical Analysis and Applications* [40].

In **Chapter 3**, we present two new numerical schemes for the cross-diffusion model (1.6)-(1.10). We use a backward Euler method in time for both schemes in order to preserve the entropy structure. The schemes differ with respect to the space discretization: The first scheme is a finite-volume scheme in the original variables (i.e. the ion concentrations u_i), while the second scheme uses a Galerkin finite-element method in the entropy variables w_i.

The FV scheme is described and analyzed in **Section 3.1**. The key idea of the discretization is to use the drift-diffusion structure of the equations and two-point flux approximations with upwind mobilities. As there is no maximum principle for the equations (1.6), the analysis of the scheme is only possible under the assumption of equal diffusion constants. For the convergence proof, we need to restrict ourselves to a simplified situation without the coupled electric potential. The resulting system cannot model ion transport, but is still of interest from a mathematical point of view. The main results are as follows:

- If $D_i = D$ for all i, we prove the existence of solutions to the fully discrete numerical scheme (Theorem 3.4). If additionally the drift part vanishes, the solution is unique. The existence proof uses a topological degree argument in finite space dimensions, while the uniqueness proof is again based on the entropy method of Gajewski [36].

- If $D_i = D$ for all i, the scheme preserves the nonnegativity and upper bounds for the concentrations. If additionally the drift part vanishes, convexity arguments show that the discrete entropy is dissipated with a discrete entropy production analogous to the continuous case (Theorem 3.5). The assumption on vanishing drift terms is needed, since a discrete version of the sum $\sum_{i=1}^{n} u_i$ has to be controlled from below; see the discussion after Theorem 3.5.

- If $D_i = D$ for all i and the drift part vanishes, the discrete solution converges to a continuous solution to (1.6) as the mesh size tends to zero (Theorem 3.6). The proof is based on a priori estimates obtained from the discrete entropy inequality. The compactness property, which is needed for the convergence, is derived from a new discrete Aubin–Lions lemma, which takes into account the nonstandard degeneracy of the equations; see Lemma 5.6 in the appendix.

The results of this section are based on a joint work with C. Chainais-Hillairet and C. Cancès from Univ. Lille 1 and A. Jüngel (TU Wien) and will appear under the title *Finite-volume scheme for a degenerate cross-diffusion model motivated from ion transport* in the

journal *Numerical Methods for Partial Differential Equations* [17].

In **Section 3.2** the FE scheme is discussed. It is based on the weak formulation of the ion transport system in entropy variables with a small regularization term. We show the following results:

- We prove the existence of discrete solutions (in entropy variables) that satisfy an entropy production inequality using a fixed point argument (Theorem 3.12). By transforming back to the original variables we immediately get the positivity and boundedness of the discrete solution.

- We show the convergence of the discrete solutions (in the original variables) to a solution of the continuous system (Theorem 3.13). In contrast to the FV case, we do not need any additional assumptions on the data. The proof makes use of arguments that are already elaborated in Section 2.3 for proving the existence of weak solutions to the continuous system.

In **Chapter 4** we present some numerical experiments to show the efficiency of both schemes in two spatial dimensions. We choose two different scenarios that are inspired by real life applications:

- The first test case is a simple model for a calcium-selective ion channel that was proposed by [59]. We observe that our simulations compare well to 1D simulations done in [16] for the same setting. Furthermore, we investigate the long-time-behavior of the numerical solutions and obtain experimental convergence rates for both schemes.

- The second experiment models a bipolar ion channel similar to an N-P semiconductor diode. The modified PNP model has not been applied before to this sort of test case, so we compare our simulation results to those of [43] and our own simulations of the classical PNP model. In particular, we investigate the rectification phenomenon that is typical for pores with asymmetric charge distribution.

The results of Section 3.2 and Chapter 4 are based on a collaboration with A. Jüngel (TU Wien) and are submitted for publication under the title *Comparison of a finite-element and finite-volume scheme for a degenerate cross-diffusion system for ion transport.*

Lastly, in **Chapter 5** we give a summary of our findings, including a comparison of the two numerical schemes, and discuss possible future research.

2 Analysis of the Cross-Diffusion Model

The aim of this chapter is to provide a detailed mathematical analysis of the ion transport model (1.6)-(1.10). In Section 2.1 we explain the key idea for the existence analysis, which is the entropy method. Then, in Section 2.2 we formulate the main results, namely the existence and uniqueness (under some assumptions) of weak solutions, and provide an overview of the strategies of the proofs. The following Sections contain the proofs in full detail, the existence proof is found in Section 2.3 and the uniqueness proof in Section 2.4.

2.1 Key Idea of the Analysis

We extend the boundedness-by-entropy method [49] to the case of nonconstant potentials and nonhomogeneous mixed boundary conditions. The key observation, already stated in [16], is that the equations (1.6) possess an entropy or gradient-flow structure. Since we need to deal with nonhomogeneous Dirichlet boundary conditions, we cannot directly use the entropy (1.11) as given in [16], but instead define a relative entropy with respect to the boundary data. The entropy or, more precisely, free energy is given by

$$\mathcal{H}(u) = \int_\Omega h(u)\, dx, \quad \text{where } u = (u_1, \dots, u_n), \tag{2.1}$$

$$h(u) = \sum_{i=0}^n \int_{\overline{u}_i}^{u_i} \log \frac{s}{\overline{u}_i}\, ds + \frac{\beta\lambda^2}{2} |\nabla(\Phi - \overline{\Phi})|^2 + \sum_{i=1}^n u_i W_i$$

and $\overline{u}_0 = 1 - \sum_{i=1}^n \overline{u}_i$. The free energy is bounded from below if $u_i \in L^\infty(\Omega)$, $\Phi \in H^1(\Omega)$ and $W_i \in L^1(\Omega)$. Note that the terms in the first summand of the entropy density can also be written in the more common way

$$\int_{\overline{u}_i}^{u_i} \log \frac{s}{\overline{u}_i}\, ds = H(u_i) - H(\overline{u}_i) - \log(\overline{u}_i)(u_i - \overline{u}_i),$$

with the convex function $H(s) := s(\log s - 1) + 1$.

Equations (1.13) can be written as a formal gradient flow in the sense

$$\partial_t u_i = \operatorname{div}\left(\sum_{j=1}^n B_{ij} \nabla w_j \right), \quad i = 1, \dots, n, \tag{2.2}$$

where $B_{ii} = D_i u_0 u_i$, $B_{ij} = 0$ if $i \neq j$ provide a diagonal positive semidefinite matrix (B_{ij}), and w_j are the entropy variables, defined by

$$\frac{\partial h}{\partial u_i} = w_i - \overline{w}_i, \quad \text{where}$$

$$w_i = \log \frac{u_i}{u_0} + \beta z_i \Phi + W_i, \quad \overline{w}_i = \log \frac{\overline{u}_i}{\overline{u}_0} + \beta z_i \overline{\Phi}, \quad i = 1, \dots, n. \tag{2.3}$$

We refer to Lemma 5.1 in the Appendix for the computation of $\partial h/\partial u_i$. In thermodynamics $\partial h/\partial u_i$ is called the chemical potential of the ith species. The advantage of the reformulation (2.2) is that the drift terms are eliminated and, in this special case, the new diffusion matrix (B_{ij}) is diagonal. Note that we have not included the boundary data into the formulation (2.2). In fact, the free energy is nonincreasing along trajectories to (1.6)-(1.10) only if the boundary data are in equilibrium, i.e. if $\nabla \overline{w}_i = 0$. In the general case, the free energy is bounded only; see (2.8) below.

There is another important benefit of formulation (2.2). Observing that the relation between $w = (w_1, \ldots, w_n)$ and $u = (u_1, \ldots, u_n)$ can be inverted explicitly according to

$$u_i = u_i(w, \Phi) = \frac{\exp(w_i - \beta z_i \Phi - W_i)}{1 + \sum_{j=1}^n \exp(w_j - \beta z_j \Phi - W_j)}, \quad i = 1, \ldots, n, \tag{2.4}$$

we see that, if $(w_1, \ldots, w_n, \Phi)$ is a solution to (1.7) and (2.2),

$$u(w, \Phi) \in \mathcal{D} := \left\{ u = (u_1, \ldots, u_n) \in (0, 1)^n : \sum_{i=1}^n u_i < 1 \right\}. \tag{2.5}$$

This provides positive lower *and* upper bounds for the concentrations $u_0, \ldots, u_n$ without the use of a maximum principle.

2.2 Main Results

We prove first the global-in-time existence of bounded weak solutions, and second the uniqueness of weak solutions under additional regularity assumptions. In the following, we detail these results. First, we specify the technical assumptions.

(H1) Domain: $\Omega \subset \mathbb{R}^d$ $(d \geq 1)$ is a bounded domain with $\partial\Omega = \Gamma_D \cup \Gamma_N \in C^{0,1}$, $\Gamma_D \cap \Gamma_N = \emptyset$, Γ_N is open in $\partial\Omega$, and $\text{meas}(\Gamma_D) > 0$.

(H2) Parameters: $T > 0$, D_i, $\beta > 0$, and $z_i \in \mathbb{R}$, $i = 1, \ldots, n$.

(H3) Given functions: $f \in L^\infty(\Omega)$, $W_i \in H^1(\Omega) \cap L^\infty(\Omega)$, and $W_i = 0$ on Γ_D, $\nabla W_i \cdot \nu = 0$ on Γ_N, $i = 1, \ldots, n$.

(H4) Initial and boundary data: $u_i^I \in L^\infty(\Omega)$, $\overline{u}_i \in H^1(\Omega)$ for $i = 1, \ldots, n$, with $u^I \in \mathcal{D}$ and $\overline{u} \in \mathcal{D}$ in Ω, and $\overline{\Phi} \in H^1(\Omega) \cap L^\infty(\Omega)$ satisfies

$$-\lambda^2 \Delta \overline{\Phi} = f \quad \text{in } \Omega, \quad \nabla \overline{\Phi} \cdot \nu = 0 \quad \text{on } \Gamma_N.$$

Clearly, it is sufficient to define the functions $\overline{u}_i$, $\overline{\Phi}$ on Γ_D. By the extension property, they can be extended to Ω, and we assume in (H4) that the extension of $\overline{\Phi}$ is done in a special way. This extension is needed to be consistent with the definition of the free energy (entropy) and the entropy variables; see Lemma 5.1. We denote these extensions again by $\overline{u}_i$, $\overline{\Phi}$. Furthermore, we introduce as in [73] the space

$$H_D^1(\Omega) = \{u \in H^1(\Omega) : u = 0 \text{ on } \Gamma_D\}.$$

The first result concerns the existence of bounded weak solutions.

Theorem 2.1 (Global existence of weak solutions)**.** *Let Assumptions (H1)-(H4) hold. Then there exists a bounded weak solution $u_1, \ldots, u_n : \Omega \times (0, T) \to \overline{\mathcal{D}}$ to (1.6)-(1.10) satisfying*

$$u_i u_0^{1/2}, \ u_0^{1/2} \in L^2(0, T; H^1(\Omega)), \quad \partial_t u_i \in L^2(0, T; H_D^1(\Omega)'),$$
$$\Phi \in L^2(0, T; H^1(\Omega)), \quad i = 1, \ldots, n,$$

and the weak formulation

$$\int_0^T \langle \partial_t u_i, \phi_i \rangle \, dt + D_i \int_0^T \int_\Omega u_0^{1/2} \big(\nabla(u_0^{1/2} u_i) - 3u_i \nabla u_0^{1/2} \big) \cdot \nabla \phi_i \, dx \, dt$$

$$+ D_i \int_0^T \int_\Omega u_i u_0 (\beta z_i \nabla \Phi + \nabla W_i) \cdot \nabla \phi_i \, dx \, dt = 0, \tag{2.6}$$

$$\lambda^2 \int_0^T \int_\Omega \nabla \Phi \cdot \nabla \theta \, dx dt = \int_0^T \int_\Omega \bigg(\sum_{i=1}^n z_i u_i + f \bigg) \theta \, dx \, dt, \tag{2.7}$$

for all $\phi_i, \theta \in L^2(0, T; H_D^1(\Omega))$, $i = 1, \ldots, n$. The initial condition is satisfied in the sense of $H_D^1(\Omega)'$, and the Dirichlet boundary conditions are given by

$$u_0 = \overline{u}_0 := 1 - \sum_{i=1}^n \overline{u}_i, \quad u_i u_0^{1/2} = \overline{u}_i (\overline{u}_0)^{1/2} \quad on \ \Gamma_D, \ i = 1, \ldots, n,$$

in the sense of traces in $L^2(\Gamma_D)$.

The proof is based on an approximation procedure. First, we show the existence of weak solutions for an approximate problem in entropy variables, that is semi-discretized in time with step size $\tau > 0$ and regularized by adding a term of the form $\varepsilon(\sum_{|\alpha|=m}(-1)^m D^{2\alpha} w + w)$ with $\varepsilon > 0$ to ensure coercivity and boundedness of the solution. Then, we use (2.4) to obtain an approximate solution $u^{(\varepsilon,\tau)}$ in the original variables. We pass first to the limit $\varepsilon \to 0$ and finally also let $\tau \to 0$.

The estimates needed for the compactness argument are derived from a discrete version of the entropy-production inequality (for simplicity, we omit the superindex (ε, τ))

$$\frac{d\mathcal{H}}{dt} = \int_\Omega \sum_{i=1}^n \partial_t u_i (w_i - \overline{w}_i) \, dx = - \int_\Omega \sum_{i=1}^n D_i u_0 u_i \nabla w_i \cdot \nabla(w_i - \overline{w}_i) \, dx$$

$$\leq -\frac{1}{2} \int_\Omega \sum_{i=1}^n D_i u_0 u_i |\nabla w_i|^2 \, dx + C(\overline{w}), \tag{2.8}$$

where the constant $C(\overline{w}) > 0$ depends on the $H^1(\Omega)$ norm of $\overline{w}$. We show in (2.19) below that

$$\sum_{i=1}^n u_i u_0 \nabla \log \frac{u_i}{u_0} = 4u_0 \sum_{i=1}^n |\nabla u_i^{1/2}|^2 + |\nabla u_0|^2 + 4|\nabla u_0^{1/2}|^2,$$

which yields an $H^1(\Omega)$ estimate for $u_0^{1/2}$ but *not* for u_i because of the factor $u_0 \geq 0$. This reflects the degenerate nature of the equations which is more apparent in the component-wise formulation $\partial_t u_i = \text{div}(D_i u_0 u_i \nabla w_i)$ (see (2.2)).

To overcome this degeneracy, we employ the technique developed in [15, 76] for the limit $\tau \to 0$. We show that $(u_0^{(\tau)} u_i^{(\tau)})$ is bounded in $H^1(\Omega)$ and that the (approximative) time derivative of $u_i^{(\tau)}$ is bounded in $H_D^1(\Omega)'$. If $u_0^{(\tau)}$ was strictly positive, we could apply the Aubin–Lions Lemma 5.3 to conclude strong convergence of (a subsequence of) $(u_i^{(\tau)})$ to some u_i which solves (1.6). However, since $u_0^{(\tau)}$ may vanish in the limit, this lemma cannot be used. The idea is to compensate the lack of the gradient estimates for $u_i^{(\tau)}$ by exploiting the uniform estimates for $u_0^{(\tau)}$. Then, by the "degenerate" Aubin–Lions lemma (see Lemma 5.4 in the Appendix), (a subsequence of) $(u_0^{(\tau)} u_i^{(\tau)})$ converges strongly to $u_0 u_i$, and u_0, u_i solve (1.6). For details, see Section 2.3.

Remark 2.2. *1. Theorem 2.1 also holds when reaction terms $f_i(u)$ are introduced on the right-hand side of (1.6). As in [49], we need that f_i is continuous and that*

$$\sum_{i=1}^{n} f_i(u) \frac{\partial h}{\partial u_i} \leq C(1 + h(u))$$

holds for some $C > 0$ and all $u \in \mathcal{D}$.

2. The approximate solution satisfies a discrete version of the entropy-production inequality; see (2.8). As explained above, the sequence $(u_i^{(\tau)})$ may not converge strongly, such that we are unable to perform the limit $\tau \to 0$ in (2.8). As a consequence, we cannot prove that the free energy (2.1) is nonincreasing along trajectories of (1.6)-(1.7), and the analysis of the large-time behavior seems to be inaccessible. Therefore, we investigate the decay of $\mathcal{H}(u)$ numerically; see Chapter 4.

3. Since the Neumann boundary condition does not appear explicitly in the weak formulation (2.6)-(2.7), we do not need to make expressions like $\nabla\Phi \cdot \nu = 0$ on Γ_N precise. We only mention along the way that terms like $\nabla\Phi \cdot \nu$ on Γ_N have to be understood in the sense of $H_{00}^{1/2}(\Gamma_N)'$ which is the dual space of $H_{00}^{1/2}(\Gamma_N)$ consisting of all functions v on Γ_N such that $v \in H_D^1(\Omega)$. This space is larger than $H^{-1/2}(\Gamma_N)$. We refer to [5, Chapter 18] for details.

The second result is the uniqueness of weak solutions.

Theorem 2.3 (Uniqueness of weak solutions). *Let Assumptions (H1)-(H4) hold, $\sum_{i=1}^{n} W_i \in L^\infty(0,T;W^{1,d}(\Omega))$, and let $D_i = 1$ and $z_i = z \in \mathbb{R}$ for $i = 1, \ldots, n$. Then there exists at most one bounded weak solution to (1.6)-(1.10) in the class of functions*

$$u_i \in H^1(0,T;H_D^1(\Omega)') \cap L^2(0,T;H^1(\Omega)), \quad \Phi \in L^\infty(0,T;W^{1,q}(\Omega))$$

with $q > d$.

The proof is a combination of standard $L^2(\Omega)$-type estimates and the entropy method of Gajewski [36]. In fact, equations (1.6) partially decouple because of the assumptions $D_i = 1$ and $z_i = z$. Summing (1.6) over $i = 1, \ldots, n$, we find that (u_0, Φ) solves

$$\partial_t u_0 = \text{div}\left(\nabla u_0 - u_0(1-u_0)(\beta z \nabla\Phi + \nabla W)\right), \quad -\lambda^2 \Delta\Phi = z(1-u_0) + f(x), \qquad (2.9)$$

where $W = \sum_{i=1}^{n} W_i$. The uniqueness of solutions is shown by taking two solutions (u_0, Φ) and (v_0, Ψ) and using $u_0 - v_0$ as a test function in the first equation of (2.9). Then, with the Gagliardo-Nirenberg inequality and the hypothesis $\nabla \Phi \in L^q(\Omega)$, we show that

$$\frac{d}{dt} \int_\Omega (u_0 - v_0)(t)^2 \, dx \leq C(\Phi) \int_\Omega (u_0 - v_0)^2 \, dx,$$

where $C(\Phi) > 0$ depends on the $W^{1,q}(\Omega)$ norm of Φ. Hence, Gronwall's lemma yields $u_0 = v_0$ and consequently, $\Phi = \Psi$.

The next step is to show, for given u_0 and Φ, that u_i is the unique solution to (1.6). Since we cannot expect that $\nabla u_i \in L^q(\Omega)$, $q > d$, for $d \geq 3$, we employ the technique of Gajewski [36] which avoids this regularity. The method seems to work only for linear mobilities u_i, which is the reason why we cannot apply it to (2.9). The idea is to introduce the semimetric

$$d(u, v) = \int_\Omega \sum_{i=1}^{n} \left(H(u_i) + H(v_i) - 2H\left(\frac{u_i + v_i}{2}\right) \right) dx \geq 0,$$

where $H(s) = s(\log s - 1) + 1$, and to show that $\partial_t d(u, v) \leq 0$. Since $d(u(0), v(0)) = 0$, this implies that $d(u(t), v(t)) = 0$ for $t > 0$ and consequently, $u(t) = v(t)$. Since expressions like $\log u_i$ are undefined when $u_i = 0$, we need to regularize the semimetric. For details, we refer to Section 2.4.

Remark 2.4. *1. The regularity $u_i \in L^2(0, T; H^1(\Omega))$ holds if u_0 is strictly positive. A standard idea for the proof is to employ $\min\{0, u_0 - me^{-\lambda t}\}^p$ as a test function in the first equation of (2.9), where $\inf_{\Gamma_D} \overline{u}_0 \geq m > 0$ and $\lambda > 0$ is sufficiently large, and to pass after some estimations to the limit $p \to \infty$. We leave the details to the reader; see, e.g., [42] for a proof in a related situation.*

2. The regularity condition $\Phi(t) \in W^{1,q}(\Omega)$ with $q > d$ is satisfied if $d \leq 3$, $\partial \Omega \in C^{1,1}$, and the Dirichlet and Neumann boundary do not meet, $\Gamma_D \cap \overline{\Gamma}_N = \emptyset$ [73, Theorem 3.29]. It is also satisfied in up to three space dimensions if $\partial \Omega \in C^3$, $\overline{\Gamma}_D \cap \overline{\Gamma}_N \in C^3$, and $\overline{\Phi} \in W^{1-1/q,q}(\Gamma_D)$, $q > d$ [68]. □

The rest of this chapter is organized as follows. The existence theorem is proved in Section 2.3, while the uniqueness result is shown in Section 2.4. The entropy variables $\partial h / \partial u_i$ are computed in the Appendix.

2.3 Proof of the Existence Result

We consider first the nonlinear Poisson equation

$$-\lambda^2 \Delta \Phi = \sum_{i=1}^{n} z_i u_i(w, \Phi) + f, \quad u_i(w, \Phi) = \frac{\exp(w_i - \beta z_i \Phi - W_i)}{1 + \sum_{j=1}^{n} \exp(w_j - \beta z_j \Phi - W_j)},$$

in Ω with the boundary conditions (1.9) for given $w_i \in L^\infty(\Omega)$. Then the right hand side $g : (x, \Phi) \mapsto \sum_{i=1}^{n} z_i u_i(w(x), \Phi) + f(x)$ is a bounded function with $|g(x, \Phi)| \leq \sum |z_i| +$

$\|f\|_{L^\infty(\Omega)}$ and a standard fixed-point argument shows that this problem has a weak solution $\Phi \in H^1(\Omega)$. Since $\Phi \mapsto g(x, \Phi)$ is Lipschitz continuous and decreasing, this solution is unique. By the maximum principle and $f \in L^\infty(\Omega)$, we have $\Phi \in L^\infty(\Omega)$. Note that $u(w(x), \Phi(x)) \in \mathcal{D}$ for $x \in \Omega$. Therefore, the following estimate holds:

$$\|\Phi\|_{H^1(\Omega)} \le C(1 + \|\overline{\Phi}\|_{H^1(\Omega)}), \tag{2.10}$$

where $C > 0$ depends on λ, z_i, and $\|f\|_{L^2(\Omega)}$.

Step 1: Solution to an approximate problem. Let $T > 0$, $N \in \mathbb{N}$, $\tau = T/N > 0$, and $m \in \mathbb{N}$ such that $m > d/2$. Then the embedding $H^m(\Omega) \hookrightarrow L^\infty(\Omega)$ is compact. Let $v^{k-1} := w^{k-1} - \overline{w} \in H_D^1(\Omega; \mathbb{R}^n) \cap L^\infty(\Omega; \mathbb{R}^n)$, $\Phi^{k-1} - \overline{\Phi} \in H_D^1(\Omega)$ be given. If $k = 1$, we set $v^0 = h'(u^I) - \overline{w}$ and let Φ^0 be the weak solution to $-\lambda^2 \Delta \Phi^0 = \sum_{i=1}^n z_i u_i^I + f(x)$ in Ω with boundary conditions (1.9). Our aim is to find $v^k \in H_D^1(\Omega; \mathbb{R}^n) \cap H^m(\Omega; \mathbb{R}^n)$, $\Phi^k - \overline{\Phi} \in H_D^1(\Omega)$ such that

$$\frac{1}{\tau} \int_\Omega \left(u(v^k + \overline{w}, \Phi^k) - u(v^{k-1} + \overline{w}, \Phi^{k-1}) \right) \cdot \phi \, dx$$

$$+ \int_\Omega \nabla \phi : B(v^k + \overline{w}, \Phi^k) \nabla(v^k + \overline{w}) \, dx$$

$$+ \varepsilon \int_\Omega \left(\sum_{|\alpha|=m} D^\alpha v^k \cdot D^\alpha \phi + v^k \cdot \phi \right) dx = 0, \tag{2.11}$$

$$\lambda^2 \int_\Omega \nabla \Phi^k \cdot \nabla \theta \, dx = \int_\Omega \left(\sum_{i=1}^n z_i u_i(v^k + \overline{w}, \Phi^k) + f \right) \theta \, dx \tag{2.12}$$

for all $\phi \in H_D^1(\Omega; \mathbb{R}^n)$ and $\theta \in H_D^1(\Omega)$. Here, $\alpha = (\alpha_1, \dots, \alpha_n) \in \mathbb{N}_0^n$ is a multi-index, $|\alpha| = \alpha_1 + \cdots + \alpha_n$, $D^\alpha = \partial^{|\alpha|}/\partial x_1^{\alpha_1} \cdots \partial x_n^{\alpha_n}$ is a partial derivative, and ":" denotes the Frobenius matrix product with summation over both indices. Since the matrix B is diagonal, we may write the second integral in (2.11) as

$$\int_\Omega \nabla \phi : B(v^k + \overline{w}, \Phi^k) \nabla(v^k + \overline{w}) \, dx$$

$$= \int_\Omega \sum_{i=1}^n D_i u_0(v^k + \overline{w}, \Phi^k) u_i(v^k + \overline{w}, \Phi^k) \nabla \phi_i \cdot \nabla(v_i^k + \overline{w}_i) \, dx.$$

Lemma 2.5 (Existence of weak solutions to the time-discrete problem)**.** *Let the assumptions of Theorem 2.1 hold. Then there exists a weak solution $v^k = w^k - \overline{w} \in H_D^1(\Omega; \mathbb{R}^n) \cap H^m(\Omega; \mathbb{R}^n)$, $\Phi^k - \overline{\Phi} \in H_D^1(\Omega)$ to (2.11)-(2.12), and the following discrete entropy production inequality holds:*

$$\mathcal{H}(u^k) + \tau \int_\Omega \nabla(w^k - \overline{w}) : B(w^k, \Phi^k) \nabla w^k \, dx$$

$$+ \varepsilon \tau C_P \|w^k - \overline{w}\|_{H^m(\Omega)}^2 \le \mathcal{H}(u^{k-1}), \tag{2.13}$$

where $\mathcal{H}$ is defined in (2.1), $u^k = u(w^k, \Phi^k)$, $u^{k-1} = u(w^{k-1}, \Phi^{k-1})$, and $C_P > 0$ is the constant of the generalized Poincaré inequality [72, Chap. II.1.4, Formula (1.39)].

Proof. We employ the Leray–Schauder fixed-point theorem. For this, let $y \in L^\infty(\Omega)$ and $\delta \in [0,1]$. Let $\Phi^k - \overline{\Phi} \in H_D^1(\Omega)$ be the unique weak solution to the nonlinear problem

$$\lambda^2 \int_\Omega \nabla \Phi^k \cdot \nabla \theta \, dx = \int_\Omega \left(\sum_{i=1}^n z_i u_i(y + \overline{w}, \Phi^k) + f \right) \theta \, dx$$

for $\theta \in H_D^1(\Omega)$. Since $y \in L^\infty(\Omega)$, the expression $u_i(y + \overline{w}, \Phi^k)$ is well-defined. Next, let $X = H_D^1(\Omega; \mathbb{R}^n) \cap H^m(\Omega; \mathbb{R}^n)$ and consider the linear problem

$$a(v, \phi) = F(\phi) \quad \text{for all } \phi \in X, \tag{2.14}$$

where

$$a(v, \phi) = \int_\Omega \nabla \phi : B(y + \overline{w}, \Phi^k) \nabla v \, dx + \varepsilon \int_\Omega \left(\sum_{|\alpha|=m} D^\alpha v \cdot D^\alpha \phi + v \cdot \phi \right) dx,$$

$$F(\phi) = -\frac{\delta}{\tau} \int_\Omega \left(u(y + \overline{w}, \Phi^k) - u(v^{k-1} + \overline{w}, \Phi^{k-1}) \right) \cdot \phi \, dx$$
$$- \delta \int_\Omega \nabla \phi : B(y + \overline{w}, \Phi^k) \nabla \overline{w} \, dx.$$

The bilinear form a and the linear form F are continuous on X. Furthermore, using the positive semi-definiteness of the matrix B and the generalized Poincaré inequality with constant $C_P > 0$ [72, Chap. II.1.4, Formula (1.39)], a is coercive:

$$a(v, v) \geq \varepsilon \int_\Omega \left(\sum_{|\alpha|=m} |D^\alpha v|^2 + |v|^2 \right) dx \geq \varepsilon C_P \|v\|_{H^m(\Omega)}^2.$$

By the lemma of Lax–Milgram, there exists a unique solution $v \in X \subset L^\infty(\Omega; \mathbb{R}^n)$ to (2.14). For later reference, we observe that, since the continuity constant for F does not depend on y,

$$C(\varepsilon) \|v\|_{H^m(\Omega)}^2 \leq a(v, v) = F(v) \leq C(\tau) \|v\|_{H^m(\Omega)}, \tag{2.15}$$

which gives a bound for v in $H^m(\Omega)$ which is independent of y and δ.

This defines the fixed-point operator $S : L^\infty(\Omega; \mathbb{R}^n) \times [0,1] \to L^\infty(\Omega; \mathbb{R}^n)$, $S(y, \delta) = v$. It clearly holds that $S(y, 0) = 0$ for all $y \in L^\infty(\Omega; \mathbb{R}^n)$. The continuity of S follows from standard arguments; see, e.g., the proof of Lemma 5 in [49]. In view of the compact embedding $H^m(\Omega) \hookrightarrow L^\infty(\Omega)$, S is also compact. The uniform estimate for all fixed points of $S(\cdot, \delta)$ follows from (2.15). Thus, by the Leray-Schauder fixed-point theorem, there exists $v^k \in X$ such that $S(v^k, 1) = v^k$ and $w^k := v^k + \overline{w}$, Φ^k solve (2.11)-(2.12).

It remains to prove inequality (2.13). To this end, we employ $\tau v^k = \tau(w^k - \overline{w}) \in X$ as a test function in the weak formulation of (2.11). Again, we set $u^k = u(w^k, \Phi^k)$, $u^{k-1} = u(w^{k-1}, \Phi^{k-1})$. Then

$$\int_\Omega (u^k - u^{k-1}) \cdot (w^k - \overline{w}) \, dx + \tau \int_\Omega \nabla(w^k - \overline{w}) : B(w^k, \Phi^k) \nabla w^k$$
$$+ \varepsilon \tau \|w^k - \overline{w}\|_{H^m(\Omega)}^2 \leq 0. \tag{2.16}$$

To estimate the first integral, we take $x \in \Omega$ and set

$$g(u) = \sum_{i=0}^{n} \int_{\overline{u}_i(x)}^{u_i} \log \frac{s}{\overline{u}_i(x)} ds, \quad u \in \mathbb{R}^n,$$

where we recall that $\overline{u}_0 = 1 - \sum_{i=1}^{n} \overline{u}_i$. Then $(\partial g/\partial u_i)(u) = \log(u_i/\overline{u}_i) - \log(u_0/\overline{u}_0)$ and g is convex. Hence, $g(u^k) - g(u^{k-1}) \le g'(u^k) \cdot (u^k - u^{k-1})$ or

$$\int_{\Omega} (g(u^k) - g(u^{k-1})) \, dx \le \int_{\Omega} \sum_{i=1}^{n} (u_i^k - u_i^{k-1}) \left(\log \frac{u_i^k}{u_0^k} - \log \frac{\overline{u}_i}{\overline{u}_0} \right) dx.$$

Moreover, we infer from the Poisson equation that

$$\beta \int_{\Omega} \sum_{i=1}^{n} z_i (u_i^k - u_i^{k-1})(\Phi^k - \overline{\Phi}) \, dx = -\beta \lambda^2 \int_{\Omega} \Delta(\Phi^k - \Phi^{k-1})(\Phi^k - \overline{\Phi}) \, dx$$

$$= \beta \lambda^2 \int_{\Omega} \nabla \big((\Phi^k - \overline{\Phi}) - (\Phi^{k-1} - \overline{\Phi}) \big) \cdot \nabla(\Phi^k - \overline{\Phi}) \, dx$$

$$\ge \frac{\beta \lambda^2}{2} \int_{\Omega} |\nabla(\Phi^k - \overline{\Phi})|^2 \, dx - \frac{\beta \lambda^2}{2} \int_{\Omega} |\nabla(\Phi^{k-1} - \overline{\Phi})|^2 \, dx.$$

In view of these estimates, the first term in (2.16) becomes

$$\int_{\Omega} (u^k - u^{k-1}) \cdot (w^k - \overline{w}) \, dx$$

$$= \int_{\Omega} \sum_{i=1}^{n} (u_i^k - u_i^{k-1}) \left(\log \frac{u_i^k}{u_0^k} - \log \frac{\overline{u}_i}{\overline{u}_0} + \beta z_i (\Phi^k - \overline{\Phi}) + W_i \right) dx$$

$$\ge \mathcal{H}(u^k) - \mathcal{H}(u^{k-1}).$$

We infer from (2.16) that (2.13) holds. $\qquad\qquad\square$

Step 2: A priori estimates. Let (w^k, Φ^k) be a weak solution to (2.11)-(2.12). Then $u^k(x) = u(w^k(x), \Phi^k(x)) \in \mathcal{D}$ for $x \in \Omega$, so (u^k) is bounded uniformly in (ε, τ).

Lemma 2.6 (A priori estimates). *The following estimates hold:*

$$\|u_i^k\|_{L^\infty(\Omega)} + \varepsilon \tau \sum_{j=1}^{k} \|w_i^j - \overline{w}_i\|_{H^m(\Omega)}^2 \le C, \qquad (2.17)$$

$$\tau \sum_{j=1}^{k} \left(\|(u_0^j)^{1/2}\|_{H^1(\Omega)}^2 + \|u_0^j\|_{H^1(\Omega)}^2 + \|(u_0^j)^{1/2} \nabla(u_i^j)^{1/2}\|_{L^2(\Omega)}^2 \right) \le C, \qquad (2.18)$$

where here and in the following, $C > 0$ is a generic constant independent of ε and τ.

Proof. We need to estimate the second term on the left-hand side of the entropy-production inequality (2.13). Since $B(w^k, \Phi^k) = \text{diag}(D_i u_i^k u_0^k)$, we obtain

$$\nabla(w^k - \overline{w}) : B(w^k, \Phi^k)\nabla w^k = \sum_{i=1}^n D_i u_i^k u_0^k |\nabla w_i^k|^2 - \sum_{i=1}^n D_i u_i^k u_0^k \nabla \overline{w}_i \cdot \nabla w_i^k$$

$$\geq \frac{D_{\min}}{2} \sum_{i=1}^n u_i^k u_0^k |\nabla w_i^k|^2 - \frac{D_{\max}}{2} \sum_{i=1}^n |\nabla \overline{w}_i|^2,$$

where $D_{\min} = \min_{i=1,\dots,n} D_i$, $D_{\max} = \max_{i=1,\dots,n} D_i$, and we used the fact that $0 \leq u_i^k \leq 1$ in Ω for $i = 0, \dots, n$. Furthermore, by definition (2.3) of the entropy variables,

$$|\nabla w_i^k|^2 = \left| \nabla \log \frac{u_i^k}{u_0^k} + \nabla(\beta z_i \Phi^k + W_i) \right|^2 \geq \frac{1}{2} \left| \nabla \log \frac{u_i^k}{u_0^k} \right|^2 - |\nabla(\beta z_i \Phi + W_i)|^2.$$

Inserting these inequalities into (2.13), it follows that

$$\mathcal{H}(u^k) + \tau \frac{D_{\min}}{4} \int_\Omega \sum_{i=1}^n u_i^k u_0^k \left| \nabla \log \frac{u_i^k}{u_0^k} \right|^2 dx + \varepsilon \tau C_P \|w^k - \overline{w}\|_{H^m(\Omega)}^2$$

$$\leq \mathcal{H}(u^{k-1}) + \tau \frac{D_{\min}}{2} \int_\Omega \sum_{i=1}^n |\nabla(\beta z_i \Phi^k + W_i)|^2 \, dx + \tau \frac{D_{\max}}{2} \int_\Omega \sum_{i=1}^n |\nabla \overline{w}_i|^2 \, dx.$$

We resolve this recursion to find that

$$\mathcal{H}(u^k) + \tau \frac{D_{\min}}{4} \sum_{j=1}^k \int_\Omega \sum_{i=1}^n u_i^j u_0^j \left| \nabla \log \frac{u_i^j}{u_0^j} \right|^2 dx + \varepsilon \tau C_P \sum_{j=1}^k \|w^j - \overline{w}\|_{H^m(\Omega)}^2$$

$$\leq \mathcal{H}(u^0) + \tau \frac{D_{\min}}{2} \sum_{j=1}^k \int_\Omega \sum_{i=1}^n |\nabla(\beta z_i \Phi^j + W_i)|^2 \, dx + \tau k \frac{D_{\max}}{2} \int_\Omega \sum_{i=1}^n |\nabla \overline{w}_i|^2 \, dx.$$

Because of the $H^1(\Omega)$ estimate (2.10) for the electric potential and $\tau k \leq T$, the right-hand side is uniformly bounded. Furthermore, using $\sum_{i=1}^n u_i^j = 1 - u_0^j$,

$$\sum_{i=1}^n u_i^j u_0^j \left| \nabla \log \frac{u_i^j}{u_0^j} \right|^2 = 4 u_0^j \sum_{i=1}^n |\nabla(u_i^j)^{1/2}|^2 - 2\nabla u_0^j \sum_{i=1}^n \nabla u_i^j + 4|\nabla(u_0^j)^{1/2}|^2 \sum_{i=1}^n u_i^j$$

$$= 4 u_0^j \sum_{i=1}^n |\nabla(u_i^j)^{1/2}|^2 + 2|\nabla u_0^j|^2 + 4|\nabla(u_0^j)^{1/2}|^2 - 4u_0^j|\nabla(u_0^j)^{1/2}|^2$$

$$= 4 u_0^j \sum_{i=1}^n |\nabla(u_i^j)^{1/2}|^2 + |\nabla u_0^j|^2 + 4|\nabla(u_0^j)^{1/2}|^2. \tag{2.19}$$

This finishes the proof. □

Step 3: Limit $\varepsilon \to 0$. We cannot perform the simultaneous limit $(\varepsilon, \tau) \to 0$ since we need an Aubin–Lions compactness result, which requires a uniform estimate for the

discrete time derivative of the concentrations in $H_D^1(\Omega; \mathbb{R}^n)'$ and not in the larger space $X' = (H_D^1(\Omega; \mathbb{R}^n) \cap H^m(\Omega; \mathbb{R}^n))'$. Let $k \in \{1, \ldots, N\}$ be fixed and let $u_i^{(\varepsilon)} = u_i^k$ and $\Phi^{(\varepsilon)} = \Phi^k$ be a weak solution to (2.11)-(2.12). Set $u_0^{(\varepsilon)} = 1 - \sum_{i=1}^n u_i^{(\varepsilon)}$. By Lemma 2.6, there exist subsequences of $(u_i^{(\varepsilon)})$ and $(\Phi^{(\varepsilon)})$, which are not relabeled, such that, as $\varepsilon \to 0$,

$$u_i^{(\varepsilon)} \rightharpoonup^* u_i \quad \text{weakly* in } L^\infty(\Omega), \tag{2.20}$$

$$(u_0^{(\varepsilon)})^{1/2} \rightharpoonup u_0^{1/2}, \quad \Phi^{(\varepsilon)} \rightharpoonup \Phi \quad \text{weakly in } H^1(\Omega), \ i = 1, \ldots, n, \tag{2.21}$$

$$u_0^{(\varepsilon)} \to u_0, \quad \Phi^{(\varepsilon)} \to \Phi \quad \text{strongly in } L^2(\Omega), \tag{2.22}$$

$$\varepsilon(w_i^{(\varepsilon)} - \overline{w}_i) \to 0 \quad \text{strongly in } H^m(\Omega). \tag{2.23}$$

We have to pass to the limit $\varepsilon \to 0$ in

$$\int_\Omega \nabla \phi : B(w^{(\varepsilon)}, \Phi^{(\varepsilon)}) \nabla w^{(\varepsilon)} \, dx = \int_\Omega \sum_{i=1}^n D_i u_i^{(\varepsilon)} u_0^{(\varepsilon)} \nabla w_i^{(\varepsilon)} \cdot \nabla \phi_i \, dx$$

$$= \int_\Omega \sum_{i=1}^n D_i \big(u_0^{(\varepsilon)} \nabla u_i^{(\varepsilon)} - u_i^{(\varepsilon)} \nabla u_0^{(\varepsilon)} + u_i^{(\varepsilon)} u_0^{(\varepsilon)} (\beta z_i \nabla \Phi^{(\varepsilon)} + \nabla W_i) \big) \cdot \nabla \phi_i \, dx$$

$$= \int_\Omega \sum_{i=1}^n D_i \Big((u_0^{(\varepsilon)})^{1/2} \nabla \big(u_i^{(\varepsilon)} (u_0^{(\varepsilon)})^{1/2} \big) - 3 u_i^{(\varepsilon)} (u_0^{(\varepsilon)})^{1/2} \nabla (u_0^{(\varepsilon)})^{1/2}$$

$$+ \beta z_i u_i^{(\varepsilon)} u_0^{(\varepsilon)} (\beta z_i \nabla \Phi^{(\varepsilon)} + \nabla W_i) \Big) \cdot \nabla \phi_i \, dx.$$

We claim that $u_i^{(\varepsilon)} (u_0^{(\varepsilon)})^{1/2} \rightharpoonup u_i u_0^{1/2}$ weakly in $H^1(\Omega)$. First, we observe that, because of (2.20) and (2.22), $u_i^{(\varepsilon)} (u_0^{(\varepsilon)})^{1/2} \rightharpoonup u_i u_0^{1/2}$ weakly in $L^2(\Omega)$. Then the claim follows from the bound

$$\big\| \nabla \big(u_i^{(\varepsilon)} (u_0^{(\varepsilon)})^{1/2} \big) \big\|_{L^2(\Omega)} \leq \| u_i^{(\varepsilon)} \|_{L^\infty(\Omega)} \| \nabla (u_0^{(\varepsilon)})^{1/2} \|_{L^2(\Omega)}$$

$$+ 2 \| (u_i^{(\varepsilon)})^{1/2} \|_{L^\infty(\Omega)} \| (u_0^{(\varepsilon)})^{1/2} \nabla (u_i^{(\varepsilon)})^{1/2} \|_{L^2(\Omega)} \leq C, \tag{2.24}$$

using (2.18). The compact embedding $H^1(\Omega) \hookrightarrow L^2(\Omega)$ implies that

$$u_i^{(\varepsilon)} (u_0^{(\varepsilon)})^{1/2} \to u_i u_0^{1/2} \quad \text{strongly in } L^2(\Omega),$$

and by the $L^\infty(\Omega)$ bounds, this convergence also holds in $L^p(\Omega)$ for $p < \infty$. This shows that, taking into account (2.21),

$$(u_0^{(\varepsilon)})^{1/2} \nabla \big(u_i^{(\varepsilon)} (u_0^{(\varepsilon)})^{1/2} \big) - 3 u_i^{(\varepsilon)} (u_0^{(\varepsilon)})^{1/2} \nabla (u_0^{(\varepsilon)})^{1/2}$$

$$\rightharpoonup u_0^{1/2} \nabla (u_i u_0^{1/2}) - 3 u_i u_0^{1/2} \nabla u_0^{1/2} \quad \text{weakly in } L^1(\Omega).$$

In fact, since this sequence is bounded in $L^2(\Omega)$, the weak convergence also holds in $L^2(\Omega)$. Furthermore, by (2.22), possibly for a subsequence,

$$u_i^{(\varepsilon)} u_0^{(\varepsilon)} \nabla \Phi^{(\varepsilon)} \rightharpoonup u_i u_0 \nabla \Phi \quad \text{weakly in } L^1(\Omega),$$

and this convergence holds also in $L^2(\Omega)$.

Then, performing the limit $\varepsilon \to 0$ in (2.11)-(2.12) leads to

$$\frac{1}{\tau} \int_\Omega (u^k - u^{k-1}) \cdot \phi \, dx + \int_\Omega \sum_{i=1}^n D_i (u_0^k)^{1/2} \big(\nabla(u_i^k (u_0^k)^{1/2}) - 3u_i^k \nabla(u_0^k)^{1/2} \big) \cdot \nabla \phi_i \, dx$$

$$+ \int_\Omega \sum_{i=1}^n D_i u_i^k u_0^k \big(\beta z_i \nabla \Phi^k + \nabla W_i \big) \cdot \nabla \phi_i \, dx, \tag{2.25}$$

$$\lambda^2 \int_\Omega \nabla \Phi^k \cdot \nabla \theta \, dx = \int_\Omega \Big(\sum_{i=1}^n z_i u_i^k + f \Big) \theta \, dx, \tag{2.26}$$

for all $\phi = (\phi_1, \ldots, \phi_n) \in X$ and $\theta \in H_D^1(\Omega)$, where $u^k := u$ and $\Phi^k := \Phi$. A density argument shows that we may take $\phi \in H_D^1(\Omega; \mathbb{R}^n)$.

By the trace theorem, $\Phi^k - \overline{\Phi} \in H_D^1(\Omega)$. To show that also $u_i^k - u_i(\overline{w}, \overline{\Phi}) \in H_D^1(\Omega; \mathbb{R}^n)$ holds, we observe that $w^{(\varepsilon)} = \overline{w}$ on Γ_D and therefore, $u_0^{(\varepsilon)} = \overline{u}_0$ on Γ_D in the sense of traces, where $\overline{u}_0 = 1 - \sum_{i=1}^n \overline{u}_i$ and $\overline{u}_i := u_i(\overline{w}, \overline{\Phi})$. Since $u_i^{(\varepsilon)}(u_0^{(\varepsilon)})^{1/2} = \overline{u}_i(\overline{u}_0)^{1/2}$ on Γ_D and $\nabla(u_i^{(\varepsilon)}(u_0^{(\varepsilon)})^{1/2}) \rightharpoonup \nabla(u_i u_0^{1/2})$ weakly in $L^2(\Omega)$ (see (2.24)), the trace theorem implies that $u_i u_0^{1/2} = \overline{u}_i(\overline{u}_0)^{1/2}$ on Γ_D.

Step 4: Limit $\tau \to 0$. Let $u^{(\tau)}(x, t) = u^k(x)$ and $\Phi^{(\tau)}(x, t) = \Phi^k(x)$ for $x \in \Omega$ and $t \in ((k-1)\tau, k\tau]$, $k = 1, \ldots, N$, be piecewise in time constant functions. At time $t = 0$, we set $u^{(\tau)}(\cdot, 0) = u^0$. We introduce the shift operator $(\sigma_\tau u^{(\tau)})(\cdot, t) = u^{k-1}$ for $t \in ((k-1)\tau, k\tau]$. Then, in view of (2.25)-(2.26), $(u^{(\tau)}, \Phi^{(\tau)})$ solves

$$\frac{1}{\tau} \int_\Omega (u^{(\tau)} - \sigma_\tau u^{(\tau)}) \cdot \phi \, dx dt$$

$$+ \int_0^T \int_\Omega \sum_{i=1}^n D_i \Big((u_0^{(\tau)})^{1/2} \nabla \big(u_i^{(\tau)}(u_0^{(\tau)})^{1/2} \big) - 3 u_i^{(\tau)}(u_0^{(\tau)})^{1/2} \nabla (u_0^{(\tau)})^{1/2} \Big) \cdot \nabla \phi_i \, dx dt$$

$$+ \int_0^T \int_\Omega \sum_{i=1}^n D_i u_i^{(\tau)} u_0^{(\tau)} \big(\beta z_i \nabla \Phi^{(\tau)} + \nabla W_i \big) \cdot \nabla \phi_i \, dx dt = 0, \tag{2.27}$$

$$\lambda^2 \int_0^T \int_\Omega \nabla \Phi^{(\tau)} \cdot \nabla \theta \, dx dt = \int_0^T \int_\Omega \Big(\sum_{i=1}^n z_i u_i^{(\tau)} + f \Big) \theta \, dx dt \tag{2.28}$$

for all piecewise constant functions ϕ_i, $\theta : (0, T) \to H_D^1(\Omega)$.

Lemma 2.6 provides the following uniform bounds:

$$\|u_i^{(\tau)}\|_{L^\infty(\Omega_T)} + \|(u_0^{(\tau)})^{1/2}\|_{L^2(0,T;H^1(\Omega))} + \|u_0^{(\tau)}\|_{L^2(0,T;H^1(\Omega))} \le C, \tag{2.29}$$

$$\|u_i^{(\tau)}(u_0^{(\tau)})^{1/2}\|_{L^2(0,T;H^1(\Omega))} \le C, \tag{2.30}$$

where $\Omega_T = \Omega \times (0, T)$ and $C > 0$ is independent of τ. Moreover,

$$\|\Phi^{(\tau)}\|_{L^2(0,T;H^1(\Omega))}^2 = \tau \sum_{k=1}^N \|\Phi^k\|_{H^1(\Omega)}^2 \le \tau N C \le T C.$$

We wish to derive a uniform bound for the discrete time derivative of $(u_i^{(\tau)})$. To this end, we estimate

$$\frac{1}{\tau}\left|\int_\Omega (u^{(\tau)} - \sigma_\tau u^{(\tau)}) \cdot \phi \, dxdt\right| \leq \int_0^T \sum_{i=1}^n D_i \|u_0^{(\tau)}\|_{L^\infty(\Omega)}^{1/2}$$
$$\times \left(\|\nabla(u_i^{(\tau)}(u_0^{(\tau)})^{1/2})\|_{L^2(\Omega)} + 3\|u_i^{(\tau)}\|_{L^\infty(\Omega)}\|\nabla(u_0^{(\tau)})^{1/2}\|_{L^2(\Omega)}\right)\|\nabla\phi_i\|_{L^2(\Omega)}dt$$
$$+ \int_0^T \sum_{i=1}^n D_i\|u_i^{(\tau)}u_0^{(\tau)}\|_{L^\infty(\Omega)}\left(\beta|z_i|\|\nabla\Phi^{(\tau)}\|_{L^2(\Omega)} + \|\nabla W_i\|_{L^2(\Omega)}\right)\|\nabla\phi_i\|_{L^2(\Omega)}dt$$
$$\leq C.$$

This holds for all piecewise constant functions $\phi_i : (0, T) \to H_D^1(\Omega)$. By a density argument, we obtain

$$\tau^{-1}\|u_i^{(\tau)} - \sigma_\tau u_i^{(\tau)}\|_{L^2(0,T;H_D^1(\Omega)')} \leq C, \quad i = 1, \ldots, n. \tag{2.31}$$

Summing these estimates for $i = 1, \ldots, n$, we also have

$$\tau^{-1}\|u_0^{(\tau)} - \sigma_\tau u_0^{(\tau)}\|_{L^2(0,T;H_D^1(\Omega)')} \leq C. \tag{2.32}$$

From these estimates, we conclude that, as $\tau \to 0$, up to a subsequence,

$$u_i^{(\tau)} \rightharpoonup^* u_i \quad \text{weakly* in } L^\infty(\Omega_T),$$
$$\Phi^{(\tau)} \rightharpoonup \Phi \quad \text{weakly in } L^2(0, T; H^1(\Omega)),$$
$$\tau^{-1}(u_i^{(\tau)} - \sigma_\tau u_i^{(\tau)}) \rightharpoonup \partial_t u_i \quad \text{weakly in } L^2(0, T; H_D^1(\Omega)'), \; i = 1, \ldots, n.$$

Taking into account (2.29) and (2.32), we can apply the Aubin–Lions lemma in the version of [26] (see Lemma 5.3 in the Appendix) to $(u_0^{(\tau)})$ to obtain the existence of a subsequence, which is not relabeled, such that $u_0^{(\tau)} \to u_0$ strongly in $L^2(\Omega_T)$, and this convergence even holds in $L^p(\Omega_T)$ for $p < \infty$. As a consequence,

$$(u_0^{(\tau)})^{1/2} \to u_0^{1/2} \quad \text{strongly in } L^p(\Omega_T), \; p < \infty. \tag{2.33}$$

Thus, by (2.29), up to a subsequence,

$$\nabla(u_0^{(\tau)})^{1/2} \rightharpoonup \nabla u_0^{1/2} \quad \text{weakly in } L^2(\Omega_T).$$

We cannot infer the strong convergence of $(u_i^{(\tau)})$ because of the degeneracy occurring in estimate (2.30). The idea is to employ the Aubin–Lions lemma in the "degenerate" version of [15, 49] (also see Lemma 5.4 in the Appendix). In view of (2.33), the $L^2(0, T; H^1(\Omega))$ estimates for $(u_i^{(\tau)}(u_0^{(\tau)})^{1/2})$ and $((u_0^{(\tau)})^{1/2})$ (see (2.29)-(2.30)), as well as estimate (2.31), there exists a subsequence (not relabeled) such that

$$u_i^{(\tau)}(u_0^{(\tau)})^{1/2} \to u_i u_0^{1/2} \quad \text{strongly in } L^2(\Omega_T). \tag{2.34}$$

Taking into account the uniform bound (2.30), we also have

$$\nabla\big(u_i^{(\tau)}(u_0^{(\tau)})^{1/2}\big) \rightharpoonup \nabla(u_i u_0^{1/2}) \quad \text{weakly in } L^2(\Omega_T).$$

This shows that

$$(u_0^{(\tau)})^{1/2}\nabla\big(u_i^{(\tau)}(u_0^{(\tau)})^{1/2}\big) - 3u_i^{(\tau)}(u_0^{(\tau)})^{1/2}\nabla(u_0^{(\tau)})^{1/2} \rightharpoonup u_0^{1/2}\nabla(u_iu_0^{1/2}) - 3u_iu_0^{1/2}\nabla u_0^{1/2}$$

weakly in $L^1(\Omega_T)$. Furthermore, by (2.33) and (2.34),

$$u_i^{(\tau)}u_0^{(\tau)} = u_i^{(\tau)}(u_0^{(\tau)})^{1/2}\cdot(u_0^{(\tau)})^{1/2} \to u_iu_0 \quad \text{strongly in } L^2(\Omega_T).$$

These convergences allow us to perform the limit $\tau \to 0$ in (2.27)-(2.28) to find that (u_i, Φ) solves (2.6)-(2.7) for all smooth test functions. By a density argument, we may take test functions from $L^2(0, T; H_D^1(\Omega))$. We can show as in Step 3 that the Dirichlet boundary conditions are satisfied, and the initial condition $u_i(\cdot, 0) = u_i^I$ in Ω follows from arguments similar as at the end of the proof of Theorem 2 in [49].

2.4 Proof of the Uniqueness Result

We prove Theorem 2.3. For this, we proceed in two steps.

Step 1. Adding (1.6) from $i = 1, \ldots, n$ and taking into account the assumptions $D_i = 1$ and $z_i = z$, we find that $u_0 = 1 - \sum_{i=1}^n u_i$ solves

$$\partial_t u_0 = \text{div}\big(\nabla u_0 - u_0(1 - u_0)(\beta z\nabla\Phi + \nabla W)\big), \quad -\lambda^2\Delta\Phi = z(1 - u_0) + f(x) \qquad (2.35)$$

in Ω, $t > 0$, where $W = \sum_{i=1}^n W_i$, together with the initial conditions $u_0(\cdot, 0) = 1 - \sum_{i=1}^n u_i^I$ and boundary conditions (1.9) and

$$\big(\nabla u_0 - u_0(1 - u_0)(\beta z\nabla\Phi + \nabla W)\big)\cdot\nu = 0 \quad \text{on } \Gamma_N, \quad u_0 = 1 - \sum_{i=1}^n \overline{u}_i \quad \text{on } \Gamma_D.$$

We show that this problem has a unique weak solution (u_0, Φ) in the class of functions $\Phi \in L^\infty(0, T; W^{1,q}(\Omega))$.

Let (u_0, Φ) and (v_0, Ψ) be two weak solutions to (2.35) with the corresponding initial and boundary conditions such that $\Phi, \Psi \in L^\infty(0, T; W^{1,q}(\Omega))$. We take $u_0 - v_0$ as a test function in the weak formulation of the difference of (2.35) satisfied by u_0 and v_0, respectively. Then

$$\begin{aligned}
\frac{1}{2}\int_\Omega &(u_0 - v_0)^2(t)\,dx + \int_0^t\int_\Omega |\nabla(u_0 - v_0)|^2\,dxds \\
&= \int_0^t\int_\Omega \Big(u_0(1 - u_0)(\beta z\nabla\Phi + \nabla W)) - v_0(1 - v_0)(\beta z\nabla\Psi + \nabla W))\Big) \\
&\quad \times \nabla(u_0 - v_0)\,dxds \\
&= \int_0^t\int_\Omega \big(u_0(1 - u_0) - v_0(1 - v_0)\big)(\beta z\nabla\Phi + \nabla W)\cdot\nabla(u_0 - v_0)\,dxds \\
&\quad + \beta z\int_0^t\int_\Omega v_0(1 - v_0)\nabla(\Phi - \Psi)\cdot\nabla(u_0 - v_0)\,dxds \\
&=: I_1 + I_2.
\end{aligned} \qquad (2.36)$$

The first integral is estimated using the identity $u_0(1-u_0) - v_0(1-v_0) = (1-u_0-v_0)(u_0-v_0)$ and Hölder's inequality with $1/p + 1/q + 1/2 = 1$, where $q > d$ (and $2 < p < \infty$ if $d \le 2$):

$$\begin{aligned}
I_1 &\le \|1 - u_0 - v_0\|_{L^\infty(Q_t)}\|u_0 - v_0\|_{L^2(0,t;L^p(\Omega))}\|\beta z \nabla\Phi + \nabla W\|_{L^\infty(0,t;L^q(\Omega))} \\
&\quad \times \|\nabla(u_0 - v_0)\|_{L^2(0,t;L^2(\Omega))} \\
&\le \frac{1}{4}\|\nabla(u_0 - v_0)\|^2_{L^2(Q_t)} + C\|u_0 - v_0\|^2_{L^2(0,t;L^p(\Omega))}.
\end{aligned}$$

By the Gagliardo-Nirenberg inequality with $\theta = d/2 - d/p \in (0,1)$,

$$\begin{aligned}
\int_0^t \|u_0 - v_0\|^2_{L^p(\Omega)} ds &\le C \int_0^t \|u_0 - v_0\|^{2\theta}_{H^1(\Omega)}\|u_0 - v_0\|^{2(1-\theta)}_{L^2(\Omega)} ds \\
&\le C\int_0^t \left(\|\nabla(u_0 - v_0)\|^{2\theta}_{L^2(\Omega)} + \|u_0 - v_0\|^{2\theta}_{L^2(\Omega)}\right)\|u_0 - v_0\|^{2(1-\theta)}_{L^2(\Omega)} ds \\
&\le \frac{1}{4}\int_0^t \|\nabla(u_0 - v_0)\|^2_{L^2(\Omega)} ds + C\int_0^t \|u_0 - v_0\|^2_{L^2(\Omega)} ds.
\end{aligned}$$

This shows that
$$I_1 \le \frac{1}{2}\|\nabla(u_0 - v_0)\|^2_{L^2(Q_t)} + C\|u_0 - v_0\|^2_{L^2(Q_t)}.$$

For the remaining integral, we employ the following elliptic estimate

$$\|\nabla(\Phi - \Psi)\|_{L^2(\Omega)} \le C\|(1 - u_0) - (1 - v_0)\|_{L^2(\Omega)} = C\|u_0 - v_0\|_{L^2(\Omega)},$$

such that

$$\begin{aligned}
I_2 &\le \beta|z|\|v_0(1-v_0)\|_{L^\infty(Q_t)}\|\nabla(\Phi - \Psi)\|_{L^2(Q_t)}\|\nabla(u_0 - v_0)\|_{L^2(Q_t)} \\
&\le C\|u_0 - v_0\|_{L^2(Q_t)}\|\nabla(u_0 - v_0)\|_{L^2(Q_t)} \le \frac{1}{2}\|\nabla(u_0 - v_0)\|^2_{L^2(Q_t)} + \frac{C}{2}\|u_0 - v_0\|^2_{L^2(Q_t)}.
\end{aligned}$$

Then, inserting the estimates for I_1 and I_2 into (2.36) leads to

$$\frac{1}{2}\int_\Omega (u_0 - v_0)^2(t)\,dx \le C\int_0^t \int_\Omega (u_0 - v_0)^2\,dxds,$$

and we conclude with Gronwall's lemma that $u_0 = v_0$. Consequently, by the Poisson equation in (2.35), $\Phi = \Psi$.

Step 2. Next, we show that $u_1, \dots, u_n$ is the unique weak solution to (1.6), written in the form

$$\partial_t u_i = \operatorname{div}(u_0 \nabla u_i - u_i \nabla V_i), \quad i = 1, \dots, n, \tag{2.37}$$

where $V_i = u_0 + \beta z\Phi + W_i$, and (u_0, Φ) is the unique solution to (2.35), together with the corresponding initial and boundary conditions. Since we have assumed that $u_i \in L^2(0,T;H^1(\Omega))$, the formulation (1.6) can be used instead of (2.6). The classical uniqueness proof requires that $\nabla V_i \in L^\infty(0,T;L^q(\Omega))$; see the first step of this proof. To avoid this condition, we use the entropy method of Gajewski [36, 37].

Let $u = (u_1, \ldots, u_n)$ and $v = (v_1, \ldots, v_n)$ be two weak solutions to (2.37) with initial and boundary conditions (1.8) and (1.10). We introduce the semimetric

$$d_\varepsilon(u,v) = \int_\Omega \sum_{i=1}^n \left(H_\varepsilon(u_i) + H_\varepsilon(v_i) - 2H_\varepsilon\left(\frac{u_i + v_i}{2}\right) \right) dx,$$

where $H_\varepsilon(s) = (s+\varepsilon)(\log(s+\varepsilon)-1)+1$ for $s \geq 0$. The regularization with $\varepsilon > 0$ is needed to avoid that expressions like $\log(u_i)$ are undefined if $u_i = 0$. Since H_ε is convex, we have $H_\varepsilon(u_i) + H_\varepsilon(v_i) - 2H_\varepsilon((u_i + v_i)/2) \geq 0$ in Ω and hence, $d_\varepsilon(u,v) \geq 0$. Now, using (2.37), we compute, similarly as in [76],

$$\frac{d}{dt} d_\varepsilon(u,v) = \sum_{i=1}^n \left\{ \left\langle \partial_t u_i, H_\varepsilon'(u_i) - H_\varepsilon'\left(\frac{u_i+v_i}{2}\right) \right\rangle + \left\langle \partial_t v_i, H_\varepsilon'(v_i) - H_\varepsilon'\left(\frac{u_i+v_i}{2}\right) \right\rangle \right\}$$

$$= -\int_\Omega \sum_{i=1}^n \left\{ (u_0 \nabla u_i - u_i \nabla V_i) \cdot \left(H_\varepsilon''(u_i) \nabla u_i - \frac{1}{2} H_\varepsilon''\left(\frac{u_i+v_i}{2}\right) \nabla(u_i+v_i) \right) \right.$$

$$\left. + (u_0 \nabla v_i - v_i \nabla V_i) \cdot \left(H_\varepsilon''(v_i) \nabla v_i - \frac{1}{2} H_\varepsilon''\left(\frac{u_i+v_i}{2}\right) \nabla(u_i+v_i) \right) \right\} dx.$$

Rearranging these terms, we arrive at

$$\frac{d}{dt} d_\varepsilon(u,v) = -4 \int_\Omega u_0 \sum_{i=1}^n \left(|\nabla \sqrt{u_i+\varepsilon}|^2 + |\nabla \sqrt{v_i+\varepsilon}|^2 - 2|\nabla \sqrt{u_i+v_i+2\varepsilon}|^2 \right) dx$$

$$- \int_\Omega \sum_{i=1}^n \left(\frac{u_i+v_i}{u_i+v_i+2\varepsilon} - \frac{u_i}{u_i+\varepsilon} \right) \nabla V_i \cdot \nabla u_i \, dx$$

$$- \int_\Omega \sum_{i=1}^n \left(\frac{u_i+v_i}{u_i+v_i+2\varepsilon} - \frac{v_i}{v_i+\varepsilon} \right) \nabla V_i \cdot \nabla v_i \, dx.$$

Lemma 10 in [76] shows that the first integral is nonnegative. Therefore, integrating the above identity in time and observing that $d_\varepsilon(u(0), v(0)) = 0$, we obtain

$$d_\varepsilon(u(t), v(t)) \leq - \int_0^t \int_\Omega \sum_{i=1}^n \left(\frac{u_i+v_i}{u_i+v_i+2\varepsilon} - \frac{u_i}{u_i+\varepsilon} \right) \nabla V_i \cdot \nabla u_i \, dxds$$

$$- \int_0^t \int_\Omega \sum_{i=1}^n \left(\frac{u_i+v_i}{u_i+v_i+2\varepsilon} - \frac{v_i}{v_i+\varepsilon} \right) \nabla V_i \cdot \nabla v_i \, dxds.$$

Arguing as in [76, Section 6], the dominated convergence theorem shows that $d_\varepsilon(u(t), v(t)) \to 0$ as $\varepsilon \to 0$ (here, we use $\nabla V_i \in L^2(\Omega_T)$). Then, since a Taylor expansion of H_ε gives

$$d_\varepsilon(u(t), v(v)) \geq \frac{1}{8} \sum_{i=1}^n \|u_i(t) - v_i(t)\|_{L^2(\Omega)}^2,$$

we infer that $u_i(t) = v_i(t)$ in Ω for $t > 0$, $i = 1, \ldots, n$, which finishes the proof.

3 Discretization of the Model Equations

In this chapter we present two different numerical schemes for the ion transport model. First, we describe a finite-volume discretization in the original variables in Section 3.1, then a finite-element discretization in the entropy variables in Section 3.2. Both sections are structured as follows. In the beginning, we detail the assumptions and notations. Next, the numerical schemes are presented in detail and the main results are stated. This includes the existence of discrete solutions, a discrete version of the entropy inequality and a convergence result for both schemes. The proofs are detailed in the following subsections.

3.1 Finite-Volume Scheme

The key observation for the finite-volume (FV) discretization is that the fluxes can be written on each cell in a "double" drift-diffusion form, i.e., both $\mathcal{F}_i = -D_i(u_0 \nabla u_i - u_i V_i)$ and $V_i = \nabla u_0 - \beta z_i u_0 \nabla \Phi$ have the structure $\nabla v + vF$, where ∇v is the diffusion term and vF is the drift term. We discretize $\mathcal{F}$ and V by using a two-point flux approximation with "double" upwind mobilities. Under certain assumptions, we can show that the structure of the equations is preserved on the discrete level. Because of the drift-diffusion structure, we are able to prove that the scheme preserves the nonnegativity, which follows from a discrete minimum principle argument. It is well known that the maximum principle generally does not hold for systems of equations. Therefore, it is not a surprise that the upper bound comes only at a price: We need to assume that all diffusion coefficients D_i are the same. Under this assumption, $u_0 = 1 - \sum_{i=1}^{n} u_i$ solves a drift-diffusion equation for which the (discrete) maximum principle can be applied. In order to prove that the scheme satisfies an entropy-dissipation inequality and also to complete the convergence analysis of the scheme successfully, we need a stronger additional assumption: We assume that the drift terms, and therefore the coupling with the Poisson equation, can be neglected. This means that our main results are obtained for a simplified degenerate cross-diffusion system, no more corresponding to the initial ion transport model but still of mathematical interest. Nevertheless, the scheme we propose can be applied to the full ion transport model, and this is done in the last chapter of the thesis. Our analytical results are stated and proved for no-flux boundary conditions on $\partial\Omega$. Mixed Dirichlet-Neumann boundary conditions could be prescribed as well, but the proofs would become even more technical.

3.1.1 Notations and Assumptions

We summarize our general hypotheses on the data:

(H1') Domain: $\Omega \subset \mathbb{R}^d$ ($d = 2$ or $d = 3$) is an open, bounded, polygonal domain with $\partial\Omega = \Gamma_D \cup \Gamma_N \in C^{0,1}$, $\Gamma_D \cap \Gamma_N = \emptyset$.

(H2') Parameters: $T > 0$, $D_i > 0$, $\beta > 0$, and $z_i \in \mathbb{R}$, $i = 1, \ldots, n$.

(H3') Background charge: $f \in L^\infty(\Omega)$, $W_i \equiv 0$.

(H4') Initial and boundary data: $u_i^I \in L^\infty(\Omega)$, $\overline{u}_i \in H^1(\Omega)$ satisfy $u_i^I \geq 0$, $\overline{u}_i \geq 0$ and $1 - \sum_{i=1}^n u_i^I \geq 0$, $1 - \sum_{i=1}^n \overline{u}_i \geq 0$ in Ω for $i = 1, \ldots, n$, and $\overline{\Phi} \in H^1(\Omega) \cap L^\infty(\Omega)$.

Remark 3.1. *Note that there are some differences compared to Assumptions (H1)-(H4) stated in Section 2.2. Regarding the spatial domain, we restrict ourselves now to two or three dimensions and consider only polygons for the sake of discretization. We also assume that the external potentials W_i vanish. This is done only for simplicity and better readability of the proofs. Finally, we emphasize that we can allow for initial and boundary data that are nonnegative instead of strictly positive, as we do not use the transformation to entropy variables for the FV scheme.*

For our main results, we need additional technical assumptions:

(A1) $\partial\Omega = \Gamma_N$, i.e., we impose no-flux boundary conditions on the whole boundary.

(A2) The diffusion constants are equal, $D_i = D > 0$ for $i = 1, \ldots, n$.

(A3) The drift terms are set to zero, $\Phi \equiv 0$.

Remark 3.2 (Discussion of the assumptions)**.** *Assumption (A1) is supposed for simplicity only. Mixed Dirichlet-Neumann boundary conditions can be included in the analysis as was done on the continuous level in the previous chapter, but the proofs become even more technical. Mixed boundary conditions are chosen in the numerical experiments; therefore, the numerical scheme is defined for that case. Assumption (A2) is needed for the derivation of an upper bound for the solvent concentration. Indeed, when $D_i = D$ for all i, summing (1.6) over $i = 1, \ldots, n$ gives*

$$\partial_t u_0 = D \operatorname{div}(\nabla u_0 - u_0 v \nabla \Phi), \quad \text{where } v = \beta \sum_{i=1}^n z_i u_i.$$

On the discrete level, we replace $u_0 v \nabla \Phi$ by an upwind approximation. This allows us to apply the discrete maximum principle showing that $u_0 \geq 0$ and hence $u = (u_1, \ldots, u_n) \in \overline{\mathcal{D}}$ with $\mathcal{D}$ defined in (2.5). Finally, Assumption (A3) is needed to derive a discrete version of the entropy inequality. Without the drift terms, the upwinding value does not depend on the index of the species, which simplifies some expressions; see Remark 3.3.

For the definition of the numerical scheme for (1.6)-(1.10), we need to introduce a suitable discretization of the domain Ω and the interval $(0, T)$. For simplicity, we consider a uniform time discretization with time step $\triangle t > 0$, and we set $t^k = k \triangle t$ for $k = 1, \ldots, N$, where $T > 0$, $N \in \mathbb{N}$ are given and $\triangle t = T/N$. The domain Ω is discretized by a regular and admissible triangulation in the sense of [33, Definition 9.1]. The triangulation consists of a family $\mathcal{T}$ of open polygonal convex subsets of Ω (so-called cells), a family $\mathcal{E}$ of edges (or faces in three dimensions), and a family of points $(x_K)_{K \in \mathcal{T}}$ associated to the cells. The admissibility assumption implies that the straight line between two centers of neighboring

cells $\overline{x_K x_L}$ is orthogonal to the edge $\sigma = K|L$ between two cells K and L. The condition is satisfied by, for instance, triangular meshes whose triangles have angles smaller than $\pi/2$ [33, Examples 9.1] or Voronoi meshes [33, Example 9.2].

We assume that the family of edges $\mathcal{E}$ can be split into internal and external edges $\mathcal{E} = \mathcal{E}_{\text{int}} \cup \mathcal{E}_{\text{ext}}$ with $\mathcal{E}_{\text{int}} = \{\sigma \in \mathcal{E} : \sigma \subset \Omega\}$ and $\mathcal{E}_{\text{ext}} = \{\sigma \in \mathcal{E} : \sigma \subset \partial\Omega\}$. Each exterior edge is assumed to be an element of either the Dirichlet or Neumann boundary, i.e. $\mathcal{E}_{\text{ext}} = \mathcal{E}_{\text{ext}}^D \cup \mathcal{E}_{\text{ext}}^N$. For given $K \in \mathcal{T}$, we define the set $\mathcal{E}_K$ of the edges of K, which is the union of internal edges and edges on the Dirichlet or Neumann boundary, and we set $\mathcal{E}_{K,\text{int}} = \mathcal{E}_K \cap \mathcal{E}_{\text{int}}$.

The size of the mesh is defined by $h(\mathcal{T}) = \sup\{\text{diam}(K) : K \in \mathcal{T}\}$. For $\sigma \in \mathcal{E}_{\text{int}}$ with $\sigma = K|L$, we denote by $\text{d}_\sigma = \text{d}(x_K, x_L)$ the Euclidean distance between x_K and x_L, while for $\sigma \in \mathcal{E}_{\text{ext}}$, we set $\text{d}_\sigma = d(x_K, \sigma)$. For a given edge $\sigma \in \mathcal{E}$, the transmissibility coefficient is defined by

$$\tau_\sigma = \frac{\text{m}(\sigma)}{\text{d}_\sigma}, \tag{3.1}$$

where $\text{m}(\sigma)$ denotes the Lebesgue measure of σ.

We impose a regularity assumption on the mesh: There exists $\zeta > 0$ such that for all $K \in \mathcal{T}$ and $\sigma \in \mathcal{E}_K$, it holds that

$$\text{d}(x_K, \sigma) \geq \zeta \text{d}_\sigma. \tag{3.2}$$

This hypothesis is needed to apply discrete functional inequalities (see [8, 33]) and a discrete compactness theorem (see [39]).

It remains to introduce suitable function spaces for the numerical discretization. The space $\mathcal{H}_\mathcal{T}$ of piecewise constant functions is defined by

$$\mathcal{H}_\mathcal{T} = \left\{ v : \overline{\Omega} \to \mathbb{R} : \exists(v_K)_{K \in \mathcal{T}} \subset \mathbb{R}, \ v(x) = \sum_{K \in \mathcal{T}} v_K \mathbf{1}_K(x) \right\}.$$

The (squared) discrete H^1 norm on this space is given by

$$\|v\|_{1,\mathcal{T}}^2 = \sum_{\sigma = K|L \in \mathcal{E}_{\text{int}}} \tau_\sigma (v_K - v_L)^2 + \sum_{K \in \mathcal{T}} \text{m}(K) v_K^2. \tag{3.3}$$

The discrete H^{-1} norm is the dual norm with respect to the L^2 scalar product,

$$\|v\|_{-1,\mathcal{T}} = \sup\left\{ \int_\Omega vw \, dx : w \in \mathcal{H}_\mathcal{T}, \ \|w\|_{1,\mathcal{T}} = 1 \right\}. \tag{3.4}$$

Then

$$\left| \int_\Omega vw \, dx \right| \leq \|v\|_{-1,\mathcal{T}} \|w\|_{1,\mathcal{T}} \quad \text{for } v, w \in \mathcal{H}_\mathcal{T}.$$

Finally, we introduce the space $\mathcal{H}_{\mathcal{T},\triangle t}$ of piecewise constant in time functions with values in $\mathcal{H}_\mathcal{T}$,

$$\mathcal{H}_{\mathcal{T},\triangle t} = \left\{ v : \overline{\Omega} \times [0,T] \to \mathbb{R} : \exists(v^k)_{k=1,\dots,N} \subset \mathcal{H}_\mathcal{T}, \ v(x,t) = \sum_{k=1}^N v^k(x) \mathbf{1}_{(t^{k-1}, t^k)}(t) \right\},$$

equipped with the discrete $L^2(0, T; H^1(\Omega))$ norm

$$\|v\|_{1,\mathcal{T},\triangle t} = \left(\sum_{k=1}^{N} \triangle t \|v^k\|_{1,\mathcal{T}}^2 \right)^{1/2}.$$

For the numerical scheme, we introduce some further definitions. Let $u_i \in \mathcal{H}_\mathcal{T}$ with values $\overline{u}_{i,\sigma}$ on the Dirichlet boundary $(i = 1, \ldots, n)$. Then we introduce

$$\mathrm{D}_{K,\sigma}(u_i) = u_{i,K,\sigma} - u_{i,K}, \tag{3.5}$$

$$\text{where} \quad u_{i,K,\sigma} = \begin{cases} u_{i,L} & \text{for } \sigma \in \mathcal{E}_{\text{int}}, \ \sigma = K|L, \\ \overline{u}_{i,\sigma} & \text{for } \sigma \in \mathcal{E}_{\text{ext},K}^D, \\ u_{i,K} & \text{for } \sigma \in \mathcal{E}_{\text{ext},K}^N, \end{cases} \qquad \overline{u}_{i,\sigma} = \frac{1}{\mathrm{m}(\sigma)} \int_\sigma \overline{u}_i \, ds.$$

The numerical fluxes $\mathcal{F}_{K,\sigma}$ should be consistent approximations to the exact fluxes through the edges $\int_\sigma \mathcal{F} \cdot \nu ds$. We impose the conservation of the numerical fluxes $\mathcal{F}_{K,\sigma} + \mathcal{F}_{L,\sigma} = 0$ for edges $\sigma = K|L$, requiring that they vanish on the Neumann boundary edges, $\mathcal{F}_{K,\sigma} = 0$ for $\sigma \in \mathcal{E}_{\text{ext},K}^N$. Then the discrete integration-by-parts formula becomes for $u \in \mathcal{H}_\mathcal{T}$

$$\sum_{K \in \mathcal{T}} \sum_{\sigma \in \mathcal{E}_K} \mathcal{F}_{K,\sigma} u_K = - \sum_{\sigma \in \mathcal{E}} \mathcal{F}_{K,\sigma} \mathrm{D}_{K,\sigma}(u) + \sum_{\sigma \in \mathcal{E}_{\text{ext}}^D} \mathcal{F}_{K,\sigma} u_{K,\sigma}.$$

When $\partial\Omega = \Gamma_N$, this formula simplifies to

$$\sum_{K \in \mathcal{T}} \sum_{\sigma \in \mathcal{E}_K} \mathcal{F}_{K,\sigma} u_K = \sum_{\sigma = K|L \in \mathcal{E}_{\text{int}}} \mathcal{F}_{K,\sigma}(u_K - u_L). \tag{3.6}$$

3.1.2 Definition of the Scheme

We need to approximate the initial, boundary, and given functions on the elements $K \in \mathcal{T}$ and edges $\sigma \in \mathcal{E}$:

$$u_{i,K}^I = \frac{1}{\mathrm{m}(K)} \int_K u_i^I(x) \, dx, \qquad\qquad f_K = \frac{1}{\mathrm{m}(K)} \int_K f(x) \, dx,$$

$$\overline{u}_{i,\sigma} = \frac{1}{\mathrm{m}(\sigma)} \int_\sigma \overline{u}_i \, ds, \qquad\qquad \overline{\Phi}_\sigma = \frac{1}{\mathrm{m}(\sigma)} \int_\sigma \overline{\Phi} \, ds,$$

and we set $u_{0,K}^I = 1 - \sum_{i=1}^n u_{i,K}^I$ and $\overline{u}_{0,\sigma} = 1 - \sum_{i=1}^n \overline{u}_{i,\sigma}$.

The numerical scheme is as follows. Let $K \in \mathcal{T}$, $k \in \{1, \ldots, N\}$, $i = 1, \ldots, n$, and $u_{i,K}^{k-1} \geq 0$ be given. Then the values $u_{i,K}^k$ are determined by the implicit Euler scheme

$$\mathrm{m}(K) \frac{u_{i,K}^k - u_{i,K}^{k-1}}{\triangle t} + \sum_{\sigma \in \mathcal{E}_K} \mathcal{F}_{i,K,\sigma}^k = 0, \tag{3.7}$$

where the fluxes $\mathcal{F}_{i,K,\sigma}^k$ are given by the upwind scheme

$$\mathcal{F}_{i,K,\sigma}^k = -\tau_\sigma D_i \Big(u_{0,\sigma}^k \mathrm{D}_{K,\sigma}(u_i^k) - u_{i,\sigma}^k \big(\mathrm{D}_{K,\sigma}(u_0^k) - \widehat{u}_{0,\sigma,i}^k \beta z_i \mathrm{D}_{K,\sigma}(\Phi^k) \big) \Big), \tag{3.8}$$

where τ_σ is defined in (3.1),

$$u_{0,K}^k = 1 - \sum_{i=1}^n u_{i,K}^k, \quad u_{0,\sigma}^k = \max\{u_{0,K}^k, u_{0,L}^k\}, \tag{3.9}$$

$$u_{i,\sigma}^k = \begin{cases} u_{i,K}^k & \text{if } \mathcal{V}_{i,K,\sigma}^k \geq 0, \\ u_{i,K,\sigma}^k & \text{if } \mathcal{V}_{i,K,\sigma}^k < 0, \end{cases}, \quad \widehat{u}_{0,\sigma,i}^k = \begin{cases} u_{0,K}^k & \text{if } z_i \mathrm{D}_{K,\sigma}(\Phi^k) \geq 0, \\ u_{0,K,\sigma}^k & \text{if } z_i \mathrm{D}_{K,\sigma}(\Phi^k) < 0, \end{cases}, \tag{3.10}$$

and $\mathcal{V}_{i,K,\sigma}^k$ is the "drift part" of the flux,

$$\mathcal{V}_{i,K,\sigma}^k = \mathrm{D}_{K,\sigma}(u_0^k) - \widehat{u}_{0,\sigma,i}^k \beta z_i \mathrm{D}_{K,\sigma}(\Phi^k) \tag{3.11}$$

for $i = 1, \ldots, n$. Observe that we employed a double upwinding: one related to the electric potential, defining $\widehat{u}_{0,\sigma,i}^k$, and another one related to the drift part of the flux, $\mathcal{V}_{i,K,\sigma}^k$. The potential is computed via

$$-\lambda^2 \sum_{\sigma \in \mathcal{E}_K} \tau_\sigma \mathrm{D}_{K,\sigma}(\Phi^k) = \mathrm{m}(K) \left(\sum_{i=1}^n z_i u_{i,K}^k + f_K \right). \tag{3.12}$$

We recall that the numerical boundary conditions are given by $\overline{u}_{i,\sigma}$ and $\overline{\Phi}_\sigma$ for $\sigma \in \mathcal{E}_{\mathrm{ext}}^D$.

We denote by $u_{i,\mathcal{T},\triangle t}$, $\Phi_{\mathcal{T},\triangle t}$ the functions in $\mathcal{H}_{\mathcal{T},\triangle t}$ associated to the values $u_{i,K}^k$ and Φ_K^k, respectively. Moreover, when dealing with a sequence of meshes $(\mathcal{T}_m)_m$ and a sequence of time steps $(\triangle t_m)_m$, we set $u_{i,m} = u_{i,\mathcal{T}_m,\triangle t_m}$, $\Phi_m = \Phi_{\mathcal{T}_m,\triangle t_m}$.

Remark 3.3 (Simplified numerical scheme). *When Assumptions (A1)-(A3) hold, the numerical scheme simplifies to*

$$\mathrm{m}(K) \frac{u_{i,K}^k - u_{i,K}^{k-1}}{\triangle t} + \sum_{\sigma \in \mathcal{E}_{K,int}} \mathcal{F}_{i,K,\sigma}^k = 0, \tag{3.13}$$

$$\mathcal{F}_{i,K,\sigma}^k = -\tau_\sigma D \Big(u_{0,\sigma}^k \big(u_{i,L}^k - u_{i,K}^k \big) - u_{i,\sigma}^k \big(u_{0,L}^k - u_{0,K}^k \big) \Big), \tag{3.14}$$

where $u_{0,K}^k$ and $u_{0,\sigma}^k$ are defined in (3.9), and the definition of $u_{i,\sigma}^k$ simplifies to

$$u_{i,\sigma}^k = \begin{cases} u_{i,K}^k & \text{if } u_{0,K}^k - u_{0,L}^k \leq 0, \\ u_{i,L}^k & \text{if } u_{0,K}^k - u_{0,L}^k > 0. \end{cases}$$

In the definition of $u_{i,\sigma}^k$, the upwinding value does not depend on i anymore such that

$$\sum_{i=0}^n u_{i,\sigma}^k = 1 + \max\{u_{0,K}^k, u_{0,L}^k\} - \min\{u_{0,K}^k, u_{0,L}^k\} = 1 + |u_{0,K}^k - u_{0,L}^k|. \tag{3.15}$$

This property is needed to control the sum $\sum_{i=1}^n u_{i,\sigma}^k$ from below in the proof of the discrete entropy inequality; see (3.27). Finally, we are able to reformulate the discrete fluxes such that we obtain a discrete version of the reformulation of the fluxes in the weak formulation (2.6) (without the drift part):

$$\mathcal{F}_{i,K,\sigma} = \tau_\sigma D \left\{ u_{0,\sigma}^{1/2} \big(u_{0,K}^{1/2} u_{i,K} - u_{0,L}^{1/2} u_{i,L} \big) - u_{i,\sigma} \big(u_{0,K}^{1/2} - u_{0,L}^{1/2} \big) \left(u_{0,\sigma}^{1/2} + 2 \frac{u_{0,K}^{1/2} + u_{0,L}^{1/2}}{2} \right) \right\}. \tag{3.16}$$

This formulation is needed in the convergence analysis.

3.1.3 Main Results

Since our scheme is implicit and nonlinear, the existence of an approximate solution is nontrivial. Therefore, our first result concerns the well-posedness of the numerical scheme.

Theorem 3.4 (Existence and uniqueness of solutions)**.** *Let (H1')-(H4') and (A2) hold. Then there exists a solution* (u, Φ) *to scheme (3.7)-(3.12) satisfying* $u^k \in \overline{\mathcal{D}}$ *and, if the initial data lie in* $\mathcal{D}$, $u^k \in \mathcal{D}$. *If additionally Assumptions (A1) and (A3) hold, the solution is unique.*

Assumption (A2) is needed to show that $u_0^k = 1 - \sum_{i=1}^n u_i^k$ is nonnegative. Indeed, summing (3.7) and (3.8) over $i = 1, \ldots, n$, we obtain

$$\mathrm{m}(K) \frac{u_{0,K}^k - u_{0,K}^{k-1}}{\triangle t} = - \sum_{\sigma \in \mathcal{E}_K} \tau_\sigma \left(u_{0,\sigma}^k \mathrm{D}_{K,\sigma} \left(\sum_{i=1}^n D_i u_i^k \right) - \sum_{i=1}^n D_i u_{i,\sigma}^k \mathcal{V}_{i,K,\sigma}^k \right).$$

Under Assumption (A2), it follows that $\sum_{i=1}^n D_i u_{i,K}^k = D(1 - u_{0,K}^k)$, and we can apply the discrete minimum principle, which then implies an L^∞ bound for u_i^k. This bound allows us to apply a topological degree argument; see [25, 31]. For the uniqueness proof, we additionally need Assumption (A3), so that we only need to deal with the simplified scheme when using the entropy method of Gajewski [36]. The idea is to prove first the uniqueness of u_0^k, which solves a discrete nonlinear equation, and then to show the uniqueness of u_i^k for $i = 1, \ldots, n$ by introducing a semimetric $d(u^k, v^k)$ for two solutions $u^k = (u_1^k, \ldots, u_n^k)$ and $v^k = (v_1^k, \ldots, v_n^k)$ and showing that it is monotone in k, such that a discrete Gronwall argument implies that $u^k = v^k$.

The second result shows that the scheme preserves a discrete version of the entropy inequality.

Theorem 3.5 (Discrete entropy inequality)**.** *Let Assumptions (H1')-(H4') and (A1)-(A3) hold. Then the solution to scheme (3.13)-(3.14) constructed in Theorem 3.4 satisfies the discrete entropy inequality*

$$\frac{\mathcal{H}^k - \mathcal{H}^{k-1}}{\triangle t} + \mathcal{I}^k \le 0, \tag{3.17}$$

with the discrete entropy

$$\mathcal{H}^k = \sum_{K \in \mathcal{T}} \mathrm{m}(K) \sum_{i=0}^n \left(u_{i,K}^k (\log u_{i,K}^k - 1) + 1 \right) \tag{3.18}$$

and the discrete entropy production

$$\mathcal{I}^k = D \sum_{\sigma = K|L \in \mathcal{E}_{int}} \tau_\sigma \left(4 \sum_{i=1}^n u_{0,\sigma}^k \left((u_{i,K}^k)^{1/2} - (u_{i,L}^k)^{1/2} \right)^2 \right.$$
$$\left. + 4 \left((u_{0,K}^k)^{1/2} - (u_{0,L}^k)^{1/2} \right)^2 + \left(u_{0,K}^k - u_{0,L}^k \right)^2 \right).$$

Assumption (A3) is required to estimate the expression $\sum_{i=1}^{n} u_{i,\sigma}^k$. In the continuous case, this sum equals $1 - u_0$. On the discrete level, this identity cannot be expected since the value of $u_{i,\sigma}^k$ depends on the upwinding value; see (3.10). If the drift part vanishes, the upwinding value does not depend on i, as mentioned in Remark 3.3, and we can derive the estimate $\sum_{i=1}^{n} u_{i,\sigma}^k \geq 1 - u_{0,\sigma}^k$; see Section 3.1.5. Note that the entropy production $\mathcal{I}^k$ is the discrete counterpart of (2.19).

The main result of this section is the convergence of the approximate solutions to a solution to the continuous cross-diffusion system.

Theorem 3.6 (Convergence of the approximate solution). *Let (H1')-(H4') and (A1)-(A3) hold and let $(\mathcal{T}_m)$ and $(\triangle t_m)$ be sequences of admissible meshes and time steps, respectively, such that $h(\mathcal{T}_m) \to 0$ and $\triangle t_m \to 0$ as $m \to \infty$. Let $(u_{0,m}, \ldots, u_{n,m})$ be the solution to (3.13)-(3.14) constructed in Theorem 3.4. Then there exist functions u_0, $u = (u_1, \ldots, u_n)$ satisfying $u(x,t) \in \overline{\mathcal{D}}$,*

$$u_0^{1/2}, \ u_0^{1/2}u_i \in L^2(0,T;H^1(\Omega)), \quad i = 1, \ldots, n,$$
$$u_{0,m}^{1/2} \to u_0^{1/2}, \ u_{0,m}^{1/2}u_{i,m} \to u_0^{1/2}u_i \quad \textit{strongly in } L^2(\Omega \times (0,T)),$$

where u is a weak solution to (1.6), (1.8)-(1.10) (with $\Gamma_N = \partial\Omega$), i.e., for all $\phi \in C_0^\infty(\overline{\Omega} \times [0,T))$ and $i = 1, \ldots, n$,

$$\int_0^T \int_\Omega u_i \partial_t \phi \, dx \, dt + \int_\Omega u_i^I \phi(\cdot, 0) \, dx = D \int_0^T \int_\Omega u_0^{1/2}\big(\nabla(u_0^{1/2}u_i) - 3u_i \nabla u_0^{1/2}\big) \cdot \nabla \phi \, dx \, dt. \tag{3.19}$$

The compactness of the concentrations follows from the discrete gradient estimates derived from the entropy inequality (3.17), for which we need Assumption (A3). By the discrete Aubin–Lions lemma (Lemma 5.5 in the Appendix), we conclude the strong convergence of the sequence $(u_{0,m}^{1/2})$. The difficult part is to show the strong convergence of $(u_{0,m}^{1/2}u_{i,m})$, since there is no control on the discrete gradient of $u_{i,m}$. The idea is to apply a discrete Aubin–Lions lemma of "degenerate" type, proved in Lemma 5.6 in the Appendix.

3.1.4 Existence and Uniqueness of Approximate Solutions

L^∞ bounds and existence of solutions

In order to prove the existence of solutions to (3.7)-(3.12), we first consider a truncated problem. This means that we truncate the expressions in (3.10); more precisely, we consider scheme (3.7), (3.8), and (3.12) with

$$u_{0,K}^k = 1 - \sum_{i=1}^{n}(u_{i,K}^k)^+, \quad u_{0,\sigma}^k = \max\{0, u_{0,K}^k, u_{0,K,\sigma}^k\},$$

$$\widehat{u}_{0,\sigma,i}^k = \begin{cases} (u_{0,K}^k)^+ & \text{if } z_i \mathrm{D}_{K,\sigma}(\Phi^k) \geq 0, \\ (u_{0,K,\sigma}^k)^+ & \text{if } z_i \mathrm{D}_{K,\sigma}(\Phi^k) < 0, \end{cases}$$

$$u_{i,\sigma}^k = \begin{cases} (u_{i,K}^k)^+ & \text{if } \mathcal{V}_{i,K,\sigma}^k \geq 0, \\ (u_{i,K,\sigma}^k)^+ & \text{if } \mathcal{V}_{i,K,\sigma}^k < 0, \end{cases} \tag{3.20}$$

where $z^+ = \max\{0, z\}$ for $z \in \mathbb{R}$ and $i = 1, \ldots, n$. We show that this truncation is, in fact, not needed if the initial data are nonnegative. In the following let (H1')-(H4') hold.

Lemma 3.7 (Nonnegativity of u_i^k)**.** *Let* (u, Φ) *be a solution to* (3.7)*,* (3.8)*,* (3.12)*, and* (3.20)*. Then* $u_{i,K}^k \geq 0$ *for all* $K \in \mathcal{T}$*,* $k \in \{1, \ldots, N\}$*, and* $i = 1, \ldots, n$*. If* $u_i^I > 0$ *and* $\overline{u}_i > 0$ *then also* $u_{i,K}^k > 0$ *for all* $K \in \mathcal{T}$*,* $k \in \{1, \ldots, N\}$*.*

Proof. We proceed by induction. For $k = 0$, the nonnegativity holds because of our assumptions on the initial data. Assume that $u_{i,L}^{k-1} \geq 0$ for all $L \in \mathcal{T}$. Then let $u_{i,K}^k = \min\{u_{i,L}^k : L \in \mathcal{T}\}$ for some $K \in \mathcal{T}$ and assume that $u_{i,K}^k < 0$. The scheme writes as

$$\mathrm{m}(K)\frac{u_{i,K}^k - u_{i,K}^{k-1}}{\triangle t} = \sum_{\sigma \in \mathcal{E}_K} \tau_\sigma D_i\big(u_{0,\sigma}^k \mathrm{D}_{K,\sigma}(u_i^k) - u_{i,\sigma}^k \mathcal{V}_{i,K,\sigma}^k\big). \tag{3.21}$$

By assumption, $\mathrm{D}_{K,\sigma}(u_i^k) \geq 0$. If $\mathcal{V}_{i,K\sigma}^k \geq 0$, we have $-u_{i,\sigma}^k \mathcal{V}_{i,K,\sigma}^k = -(u_{i,K})^+ \mathcal{V}_{i,K,\sigma} = 0$ and if $\mathcal{V}_{i,K,\sigma}^k < 0$, it follows that $-u_{i,\sigma}^k \mathcal{V}_{i,K,\sigma}^k = -(u_{i,K,\sigma}^k)^+ \mathcal{V}_{i,K,\sigma}^k \geq 0$. Hence, the right-hand side of (3.21) is nonnegative. However, the left-hand side is negative, which is a contradiction. We infer that $u_{i,K}^k \geq 0$ and consequently, $u_{i,L}^k \geq 0$ for all $L \in \mathcal{T}$. When the initial data are positive, similar arguments show the positivity of $u_{i,L}^k$ for $L \in \mathcal{T}$. $\qquad\square$

We are able to show the nonnegativity of $u_{0,K}^k = 1 - \sum_{i=1}^n u_{i,K}^k$ only if the diffusion coefficients are the same. The reason is that we derive an equation for $u_{0,K}^k$ by summing (3.7) for $i = 1, \ldots, n$, and this gives an equation for $u_{0,K}^k$ only if $D_i = D$ for all $i = 1, \ldots, n$.

Lemma 3.8 (Nonnegativity of u_0^k)**.** *Let Assumption (A2) hold and let* (u, Φ) *be a solution to* (3.7)*,* (3.8)*,* (3.12)*, and* (3.20)*. Then* $u_{0,K}^k \geq 0$ *for all* $K \in \mathcal{T}$*,* $k \in \{1, \ldots, N\}$*. If* $u_0^I > 0$ *and* $\overline{u}_i > 0$ *then also* $u_{0,K}^k > 0$ *for all* $K \in \mathcal{T}$*,* $k \in \{1, \ldots, N\}$*.*

Proof. Again, we proceed by induction. The case $k = 0$ follows from the assumptions. Assume that $u_{0,L}^{k-1} \geq 0$ for all $L \in \mathcal{T}$. Then let $u_{0,K}^k = \min\{u_{0,L}^k : L \in \mathcal{T}\}$ for some $K \in \mathcal{T}$ and assume that $u_{0,K}^k < 0$. Summing equations (3.7) from $i = 1, \ldots, n$, we obtain

$$\mathrm{m}(K)\frac{u_{0,K}^k - u_{0,K}^{k-1}}{\triangle t} = D \sum_{\sigma \in \mathcal{E}_K} \tau_\sigma \Big(u_{0,\sigma}^k \mathrm{D}_{K,\sigma}(u_0^k) + \sum_{i=1}^n u_{i,\sigma}^k \big(\mathrm{D}_{K,\sigma}(u_0^k) - \beta z_i \widehat{u}_{0,\sigma,i}^k \mathrm{D}_{K,\sigma}(\Phi^k)\big)\Big)$$

$$\geq -D \sum_{\sigma \in \mathcal{E}_K} \tau_\sigma \sum_{i=1}^n \beta z_i \widehat{u}_{0,\sigma,i}^k \mathrm{D}_{K,\sigma}(\Phi^k), \tag{3.22}$$

since $u_{0,\sigma}^k \geq 0$ and $u_{i,\sigma}^k \geq 0$ by construction and $\mathrm{D}_{K,\sigma}(u_0^k) \geq 0$ because of the minimality property of $u_{0,K}^k$. The remaining expression is nonnegative:

$$-\widehat{u}_{0,\sigma_i}^k z_i \mathrm{D}_{K,\sigma}(\Phi^k) = \begin{cases} -(u_{0,K}^k)^+ z_i \mathrm{D}_{K,\sigma}(\Phi^k) = 0 & \text{if } z_i \mathrm{D}_{K,\sigma}(\Phi^k) \geq 0, \\ -(u_{0,L}^k)^+ z_i \mathrm{D}_{K,\sigma}(\Phi^k) \geq 0 & \text{if } z_i \mathrm{D}_{K,\sigma}(\Phi^k) < 0. \end{cases}$$

However, the left-hand side of (3.22) is negative by induction hypothesis, which gives a contradiction. $\qquad\square$

Lemmas 3.7 and 3.8 imply that we may remove the truncation in (3.20). Moreover, by definition, we have $1 - \sum_{i=1}^{n} u_{i,K}^{k} = u_{0,K}^{k} \geq 0$ such that $u_K^k = (u_{1,K}^k, \ldots, u_{n,K}^k) \in \overline{\mathcal{D}}$ or, if the initial and boundary data are positive, $u_K^k \in \mathcal{D}$.

Proposition 3.9 (Existence for the numerical scheme)**.** *Let Assumption (A2) hold. Then the scheme* (3.7)-(3.12) *has a solution* (u, Φ) *which satisfies* $u_K^k \in \overline{\mathcal{D}}$ *for all* $K \in \mathcal{T}$ *and* $k \in \mathbb{N}$.

Proof. We argue by induction. For $k = 0$, we have $u_K^0 \in \overline{\mathcal{D}}$ by assumption. The function Φ^0 is uniquely determined by scheme (3.12), as this is a linear system of equations with positive definite matrix. Assume the existence of a solution (u^{k-1}, Φ^{k-1}) with $u_K^{k-1} \in \overline{\mathcal{D}}$. Let $m \in \mathbb{N}$ be the product of the number of species n and the number of cells $K \in \mathcal{T}$. For given $K \in \mathcal{T}$ and $i = 1, \ldots, n$, we define the function $F_{i,K} : \mathbb{R}^m \times [0, 1] \to \mathbb{R}$ by

$$
F_{i,K}(u, \rho) = \mathrm{m}(K) \frac{u_{i,K} - u_{i,K}^{k-1}}{\triangle t}
$$
$$
- \rho D \sum_{\sigma \in \mathcal{E}_K} \tau_\sigma \Big(u_{0,\sigma} \mathrm{D}_{K,\sigma}(u_i) - u_{i,\sigma} \big(\mathrm{D}_{K,\sigma}(u_0) - \widehat{u}_{0,\sigma,i} \beta z_i \mathrm{D}_{K,\sigma}(\Phi) \big) \Big).
$$

where $u_{0,K}$, $u_{i,\sigma}$, $u_{0,\sigma}$, and $\widehat{u}_{0,\sigma_i}$ are defined in (3.20), and Φ is uniquely determined by (3.12). Let $F = (F_{i,K})_{i=1,\ldots,n,\, K \in \mathcal{T}}$. Then $F : \mathbb{R}^m \times [0, 1] \to \mathbb{R}^m$ is a continuous function. We wish to apply the fixed-point theorem of [34, Theorem 5.1]. For this, we need to verify three assumptions:

- The function $u \mapsto F_{i,K}(u, 0) = \mathrm{m}(K)(u_{i,K} - u_{i,K}^{k-1})/\triangle t$ is affine.

- We have proved above that any solution to $F(u, 1) = 0$ satisfies $u \in \mathcal{D}$ or $\|u\|_\infty < 2$. A similar proof shows that any solution to $F(u, \rho) = 0$ with $\rho \in (0, 1)$ satisfies $\|u\|_\infty < 2$, too.

- The equation $F(u, 0) = 0$ has the unique solution $u = u^{k-1}$ and consequently, $\|u\|_\infty = \|u^{k-1}\|_\infty < 2$.

We infer the existence of a solution u^k to $F(u^k, 1) = 0$ satisfying $\|u^k\|_\infty < 2$. In fact, by Lemmas 3.7 and 3.8, we find that $u^k \in \overline{\mathcal{D}}$. Hence, u^k solves the original scheme (3.7)-(3.12). $\qquad \square$

Uniqueness of solutions

The proof of Theorem 3.4 is completed when we show the uniqueness of solutions to scheme (3.7)-(3.12) under the additional conditions (A1) and (A3). Recall that in this case, the scheme is given by (3.13)-(3.14),

Step 1: uniqueness for u_0. If $k = 0$, the solution is uniquely determined by the initial condition. Assume that u_0^{k-1} is given. Thanks to Assumptions (A2)-(A3), the sum of (3.13)-(3.14) for $i = 1, \ldots, n$ gives an equation for $u_0^k = 1 - \sum_{i=1}^{n} u_i^k$ (in the following,

we omit the superindices k):

$$\mathrm{m}(K)\frac{u_{0,K} - u_{0,K}^{k-1}}{\triangle t} = -D \sum_{\sigma \in \mathcal{E}_{K,\mathrm{int}}} \tau_\sigma (u_{0,K} - u_{0,L})\left(u_{0,\sigma} + \sum_{i=1}^n u_{i,\sigma}\right)$$

$$= -D \sum_{\sigma \in \mathcal{E}_{K,\mathrm{int}}} \tau_\sigma (u_{0,K} - u_{0,L})\big(1 + |u_{0,K} - u_{0,L}|\big),$$

where we used (3.15) in the last step.

Let u_0 and v_0 be two solutions to the previous equation and set $w_0 := u_0 - v_0$. Then w_0 solves

$$0 = \mathrm{m}(K)\frac{w_{0,K}}{\triangle t} + D \sum_{\sigma \in \mathcal{E}_{K,\mathrm{int}}} \tau_\sigma (w_{0,K} - w_{0,L})$$

$$+ D \sum_{\sigma \in \mathcal{E}_{K,\mathrm{int}}} \tau_\sigma \big((u_{0,K} - u_{0,L})|u_{0,K} - u_{0,L}| - (v_{0,K} - v_{0,L})|v_{0,K} - v_{0,L}|\big).$$

We multiply this equation by $w_{0,K}/D$, sum over $K \in \mathcal{T}$, and use discrete integration by parts (3.6):

$$0 = \sum_{K \in \mathcal{T}} \frac{\mathrm{m}(K)}{D}\frac{w_{0,K}^2}{\triangle t} + \sum_{\sigma = K|L \in \mathcal{E}_{\mathrm{int}}} \tau_\sigma (w_{0,K} - w_{0,L})^2$$

$$+ \sum_{\sigma = K|L \in \mathcal{E}_{\mathrm{int}}} \tau_\sigma \big((u_{0,K} - u_{0,L})|u_{0,K} - u_{0,L}| - (v_{0,K} - v_{0,L})|v_{0,K} - v_{0,L}|\big)(w_{0,K} - w_{0,L}).$$

The first two terms on the right-hand side are clearly nonnegative. We infer from the elementary inequality $(y|y| - z|z|)(y - z) \geq 0$ for $y, z \in \mathbb{R}$, which is a consequence of the monotonicity of $z \mapsto z|z|$, that the third term is nonnegative, too. Consequently, the three terms must vanish and this implies that $w_{0,K} = 0$ for all $K \in \mathcal{T}$. This shows the uniqueness for u_0.

Step 2: uniqueness for u_i. Let u_0 be the uniquely determined solution from the previous step and let $u^k = (u_1^k, \ldots, u_n^k)$ and $v^k = (v_1^k, \ldots, v_n^k)$ be two solutions to (3.7). Similarly as in [36], we introduce the semimetric

$$d_\varepsilon(u^k, v^k) = \sum_{K \in \mathcal{T}} \mathrm{m}(K) \sum_{i=1}^n H_1^\varepsilon(u_{i,K}^k, v_{i,K}^k), \quad \text{where}$$

$$H_1^\varepsilon(a, b) = h_\varepsilon(a) + h_\varepsilon(b) - 2h_\varepsilon\left(\frac{a + b}{2}\right)$$

and $h_\varepsilon(z) = (z + \varepsilon)(\log(z + \varepsilon) - 1) + 1$. The parameter $\varepsilon > 0$ is needed since $u_{i,K}^k$ or $v_{i,K}^k$ may vanish and then the logarithm of $u_{i,K}^k$ or $v_{i,K}^k$ may be undefined. The objective is to verify that $\lim_{\varepsilon \to 0} d_\varepsilon(u^k, v^k) = 0$ by estimating the discrete time derivative of the semimetric, implying that $u^k = v^k$.

First, we write

$$d_\varepsilon(u^k, v^k) - d_\varepsilon(u^{k-1}, v^{k-1}) = \sum_{K \in \mathcal{T}} \mathrm{m}(K) \sum_{i=1}^n \big(H_1^\varepsilon(u_{i,K}^k, v_{i,K}^k) - H_1^\varepsilon(u_{i,K}^{k-1}, v_{i,K}^{k-1})\big).$$

The function H_1^ε is convex since

$$D^2 H_1^\varepsilon(a,b) = \frac{1}{(a+\varepsilon)(b+\varepsilon)(a+b+2\varepsilon)} \begin{pmatrix} (b+\varepsilon)^2 & -(a+\varepsilon)(b+\varepsilon) \\ -(a+\varepsilon)(b+\varepsilon) & (a+\varepsilon)^2 \end{pmatrix}.$$

Therefore, a Taylor expansion of H_1^ε around $(u_{i,K}^k, v_{i,K}^k)$ leads to

$$\frac{1}{\triangle t}\big(d_\varepsilon(u^k, v^k) - d_\varepsilon(u^{k-1}, v^{k-1})\big)$$

$$\leq \sum_{K \in \mathcal{T}} \frac{\mathrm{m}(K)}{\triangle t} \sum_{i=1}^n \left\{ DH_1^\varepsilon(u_{i,K}^k, v_{i,K}^k)\left(\begin{pmatrix} u_{i,K}^k \\ v_{i,K}^k \end{pmatrix} - \begin{pmatrix} u_{i,K}^{k-1} \\ v_{i,K}^{k-1} \end{pmatrix} \right) \right\}$$

$$= \sum_{i=1}^n \sum_{K \in \mathcal{T}} \mathrm{m}(K) \frac{u_{i,K}^k - u_{i,K}^{k-1}}{\triangle t} \left(h_\varepsilon'(u_{i,K}^k) - h_\varepsilon'\left(\frac{u_{i,K}^k + v_{i,K}^k}{2} \right) \right)$$

$$+ \sum_{i=1}^n \sum_{K \in \mathcal{T}} \mathrm{m}(K) \frac{v_{i,K}^k - v_{i,K}^{k-1}}{\triangle t} \left(h_\varepsilon'(v_{i,K}^k) - h_\varepsilon'\left(\frac{u_{i,K}^k + v_{i,K}^k}{2} \right) \right).$$

We insert the scheme (3.13)-(3.14) and use discrete integration by parts:

$$\frac{1}{\triangle t}\big(d_\varepsilon(u^k, v^k) - d_\varepsilon(u^{k-1}, v^{k-1})\big) \leq S_1^k + S_2^k + \varepsilon S_3^k,$$

where

$$S_1^k = -D \sum_{i=1}^n \sum_{\sigma = K|L \in \mathcal{E}_{\mathrm{int}}} \tau_\sigma u_{0,\sigma}^k \bigg\{ \big(u_{i,K}^k - u_{i,L}^k\big)\big(\log(u_{i,K}^k + \varepsilon) - \log(u_{i,L}^k + \varepsilon)\big)$$

$$+ \big(v_{i,K}^k - v_{i,L}^k\big)\big(\log(v_{i,K}^k + \varepsilon) - \log(v_{i,L}^k + \varepsilon)\big)$$

$$- 2\left(\frac{u_{i,K}^k + v_{i,K}^k}{2} - \frac{u_{i,L}^k + v_{i,L}^k}{2} \right)\left(\log\left(\frac{u_{i,K}^k + v_{i,K}^k}{2} + \varepsilon \right) - \log\left(\frac{u_{i,L}^k + v_{i,L}^k}{2} + \varepsilon \right) \right) \bigg\},$$

$$S_2^k = D \sum_{i=1}^n \sum_{\sigma = K|L \in \mathcal{E}_{\mathrm{int}}} \tau_\sigma(u_{0,K}^k - u_{0,L}^k) \bigg\{ (u_{i,\sigma}^k + \varepsilon)\big(\log(u_{i,K}^k + \varepsilon) - \log(u_{i,L}^k + \varepsilon)\big)$$

$$+ (v_{i,\sigma}^k + \varepsilon)\big(\log(v_{i,K}^k + \varepsilon) - \log(v_{i,L}^k + \varepsilon)\big)$$

$$- 2\left(\frac{u_{i,\sigma}^k + v_{i,\sigma}^k}{2} + \varepsilon \right)\left(\log\left(\frac{u_{i,K}^k + v_{i,K}^k}{2} + \varepsilon \right) - \log\left(\frac{u_{i,L}^k + v_{i,L}^k}{2} + \varepsilon \right) \right) \bigg\},$$

$$S_3^k = -D \sum_{i=1}^n \sum_{\sigma = K|L \in \mathcal{E}_{\mathrm{int}}} \tau_\sigma(u_{0,K}^k - u_{0,L}^k) \bigg\{ \big(\log(u_{i,K}^k + \varepsilon) - \log(u_{i,L}^k + \varepsilon)\big)$$

$$+ \big(\log(v_{i,K}^k + \varepsilon) - \log(v_{i,L}^k + \varepsilon)\big)$$

$$- 2\left(\log\left(\frac{u_{i,K}^k + v_{i,K}^k}{2} + \varepsilon \right) - \log\left(\frac{u_{i,L}^k + v_{i,L}^k}{2} + \varepsilon \right) \right) \bigg\}.$$

We claim that $S_1^k \leq 0$ and $S_2^k \leq 0$. Indeed, with $H_2^\varepsilon(a,b) = (a-b)(\log(a+\varepsilon) - \log(b+\varepsilon))$, we can reformulate S_1^k as

$$S_1^k = -D \sum_{i=1}^n \sum_{\sigma=K|L\in\mathcal{E}_{\text{int}}} \tau_\sigma u_{0,\sigma}^k \left\{ H_2^\varepsilon\big(u_{i,K}^k, u_{i,L}^k\big) + H_2^\varepsilon\big(v_{i,K}^k, v_{i,L}^k\big) \right.$$
$$\left. - 2H_2^\varepsilon\left(\frac{u_{i,K}^k + v_{i,K}^k}{2}, \frac{u_{i,L}^k + v_{i,L}^k}{2}\right) \right\}.$$

The Hessian of H_2^ε,

$$D^2 H_2^\varepsilon(a,b) = \begin{pmatrix} \frac{a+b+2\varepsilon}{(a+\varepsilon)^2} & -\frac{a+b+2\varepsilon}{(a+\varepsilon)(b+\varepsilon)} \\ -\frac{a+b+2\varepsilon}{(a+\varepsilon)(b+\varepsilon)} & \frac{a+b+2\varepsilon}{(b+\varepsilon)^2} \end{pmatrix},$$

is positive semidefinite. Therefore, performing a Taylor expansion up to second order, we see that $S_1^k \leq 0$.

Next, we show that $S_2^k \leq 0$. For this, we assume without loss of generality for some fixed $\sigma = K|L$ that $u_{0,K}^k \leq u_{0,L}^k$. By definition of the scheme, $u_{i,\sigma}^k = u_{i,K}^k$ and $v_{i,\sigma}^k = v_{i,K}^k$. Set $H_3^\varepsilon(a,b) = (a+\varepsilon)(\log(a+\varepsilon) - \log(b+\varepsilon))$. The term in the curly bracket in S_2^k then takes the form

$$\big(u_{0,K}^k - u_{0,L}^k\big) \left\{ H_3^\varepsilon\big(u_{i,K}^k, u_{i,L}^k\big) + H_3^\varepsilon\big(v_{i,K}^k, v_{i,L}^k\big) - 2H_3^\varepsilon\left(\frac{u_{i,K}^k + v_{i,K}^k}{2}, \frac{u_{i,L}^k + v_{i,L}^k}{2}\right) \right\}. \quad (3.23)$$

The Hessian of H_3^ε,

$$D^2 H_3^\varepsilon(a,b) = \begin{pmatrix} \frac{1}{a+\varepsilon} & -\frac{1}{b+\varepsilon} \\ -\frac{1}{b+\varepsilon} & \frac{a+\varepsilon}{(b+\varepsilon)^2} \end{pmatrix},$$

is also positive semidefinite, showing that (3.23) is nonpositive as $u_{0,K}^k - u_{0,L}^k \leq 0$. If $u_{0,K}^k > u_{0,L}^k$, both factors of the product (3.23) change their sign, so that we arrive at the same conclusion. Hence, $S_2^k \leq 0$. We conclude that

$$d_\varepsilon(u^k, v^k) - d_\varepsilon(u^{k-1}, v^{k-1}) \leq \varepsilon \triangle t S_3^k.$$

Since $d_\varepsilon(u^0, v^0) = 0$, we find after resolving the recursion that

$$d_\varepsilon(u^k, v^k) \leq \varepsilon \triangle t \sum_{\ell=1}^k S_3^\ell.$$

As the densities $u_{i,K}^\ell$ are nonnegative and bounded by 1 for all $K \in \mathcal{T}$, for all $\ell \geq 0$ and for all $1 \leq i \leq n$, it is clear that $\sum_{\ell=1}^k \varepsilon S_3^\ell \to 0$ when $\varepsilon \to 0$. Then, we may perform the limit $\varepsilon \to 0$ in the previous inequality yielding $d_\varepsilon(u^k, v^k) \to 0$. A Taylor expansion as in [76, end of Section 6] shows that $d_\varepsilon(u^k, v^k) \geq \frac{1}{8} \sum_{K\in\mathcal{T}} \text{m}(K) \sum_{i=1}^n (u_{i,K}^k - v_{i,K}^k)^2$. We infer that $u^k = v^k$, finishing the proof. $\qquad \square$

3.1.5 Discrete Entropy Inequality and Uniform Estimates

Discrete entropy inequality

First, we prove (3.17).

Proof of Theorem 3.5. The idea is to multiply (3.7) by $\log(u_{i,K}^{k,\varepsilon}/u_{0,K}^{k,\varepsilon})$, where we set $u_{i,K}^{k,\varepsilon} := u_{i,K}^{k} + \varepsilon$ for $i = 0, \ldots, n$. The regularization is necessary to avoid issues when the concentrations vanish. After this multiplication, we sum the equations over $i = 1, \ldots, n$ and $K \in \mathcal{T}$ and use discrete integration by parts to obtain

$$
\begin{aligned}
0 = & \sum_{K \in \mathcal{T}} \frac{\mathrm{m}(K)}{\triangle t D} \sum_{i=1}^{n} (u_{i,K}^{k} - u_{i,K}^{k-1}) \log \frac{u_{i,K}^{k,\varepsilon}}{u_{0,K}^{k,\varepsilon}} \\
& + \sum_{\sigma = K|L \in \mathcal{E}_{\mathrm{int}}} \tau_\sigma \Big(u_{0,\sigma}^{k} \big(u_{i,K}^{k} - u_{i,L}^{k} \big) - u_{i,\sigma}^{k} \big(u_{0,K}^{k} - u_{0,L}^{k} \big) \Big) \Big(\log \frac{u_{i,K}^{k,\varepsilon}}{u_{0,K}^{k,\varepsilon}} - \log \frac{u_{i,L}^{k,\varepsilon}}{u_{0,L}^{k,\varepsilon}} \Big) \quad (3.24) \\
= & A_0 + \sum_{\sigma = K|L \in \mathcal{E}_{\mathrm{int}}} \tau_\sigma (A_1 + A_2 + B_1 + B_2),
\end{aligned}
$$

where

$$
A_0 = \sum_{K \in \mathcal{T}} \frac{\mathrm{m}(K)}{\triangle t D} \sum_{i=0}^{n} (u_{i,K}^{k,\varepsilon} - u_{i,K}^{k-1,\varepsilon}) \log u_{i,K}^{k,\varepsilon},
$$

$$
A_1 = \sum_{i=1}^{n} u_{0,\sigma}^{k} \big(u_{i,K}^{k,\varepsilon} - u_{i,L}^{k,\varepsilon} \big) \big(\log u_{i,K}^{k,\varepsilon} - \log u_{i,L}^{k,\varepsilon} \big),
$$

$$
A_2 = - \sum_{i=1}^{n} u_{0,\sigma}^{k} \big(u_{i,K}^{k} - u_{i,L}^{k} \big) \big(\log u_{0,K}^{k,\varepsilon} - \log u_{0,L}^{k,\varepsilon} \big),
$$

$$
B_1 = - \sum_{i=1}^{n} u_{i,\sigma}^{k} \big(u_{0,K}^{k} - u_{0,L}^{k} \big) \big(\log u_{i,K}^{k,\varepsilon} - \log u_{i,L}^{k,\varepsilon} \big),
$$

$$
B_2 = \sum_{i=1}^{n} u_{i,\sigma}^{k} \big(u_{0,K}^{k} - u_{0,L}^{k} \big) \big(\log u_{0,K}^{k,\varepsilon} - \log u_{0,L}^{k,\varepsilon} \big).
$$

The convexity of $h(z) = z(\log z - 1) + 1$ implies the inequality $h(u) - h(v) \le h'(u)(u - v)$ for all $u, v \in \mathbb{R}$. Consequently,

$$
A_0 \ge \sum_{K \in \mathcal{T}} \frac{\mathrm{m}(K)}{\triangle t D} \sum_{i=0}^{n} \big(u_{i,K}^{k,\varepsilon} (\log u_{i,K}^{k,\varepsilon} - 1) - u_{i,K}^{k-1,\varepsilon} (\log u_{i,K}^{k-1,\varepsilon} - 1) \big).
$$

In order to estimate the remaining terms, we recall two elementary inequalities. Let y, $z > 0$. Then, by the Cauchy–Schwarz inequality,

$$
\big(\sqrt{y} - \sqrt{z} \big)^2 = \Big(\int_z^y \frac{ds}{2\sqrt{s}} \Big)^2 \le \int_z^y \frac{ds}{4} \int_z^y \frac{ds}{s} = \frac{1}{4}(y - z)(\log y - \log z), \quad (3.25)
$$

and by the concavity of the logarithm,

$$y(\log y - \log z) \geq y - z \geq z(\log y - \log z). \tag{3.26}$$

Inequality (3.25) shows that

$$A_1 \geq 4 \sum_{i=1}^{n} u_{0,\sigma}^k \big((u_{i,K}^{k,\varepsilon})^{1/2} - (u_{i,L}^{k,\varepsilon})^{1/2} \big).$$

We use the definition of $u_{0,K}^k = 1 - \sum_{i=1}^{n} u_{i,K}^k$ in A_2 to find that

$$A_2 = u_{0,\sigma}^k \big(u_{0,K}^k - u_{0,L}^k \big) \big(\log u_{0,K}^{k,\varepsilon} - \log u_{0,L}^{k,\varepsilon} \big).$$

We rewrite B_1 by using the abbreviation $u_{i,\sigma}^{k,\varepsilon} = u_{i,\sigma}^k + \varepsilon$:

$$B_1 = - \sum_{i=1}^{n} u_{i,\sigma}^{k,\varepsilon} \big(u_{0,K}^k - u_{0,L}^k \big) \big(\log u_{i,K}^{k,\varepsilon} - \log u_{i,L}^{k,\varepsilon} \big)$$

$$+ \varepsilon \sum_{i=1}^{n} \big(u_{0,K}^k - u_{0,L}^k \big) \big(\log u_{i,K}^{k,\varepsilon} - \log u_{i,L}^{k,\varepsilon} \big)$$

$$=: B_{11} + \varepsilon B_{12}.$$

We apply inequality (3.26) to B_{11}. Indeed, if $u_{0,K}^k \leq u_{0,L}^k$, we have $u_{i,\sigma}^k = u_{i,K}^k$ and we use the first inequality in (3.26). If $u_{0,K}^k > u_{0,L}^k$ then $u_{i,\sigma}^k = u_{i,L}^k$ and we employ the second inequality in (3.26). In both cases, it follows that

$$B_{11} \geq - \sum_{i=1}^{n} \big(u_{0,K}^k - u_{0,L}^k \big) \big(u_{i,K}^{k,\varepsilon} - u_{i,L}^{k,\varepsilon} \big)$$

$$= - \big(u_{0,K}^k - u_{0,L}^k \big) \sum_{i=1}^{n} \big(u_{i,K}^{k,\varepsilon} - u_{i,L}^{k,\varepsilon} \big) = \big(u_{0,K}^k - u_{0,L}^k \big)^2.$$

Finally, we consider B_2. In view of Assumption (A3), equation (3.15) gives

$$\sum_{i=1}^{n} u_{i,\sigma}^k = 1 - \min\{u_{0,K}^k, u_{0,L}^k\} \geq 1 - u_{0,\sigma}^k, \tag{3.27}$$

and therefore, by (3.25),

$$B_2 \geq \big(1 - u_{0,\sigma}^k \big) \big(u_{0,K}^{k,\varepsilon} - u_{0,L}^{k,\varepsilon} \big) \big(\log u_{0,K}^{k,\varepsilon} - \log u_{0,L}^{k,\varepsilon} \big)$$

$$\geq 4 \big((u_{0,K}^{k,\varepsilon})^{1/2} - (u_{0,L}^{k,\varepsilon})^{1/2} \big)^2 - u_{0,\sigma}^k \big(u_{0,K}^k - u_{0,L}^k \big) \big(\log u_{0,K}^{k,\varepsilon} - \log u_{0,L}^{k,\varepsilon} \big).$$

The last expression cancels with A_2 such that

$$A_2 + B_2 \geq 4 \big((u_{0,K}^{k,\varepsilon})^{1/2} - (u_{0,L}^{k,\varepsilon})^{1/2} \big)^2.$$

Putting together the estimates for A_0, A_1, B_1, and $A_2 + B_2$, we deduce from (3.24) that

$$\sum_{K \in \mathcal{T}} \frac{\mathrm{m}(K)}{\triangle t} \sum_{i=0}^{n} u_{i,K}^{k,\varepsilon} (\log u_{i,K}^{k,\varepsilon} - 1) - \sum_{K \in \mathcal{T}} \frac{\mathrm{m}(K)}{\triangle t} \sum_{i=1}^{n} u_{i,K}^{k-1,\varepsilon} (\log u_{i,K}^{k-1,\varepsilon} - 1)$$

$$+ D \sum_{\sigma = K|L \in \mathcal{E}_{\mathrm{int}}} \tau_\sigma \left\{ 4 \sum_{i=1}^{n} u_{0,\sigma} \big((u_{i,K}^{k,\varepsilon})^{1/2} - (u_{i,L}^{k,\varepsilon})^{1/2} \big)^2 \right.$$

$$\left. + 4 \big((u_{0,K}^{k,\varepsilon})^{1/2} - (u_{0,L}^{k,\varepsilon})^{1/2} \big)^2 + \big(u_{0,K}^{k} - u_{0,L}^{k} \big)^2 \right\}$$

$$\leq -\varepsilon D \big(u_{0,K}^{k} - u_{0,L}^{k} \big) \sum_{i=1}^{n} \big(\log u_{i,K}^{k,\varepsilon} - \log u_{i,L}^{k,\varepsilon} \big).$$

Since the right-hand side converges to zero as $\varepsilon \to 0$, we infer that (3.17) holds. $\qquad\square$

A priori estimates

For the proof of the convergence result, we need estimates uniform in the mesh size $h(\mathcal{T})$ and time step $\triangle t$. The scheme provides uniform L^∞ bounds. Further bounds are derived from the discrete entropy inequality of Theorem 3.5. We introduce the discrete time derivative for functions $v \in \mathcal{H}_{\mathcal{T}, \triangle t}$ by

$$\partial_t^{\triangle t} v^k = \frac{v^k - v^{k-1}}{\triangle t}, \quad k = 1, \dots, N. \tag{3.28}$$

Lemma 3.10 (A priori estimates)**.** *Let (H1')-(H4') and (A1)-(A3) hold. The solution u to scheme (3.13)-(3.14) satisfies the following uniform estimates:*

$$\|u_0^{1/2}\|_{1,\mathcal{T},\triangle t} + \|u_0^{1/2} u_i\|_{1,\mathcal{T},\triangle t} \leq C, \quad i = 1, \dots, n, \tag{3.29}$$

$$\sum_{k=1}^{N} \triangle t \|\partial_t^{\triangle t} u_i^k\|_{-1,\mathcal{T}}^2 \leq C, \quad i = 0, \dots, n, \tag{3.30}$$

where the constant $C > 0$ is independent of the mesh $\mathcal{T}$ and time step size $\triangle t$.

Proof. We claim that estimates (3.29) follow from the discrete entropy inequality (3.17). Indeed, we sum (3.17) over $k = 1, \dots, N$ to obtain

$$\mathcal{H}^N + D \sum_{k=1}^{N} \triangle t \sum_{\sigma = K|L \in \mathcal{E}_{\mathrm{int}}} \tau_\sigma \left(4 \sum_{i=1}^{n} u_{0,\sigma}^{k} \big((u_{i,K}^{k})^{1/2} - (u_{i,L}^{k})^{1/2} \big)^2 \right.$$

$$\left. + 4 \big((u_{0,K}^{k})^{1/2} - (u_{0,L}^{k})^{1/2} \big)^2 + \big(u_{0,K}^{k} - u_{0,L}^{k} \big)^2 \right) \leq \mathcal{H}^0.$$

Since the entropy at time $t = 0$ is bounded independently of the discretization, we infer immediately the bound for $u_0^{1/2}$ in $\mathcal{H}_{\mathcal{T}, \triangle t}$. For the bound on $u_0^{1/2} u_i$ in $\mathcal{H}_{\mathcal{T}, \triangle t}$, we observe that

$$(u_{0,K}^{k})^{1/2} u_{i,K}^{k} - (u_{0,L}^{k})^{1/2} u_{i,L}^{k}$$
$$= u_{i,K}^{k} \big((u_{0,K}^{k})^{1/2} - (u_{0,L}^{k})^{1/2} \big) + (u_{0,L}^{k})^{1/2} \big((u_{i,K}^{k})^{1/2} + (u_{i,L}^{k})^{1/2} \big) \big((u_{i,K}^{k})^{1/2} - (u_{i,L}^{k})^{1/2} \big).$$

43

Therefore, together with the L^∞ bounds on u_i,

$$\sum_{\sigma=K|L\in\mathcal{E}_{\text{int}}} \tau_\sigma\big((u_{0,K}^k)^{1/2}u_{i,K}^k - (u_{0,L}^k)^{1/2}u_{i,L}^k\big)^2$$

$$\leq \sum_{\sigma=K|L\in\mathcal{E}_{\text{int}}} \tau_\sigma\big((u_{0,K}^k)^{1/2} - (u_{0,L}^k)^{1/2}\big)^2 + 2\sum_{\sigma=K|L\in\mathcal{E}_{\text{int}}} \tau_\sigma u_{0,\sigma}^k\big((u_{i,K}^k)^{1/2} - (u_{i,L}^k)^{1/2}\big)^2.$$

Then, summing over $k = 0, \ldots, N$ and using the estimates from the entropy inequality, we achieve the bound on $u_0^{1/2}u_i$.

It remains to prove estimate (3.30). To this end, let $\phi \in \mathcal{H}_\mathcal{T}$ be such that $\|\phi\|_{1,\mathcal{T}} = 1$ and let $k \in \{1, \ldots, N\}$ and $i \in \{1, \ldots, n\}$. We multiply the scheme (3.13) by Φ_K and we sum over $K \in \mathcal{T}$. Using successively discrete integration by parts, the rewriting of the numerical fluxes (3.16), the Cauchy–Schwarz inequality, and the L^∞ bounds on u_i, we compute

$$\sum_{K\in\mathcal{T}} \frac{\text{m}(K)}{\triangle t}\big(u_{i,K}^k - u_{i,K}^{k-1}\big)\phi_K$$

$$= D\sum_{\sigma=K|L\in\mathcal{E}_{\text{int}}} \tau_\sigma(u_{0,\sigma}^k)^{1/2}\big((u_{0,K}^k)^{1/2}u_{i,K}^k - (u_{0,L}^k)^{1/2}u_{i,L}^k\big)(\phi_K - \phi_L)$$

$$- D\sum_{\sigma=K|L\in\mathcal{E}_{\text{int}}} \tau_\sigma\big((u_{0,K}^k)^{1/2} - (u_{0,L}^k)^{1/2}\big)$$

$$\times u_{i,\sigma}^k\left((u_{0,\sigma}^k)^{1/2} + 2\frac{(u_{0,K}^k)^{1/2} + (u_{0,L}^k)^{1/2}}{2}\right)(\phi_K - \phi_L)$$

$$\leq D\bigg(\sum_{\sigma=K|L\in\mathcal{E}_{\text{int}}} \tau_\sigma\big((u_{0,K}^k)^{1/2}u_{i,K}^k - (u_{0,L}^k)^{1/2}u_{i,L}^k\big)^2\bigg)^{1/2}\bigg(\sum_{\sigma=K|L\in\mathcal{E}_{\text{int}}} \tau_\sigma(\phi_K - \phi_L)^2\bigg)^{1/2}$$

$$+ 3D\bigg(\sum_{\sigma=K|L\in\mathcal{E}_{\text{int}}} \tau_\sigma\big((u_{0,K}^k)^{1/2} - (u_{0,L}^k)^{1/2}\big)^2\bigg)^{1/2}\bigg(\sum_{\sigma=K|L\in\mathcal{E}_{\text{int}}} \tau_\sigma(\phi_K - \phi_L)^2\bigg)^{1/2}.$$

This shows that, for $i = 1, \ldots, n$,

$$\sum_{k=1}^N \triangle t\left\|\frac{u_i^k - u_i^{k-1}}{\triangle t}\right\|_{-1,\mathcal{T}}^2 \leq 2D^2\sum_{k=1}^N \triangle t\Big(\big\|(u_0^k)^{1/2}u_i^k\big\|_{1,\mathcal{T}}^2 + 9\big\|(u_0^k)^{1/2}\big\|_{1,\mathcal{T}}^2\Big) \leq C,$$

as a consequence of (3.29). The estimate for $\triangle t^{-1}(u_0^k - u_0^{k-1}) = -\triangle t^{-1}\sum_{i=1}^n(u_i^k - u_i^{k-1})$ follows from those for $i = 1, \ldots, n$, completing the proof. $\qquad\square$

3.1.6 Convergence of the Scheme

In this section, we establish the convergence of the sequence of approximate solutions, constructed in Theorem 3.4, to a weak solution to (1.6), i.e., we prove Theorem 3.6.

Compactness of the approximate solutions

In order to achieve the convergence in the fluxes, we proceed as in [20] by defining the approximate gradient on a dual mesh. For $\sigma = K|L \in \mathcal{E}_{\text{int}}$, we define the new cell T_{KL} as

the cell with the vertexes x_K, x_L and those of σ. For $\sigma \in \mathcal{E}_{\text{ext}} \cap \mathcal{E}_K$, we define $T_{K\sigma}$ as the cell with vertex x_K and those of σ. Then Ω can be decomposed as

$$\overline{\Omega} = \bigcup_{K \in \mathcal{T}} \left\{ \left(\bigcup_{L \in \mathcal{N}_K} \overline{T}_{KL} \right) \cup \left(\bigcup_{\sigma \in \mathcal{E}_{\text{ext},K}} \overline{T}_{K\sigma} \right) \right\},$$

where $\mathcal{N}_K$ denotes the set of neighboring cells of K. The discrete gradient $\nabla_{\mathcal{T},\triangle t} v$ on $\Omega_T := \Omega \times (0, T)$ for piecewise constant functions $v \in \mathcal{H}_{\mathcal{T},\triangle t}$ is defined by

$$\nabla_{\mathcal{T},\triangle t} v(x, t) = \begin{cases} \dfrac{\mathrm{m}(\sigma)(v_L^k - v_K^k)}{\mathrm{m}(T_{KL})} \mathbf{n}_{KL} & \text{for } x \in T_{KL}, \ t \in (t^k, t^{k+1}), \\ 0 & \text{for } x \in T_{K\sigma}, \ t \in (t^k, t^{k+1}), \end{cases} \tag{3.31}$$

where $\mathbf{n}_{KL}$ denotes the unit normal on $\sigma = K|L$ oriented from K to L. To simplify the notation, we set $\nabla_m := \nabla_{\mathcal{T}_m, \triangle t_m}$. The solution to the approximate scheme (3.13)-(3.14) is called $u_{0,m}, u_{1,m}, \dots, u_{n,m}$.

Lemma 3.11. *There exist functions $u_0 \in L^\infty(\Omega_T) \cap L^2(0, T; H^1(\Omega))$ and $u_i \in L^\infty(\Omega_T)$ such that, possibly for subsequences, as $m \to \infty$,*

$$u_{0,m} \to u_0, \quad u_{0,m}^{1/2} \to u_0^{1/2} \quad \text{strongly in } L^2(\Omega_T), \tag{3.32}$$

$$\nabla_m u_{0,m} \rightharpoonup \nabla u_0, \quad \nabla_m u_{0,m}^{1/2} \rightharpoonup \nabla u_0^{1/2} \quad \text{weakly in } L^2(\Omega_T), \tag{3.33}$$

$$u_{0,m}^{1/2} u_{i,m} \to u_0^{1/2} u_i \quad \text{strongly in } L^2(\Omega_T), \tag{3.34}$$

$$\nabla_m \big(u_{0,m}^{1/2} u_{i,m} \big) \rightharpoonup \nabla \big(u_0^{1/2} u_i \big) \quad \text{weakly in } L^2(\Omega_T), \tag{3.35}$$

where $i \in \{1, \dots, n\}$.

Proof. First, we claim that $(u_{0,m})$ is uniformly bounded in $\mathcal{H}_{\mathcal{T},\triangle t}$. Indeed, by the L^∞ bounds and estimate (3.29),

$$\|u_{0,m}\|_{1,\mathcal{T},\triangle t}^2 = \sum_{k=1}^N \triangle t \left(\sum_{\sigma = K|L \in \mathcal{E}_{\text{int}}} \tau_\sigma (u_{0,K}^k - u_{0,L}^k)^2 + \sum_{K \in \mathcal{T}} \mathrm{m}(K)(u_{0,K}^k)^2 \right)$$

$$= \sum_{k=1}^N \triangle t \left(\sum_{\sigma = K|L \in \mathcal{E}_{\text{int}}} \tau_\sigma \big((u_{0,K}^k)^{1/2} + (u_{0,L}^k)^{1/2} \big)^2 \big((u_{0,K}^k)^{1/2} - (u_{0,L}^k)^{1/2} \big)^2 \right.$$

$$\left. + \sum_{K \in \mathcal{T}} \mathrm{m}(K)(u_{0,K}^k)^2 \right) \tag{3.36}$$

$$\leq 4 \|u_{0,m}\|_{L^\infty(\Omega_T)} \|u_{0,m}^{1/2}\|_{1,\mathcal{T},\triangle t}^2 + \|u_{0,m}\|_{L^2(\Omega_T)}^2 \leq C.$$

By estimate (3.30), $(\partial_t^{\triangle t} u_{0,m})$ is uniformly bounded. Therefore, by the discrete Aubin–Lions lemma (see Lemma 5.5 in the appendix), we conclude the existence of a subsequence (not relabeled) such that the first convergence in (3.32) holds. The strong convergence implies (up to a subsequence) that $u_{0,m} \to u_0$ pointwise in Ω_T and consequently also

$u_{0,m}^{1/2} \to u_0^{1/2}$ pointwise in Ω_T. Thus, together with the L^∞ bound for $u_{0,m}^{1/2}$, we infer the second convergence in (3.32).

The convergences in (3.33) are a consequence of the uniform estimates (3.29) and (3.36) and the compactness result in [33, proof of Theorem 10.3]. Applying the discrete Aubin–Lions lemma of "degenerate" type (Lemma 5.6 in the appendix) to $y_m = u_{0,m}^{1/2}$ and $z_m = u_{i,m}$ for fixed $i \in \{1, \ldots, n\}$, we deduce convergence (3.34). Finally, convergence (3.35) is a consequence of (3.34) and the weak compactness of $(u_{0,m}^{1/2} u_{i,m})$, thanks to the uniform bound in (3.29). $\qquad\square$

The limit $m \to \infty$

We finish the proof of Theorem 3.6 by verifying that the limit function $u = (u_1, \ldots, u_n)$, as defined in Lemma 3.11, is a weak solution in the sense of the theorem.

Let $\phi \in C_0^\infty(\overline\Omega \times [0, T))$ and let $m \in \mathbb{N}$ be large enough such that $\operatorname{supp}\phi \subset \overline\Omega \times [0, (N_m - 1)\triangle t_m)$ (recall that $T = N_m \triangle t_m$). For the limit, we follow the strategy used, for instance, in [20] and introduce the following notations:

$$F_{10}(m) = -\int_0^T \int_\Omega u_{i,m} \partial_t \phi \, dx \, dt - \int_\Omega u_{i,m}(0)\phi(0) \, dx,$$

$$F_{20}(m) = \int_0^T \int_\Omega u_{0,m}^{1/2} \nabla_m (u_{0,m}^{1/2} u_{i,m}) \nabla \phi \, dx \, dt,$$

$$F_{30}(m) = 3 \int_0^T \int_\Omega u_{0,m}^{1/2} u_{i,m} \nabla_m (u_{0,m}^{1/2}) \nabla \phi \, dx \, dt.$$

The convergence results of Lemma 3.11 show that, as $m \to \infty$,

$$F_{10}(m) + D F_{20}(m) - D F_{30}(m) \to -\int_0^T \int_\Omega u_i \partial_t \phi \, dx \, dt - \int_\Omega u_i^0 \phi(0) \, dx \tag{3.37}$$

$$+ D \int_0^T \int_\Omega \left(u_0^{1/2} \nabla(u_0^{1/2} u_i) - 3 u_0^{1/2} u_i \nabla u_0^{1/2} \right) dx \, dt.$$

Next, setting $\phi_K^k = \phi(x_K, t^k)$, we multiply scheme (3.13) by $\triangle t_m \phi_K^{k-1}$ and sum over $K \in \mathcal{T}_m$ and $k = 1, \ldots, N_m$. Then

$$F_1(m) + D F_2(m) - D F_3(m) = 0, \tag{3.38}$$

where, omitting the subscript m from now on to simplify the notation,

$$F_1(m) = \sum_{k=1}^{N} \sum_{K \in \mathcal{T}} \mathrm{m}(K)\big(u_{i,K}^k - u_{i,K}^{k-1}\big)\phi_K^{k-1},$$

$$F_2(m) = \sum_{k=1}^{N} \triangle t \sum_{K \in \mathcal{T}} \sum_{\sigma \in \mathcal{E}_{K,\mathrm{int}}} \tau_\sigma (u_{0,\sigma}^k)^{1/2}\big((u_{0,K}^k)^{1/2}u_{i,K}^k - (u_{0,L}^k)^{1/2}u_{i,L}^k\big)\phi_K^{k-1},$$

$$F_3(m) = \sum_{k=1}^{N} \triangle t \sum_{K \in \mathcal{T}} \sum_{\sigma \in \mathcal{E}_{K,\mathrm{int}}} \tau_\sigma\big((u_{0,K}^k)^{1/2} - (u_{0,L}^k)^{1/2}\big)$$

$$\times u_{i,\sigma}^k\left((u_{0,\sigma}^k)^{1/2} + 2\frac{(u_{0,K}^k)^{1/2} + (u_{0,L}^k)^{1/2}}{2}\right)\phi_K^{k-1}.$$

The aim is to show that $F_{i0}(m) - F_i(m) \to 0$ as $m \to \infty$ for $i = 1, 2, 3$. Then, because of (3.38), $F_{10}(m) + DF_{20}(m) - DF_{30}(m) \to 0$, which finishes the proof. We start by verifying that $F_{10}(m) - F_1(m) \to 0$. For this, we rewrite $F_1(m)$ and $F_{10}(m)$, using $\phi_K^N = 0$:

$$F_1(m) = \sum_{k=1}^{N} \sum_{K \in \mathcal{T}} \mathrm{m}(K)u_{i,K}^k\big(\phi_K^{k-1} - \phi_K^k\big) - \sum_{K \in \mathcal{T}} \mathrm{m}(K)\phi_K^0 u_{i,K}^0,$$

$$= -\sum_{k=1}^{N} \sum_{K \in \mathcal{T}} \int_{t^{k-1}}^{t^k} \int_K u_{i,K}^k \partial_t \phi(x_K, t)\, dx\, dt - \sum_{K \in \mathcal{T}} \int_K u_{i,K}^0 \phi(x_K, 0)\, dx,$$

$$F_{10}(m) = -\sum_{k=1}^{N} \sum_{K \in \mathcal{T}} \int_{t^{k-1}}^{t^k} \int_K u_{i,K}^k \partial_t \phi(x, t)\, dx\, dt - \sum_{K \in \mathcal{T}} \int_K u_{i,K}^0 \phi(x, 0)\, dx.$$

In view of the regularity of ϕ and the uniform L^∞ bound on u_i, we find that

$$|F_{10}(m) - F_1(m)| \le CT\mathrm{m}(\Omega)\|\phi\|_{C^2} h(\mathcal{T}_m) \to 0 \quad \text{as } m \to \infty.$$

Using discrete integration by parts, the second integral becomes

$$F_2(m) = \sum_{k=1}^{N} \triangle t \sum_{\sigma = K|L \in \mathcal{E}_{\mathrm{int}}} \tau_\sigma (u_{0,\sigma}^k)^{1/2}\big((u_{0,K}^k)^{1/2}u_{i,K}^k - (u_{0,L}^k)^{1/2}u_{i,L}^k\big)\big(\phi_K^{k-1} - \phi_L^{k-1}\big)$$

$$= F_{21}(m) + F_{22}(m),$$

where we have decomposed $(u_{0,\sigma}^k)^{1/2} = (u_{0,K}^k)^{1/2} + ((u_{0,\sigma}^k)^{1/2} - (u_{0,K}^k)^{1/2})$, i.e.

$$F_{21}(m) = \sum_{k=1}^{N} \triangle t \sum_{\sigma = K|L \in \mathcal{E}_{\mathrm{int}}} \tau_\sigma (u_{0,K}^k)^{1/2}\big((u_{0,K}^k)^{1/2}u_{i,K}^k - (u_{0,L}^k)^{1/2}u_{i,L}^k\big)\big(\phi_K^{k-1} - \phi_L^{k-1}\big),$$

$$F_{22}(m) = \sum_{k=1}^{N} \triangle t \sum_{\sigma = K|L \in \mathcal{E}_{\mathrm{int}}} \tau_\sigma\big((u_{0,\sigma}^k)^{1/2} - (u_{0,K}^k)^{1/2}\big)\big((u_{0,K}^k)^{1/2}u_{i,K}^k - (u_{0,L}^k)^{1/2}u_{i,L}^k\big)$$

$$\times \big(\phi_K^{k-1} - \phi_L^{k-1}\big).$$

Furthermore, we write $F_{20}(m) = G_1(m) + G_2(m)$, where

$$G_1(m) = \sum_{k=1}^{N} \sum_{\sigma=K|L\in\mathcal{E}_{\text{int}}} \frac{\text{m}(\sigma)}{\text{m}(T_{KL})} (u_{0,K}^k)^{1/2} \big((u_{0,K}^k)^{1/2} u_{i,K}^k - (u_{0,L}^k)^{1/2} u_{i,L}^k\big)$$

$$\times \int_{t^{k-1}}^{t^k} \int_{T_{KL}} \nabla\phi(x,t) \cdot \mathbf{n}_{K\sigma} \, dx \, dt,$$

$$G_2(m) = \sum_{k=1}^{N} \sum_{\sigma=K|L\in\mathcal{E}_{\text{int}}} \frac{\text{m}(\sigma)}{\text{m}(T_{KL})} \big((u_{0,L}^k)^{1/2} - (u_{0,K}^k)^{1/2}\big)\big((u_{0,K}^k)^{1/2} u_{i,K}^k - (u_{0,L}^k)^{1/2} u_{i,L}^k\big)$$

$$\times \int_{t^{k-1}}^{t^k} \int_{T_{KL}\cap L} \nabla\phi(x,t) \cdot \mathbf{n}_{K\sigma} \, dx \, dt.$$

The aim is to show that $F_{21}(m) - G_1(m) \to 0$, $F_{22}(m) \to 0$, and $G_2(m) \to 0$. This implies that

$$|F_{20}(m) - F_2(m)| = \big|(G_1(m) + G_2(m)) - (F_{21}(m) + F_{22}(m))\big|$$
$$\leq |G_1 - F_{21}| + |G_2| + |F_{22}| \to 0.$$

First we notice that, due to the admissibility of the mesh and the regularity of ϕ, by taking the mean value over T_{KL},

$$\left| \int_{t^{k-1}}^{t^k} \left(\frac{\phi_K^{k-1} - \phi_L^{k-1}}{\text{d}_\sigma} - \frac{1}{\text{m}(T_{KL})} \int_{T_{KL}} \nabla\phi(x,t) \cdot \mathbf{n}_{K\sigma} \, dx \right) dt \right| \leq C\triangle th(\mathcal{T}), \qquad (3.39)$$

where the constant $C > 0$ only depends on ϕ. It yields

$$|F_{21}(m) - G_1(m)| \leq Ch(\mathcal{T}) \sum_{k=1}^{N} \triangle t \sum_{\sigma=K|L\in\mathcal{E}_{\text{int}}} \text{m}(\sigma) \big|(u_{0,K}^k)^{1/2} u_{i,K} - (u_{0,L}^k)^{1/2} u_{i,L}\big|$$
$$\leq Ch(\mathcal{T}) \|u_0^{1/2} u_i\|_{1,\mathcal{T},\triangle t} (T\text{m}(\Omega))^{1/2},$$

where the last estimate follows from the Cauchy–Schwarz inequality. This proves that $|F_{21}(m) - G_1(m)| \to 0$ as $m \to \infty$.

It remains to analyze the expressions $F_{22}(m)$ and $G_2(m)$. To this end, we remark that $\text{d}_\sigma \leq h(\mathcal{T})$ and hence, together with the regularity of ϕ, and the Cauchy–Schwarz inequality,

$$|F_{22}(m)| \leq \sum_{k=1}^{N} \triangle t \sum_{\sigma=K|L\in\mathcal{E}_{\text{int}}} \tau_\sigma \big|(u_{0,\sigma}^k)^{1/2} - (u_{0,K}^k)^{1/2}\big| \big|(u_{0,K}^k)^{1/2} u_{i,K}^k - (u_{0,L}^k)^{1/2} u_{i,L}^k\big|$$
$$\times \frac{|\phi_K^{k-1} - \phi_L^{k-1}|}{\text{d}_\sigma} \text{d}_\sigma$$
$$\leq Ch(\mathcal{T}) \|\phi\|_{C^1} \sum_{k=1}^{N} \triangle t \sum_{\sigma=K|L\in\mathcal{E}_{\text{int}}} \tau_\sigma \big|(u_{0,\sigma}^k)^{1/2} - (u_{0,K}^k)^{1/2}\big|$$
$$\times \big|(u_{0,K}^k)^{1/2} u_{i,K}^k - (u_{0,L}^k)^{1/2} u_{i,L}^k\big|$$
$$\leq Ch(\mathcal{T}) \|\phi\|_{C^1} \|u_0^{1/2}\|_{1,\mathcal{T},\triangle t} \|u_0^{1/2} u_i\|_{1,\mathcal{T},\triangle t} \leq Ch(\mathcal{T}),$$

The term $G_2(m)$ can be estimated in a similar way.

Finally, we need to show that $|F_{30}(m) - F_3(m)| \to 0$. The proof is completely analogous to the previous arguments, since

$$\left| 3(u_{0,K}^k)^{1/2} u_{i,K}^k - u_{i,\sigma}^k \left((u_{0,\sigma}^k)^{1/2} + 2 \frac{(u_{0,K}^k)^{1/2} + (u_{0,L}^k)^{1/2}}{2} \right) \right|$$
$$\leq C \left((u_{0,\sigma}^k)^{1/2} |u_{i,K}^k - u_{i,L}^k| + |(u_{0,K}^k)^{1/2} - (u_{0,L}^k)^{1/2}| \right).$$

Summarizing, we have proved that $|F_{i0}(m) - F_i(m)| \to 0$ for $i = 1, 2, 3$, and since $F_1(m) + DF_2(m) - DF_3(m) = 0$, the convergence (3.37) shows that u solves (3.19). This completes the proof of Theorem 3.6.

3.2 Finite-Element Scheme

In this section, we propose a structure-preserving implicit Euler finite-element (FE) scheme for the cross-diffusion model. The scheme is based on the formulation of the model in entropy variables (2.2). Therefore, the analysis of the scheme can be done in a similar way as the analysis of the continuous model. We show that the scheme preserves the nonnegativity and upper bounds of the ion concentrations and the total relative mass, and that it dissipates the entropy (or free energy). The existence of discrete solutions to the scheme and their convergence towards the solution to the continuous system is proved. For this, many arguments from Chapter 2 are reused.

3.2.1 Notations and Assumptions

For the FE discretization we need to make similar assumptions as we did in the previous section for the FV scheme. More precisely, we still assume (H1')-(H3') to hold, but we replace (H4') by

(H4") Initial and boundary data: $u_i^I \in H^2(\Omega)$, $\overline{u}_i \in H^2(\Omega)$ satisfy $u_i^I > 0$, $\overline{u}_i > 0$ and $1 - \sum_{i=1}^n u_i^I > 0$, $1 - \sum_{i=1}^n \overline{u}_i > 0$ in Ω for $i = 1, \dots, n$, and $\overline{\Phi} \in H^2(\Omega) \cap L^\infty(\Omega)$.

The H^2 regularity of the initial and boundary data ensures that the standard interpolation converges to the given data, see (3.42) below. We also assume strict positivity of the initial and boundary data, since otherwise the transformation to entropy variables cannot be performed. In practice, when dealing with only nonnegative initial data, a regularization has to be done.

We consider the model equations (1.6) on a finite time interval $(0, T)$ with $T > 0$ fixed. For simplicity, we again use a uniform time discretization with time step $\tau > 0$, and set $t^k = k\tau$ for $k = 1, \dots, N$ where $N \in \mathbb{N}$ is given and $\tau = T/N$.

For the space discretization, we introduce a family $\mathcal{T}_h$ ($h > 0$) of triangulations of Ω, consisting of open polygonal convex subsets of Ω (the so-called cells) such that $\overline{\Omega} = \cup_{K \in \mathcal{T}_h} \overline{K}$ with maximal diameter $h = \max_{K \in \mathcal{T}_h} \text{diam}(K)$. We assume that the corresponding family of edges $\mathcal{E}$ can be split into internal and external edges $\mathcal{E} = \mathcal{E}_{\text{int}} \cup \mathcal{E}_{\text{ext}}$ with $\mathcal{E}_{\text{int}} = \{\sigma \in \mathcal{E} :$

$\sigma \subset \Omega\}$ and $\mathcal{E}_{\text{ext}} = \{\sigma \in \mathcal{E} : \sigma \subset \partial\Omega\}$. Each exterior edge is assumed to be an element of either the Dirichlet or Neumann boundary, i.e. $\mathcal{E}_{\text{ext}} = \mathcal{E}_{\text{ext}}^D \cup \mathcal{E}_{\text{ext}}^N$.

In the FE setting, the triangulation $(\mathcal{T}_h, \mathcal{E}, \mathcal{N})$ is completed by the set of nodes $\mathcal{N} = \{p_j\}_{j \in J}$. We have to impose the following regularity assumption on the mesh: There exists a constant $\gamma > 0$ such that

$$\rho_K \leq h_K \leq \gamma \rho_K \quad \text{for all } K \in \mathcal{T}_h, \tag{3.40}$$

where ρ_K is the radius of the incircle and h_K is the diameter of K.

We associate with $\mathcal{T}_h$ the usual conforming finite-element spaces of piecewise linear functions,

$$\mathcal{S}(\mathcal{T}_h) := \{\xi \in C(\overline{\Omega}) : \xi|_K \text{ is linear } \forall K \in \mathcal{T}_h\} \subset H^1(\Omega), \tag{3.41}$$
$$\mathcal{S}_D(\mathcal{T}_h) := \mathcal{S}(\mathcal{T}_h) \cap H_D^1(\Omega).$$

Let $\{\chi_j\}_{j \in J}$ be the standard basis functions for $\mathcal{S}(\mathcal{T}_h)$ with $\chi_j(p_i) = \delta_{ij}$ for all $i, j \in J$. We define the nodal interpolation operator $I_h : C(\overline{\Omega}) \to \mathcal{S}(\mathcal{T}_h)$ via $(I_h \xi)(p_j) = \xi(p_j)$ for all $j \in J$. Due to the regularity assumptions on the mesh, I_h has the following important approximation property (see e.g. [22, Chapter 3]):

$$\lim_{h \to 0} \|\phi - I_h \phi\|_{H^1(\Omega)} = 0 \quad \text{for all } \phi \in H^2(\Omega). \tag{3.42}$$

3.2.2 Definition of the Scheme

In order to define the scheme we need to approximate the initial and boundary data. We set $w_i^0 = I_h(\log(u_i^I/u_0^I) + \beta z_i \Phi^I)$ and let Φ^0 be the standard FE solution of the linear equation $-\lambda^2 \Delta \Phi^0 = \sum_{i=1}^n z_i u_i^I + f(x)$. Also, we set $\overline{w}_h = I_h(\log(\overline{u}_i/\overline{u}_0) + \beta z_i \overline{\Phi})$ and $\overline{\Phi}_h = I_h(\overline{\Phi})$.

The FE scheme is now defined as follows. Given $w^{k-1} \in \mathcal{S}(\mathcal{T}_h)^n$ and $\Phi^{k-1} \in \mathcal{S}(\mathcal{T}_h)$ find $w^k - \overline{w}_h \in \mathcal{S}_D(\mathcal{T}_h)^n$, $\Phi^k - \overline{\Phi}_h \in \mathcal{S}_D(\mathcal{T}_h)$ such that

$$\frac{1}{\tau} \int_\Omega \left(u(w^k, \Phi^k) - u(w^{k-1}, \Phi^{k-1}) \right) \cdot \phi \, dx$$

$$+ \int_\Omega \nabla\phi : B(w^k, \Phi^k) \nabla w^k dx + \varepsilon \int_\Omega (w^k - \overline{w}_h) \cdot \phi \, dx = 0, \tag{3.43}$$

$$\lambda^2 \int_\Omega \nabla\Phi^k \cdot \nabla\theta \, dx = \int_\Omega \left(\sum_{i=1}^n z_i u_i(w^k, \Phi^k) + f \right) \theta \, dx \tag{3.44}$$

for all $\phi \in \mathcal{S}_D(\mathcal{T}_h)^n$ and $\theta \in \mathcal{S}_D(\mathcal{T}_h)$. The symbol ":" signifies the Frobenius matrix product; here, the expression reduces to

$$\nabla\phi : B(w^k, \Phi^k) \nabla w^k = \sum_{i=1}^n D_i u_i(w^k, \Phi^k) u_0(w^k, \Phi^k) \nabla\phi_i \cdot \nabla w_i^k.$$

The term involving the parameter $\varepsilon > 0$ is only needed to guarantee the coercivity of (3.43)-(3.44). Indeed, the diffusion matrix $B(w^k, \Phi^k)$ degenerates when $w_i^k \to -\infty$, and the corresponding bilinear form is only positive semidefinite. To emphasize the dependence on

the mesh and ε, we should rather write $w^{(h,\varepsilon,k)}$ instead of w^k and similarly for Φ^k; however, for the sake of presentation we will mostly omit the additional superscripts. In order to obtain an approximation in the original variables, we just need to compute $u^{(h,\varepsilon,k)} = u(w^{(h,\varepsilon,k)}, \Phi^{(h,\varepsilon,k)})$ according to (2.4). Setting $u^{(\tau)}(x,t) = u^k(x)$ for $x \in \Omega$, $t \in ((k-1)\tau, k\tau]$, $k = 1, \dots, N$, and $u^{(\tau)}(\cdot, 0) = I_h u^I$ as well as similarly for $\Phi^{(\tau)}$, we obtain piecewise constant in time functions.

3.2.3 Main Results

The first result concerns the existence of solutions to the nonlinear FE scheme (3.43)-(3.44).

Theorem 3.12 (Existence of solutions and entropy inequality for the FE scheme). *Let Assumptions (H1')-(H3') and (H4") hold. Then there exists a solution to the FE scheme* (3.43)-(3.44) *that satisfies the following discrete entropy inequality:*

$$\mathcal{H}(u^k) + \tau \int_\Omega \nabla(w^k - \overline{w}_h) : B(w^k, \Phi^k)\nabla w^k dx + \varepsilon\tau \|w^k - \overline{w}_h\|^2_{L^2(\Omega)} \le \mathcal{H}(u^{k-1}), \quad (3.45)$$

where $\mathcal{H}(u)$ is defined in (2.1), *and $u^k = u(w^k, \Phi^k)$, $u^{k-1} = u(w^{k-1}, \Phi^{k-1})$ for $k = 1, \dots, n$.*

Since the scheme is inspired from the approximate problem used in the existence proof for the continuous equations, we can prove this theorem similarly as Theorem 2.1 in Chapter 2 with a fixed point argument. The main difference is that for Theorem 2.1, a regularization term of the type $\varepsilon((-\Delta)^m w^k + w^k)$ has been added to achieve via $H^m(\Omega) \hookrightarrow L^\infty(\Omega)$ compactness and L^∞ solutions. In the finite-dimensional setting, this embedding is not necessary but we still need the regularization εw^k to conclude coercivity. We conjecture that this regularization is just technical but currently, we are not able to remove it. Note, however, that we can use arbitrarily small values of ε in the numerical simulations such that the additional term does not affect the solution practically.

The most important result of this section is the convergence of the FE solution to a weak solution of the ion transport model.

Theorem 3.13 (Convergence of the approximate FE solution). *Let Assumptions (H1')-(H3') and (H4") hold and let $u^{(h,\varepsilon,\tau)}, \Phi^{(h,\varepsilon,\tau)}$ be the approximate solution constructed from the FE scheme* (3.43)-(3.44). *Set $u_0^{(h,\varepsilon,\tau)} = 1 - \sum_i u_i^{(h,\varepsilon,\tau)}$. Then there exist functions u_0, $u = (u_1, \dots, u_n)$, Φ, satisfying $u(x,t) \in \overline{\mathcal{D}}$, $u_0 = 1 - \sum_i u_i$ in Ω, the regularity*

$$u_0^{1/2}, \, u_0^{1/2}u_i, \, \Phi \in L^2(0,T;H^1(\Omega)), \quad \partial_t u_i \in L^2(0,T;H_D^1(\Omega)')$$

for $i = 1, \dots, n$, such that as $(h, \varepsilon, \tau) \to 0$,

$$(u_0^{(h,\varepsilon,\tau)})^{1/2} \to u_0^{1/2}, \, (u_0^{(h,\varepsilon,\tau)})^{1/2}u_i^{(h,\varepsilon,\tau)} \to u_0^{1/2}u_i \quad \text{strongly in } L^2(\Omega \times (0,T)),$$
$$\Phi^{(h,\varepsilon,\tau)} \to \Phi \quad \text{strongly in } L^2(\Omega \times (0,T)),$$

and u and Φ are a weak solution to (1.6)-(1.10), i.e., for all $\phi \in L^2(0,T; H_D^1(\Omega)^n)$ and $i = 1, \ldots, n$,

$$\int_0^T \langle \partial_t u_i, \phi \rangle \, dt + D_i \int_0^T \int_\Omega u_0^{1/2} \big(\nabla(u_0^{1/2} u_i) - 3u_i \nabla u_0^{1/2} \big) \cdot \nabla \phi \, dx \, dt$$

$$+ D_i \int_0^T \int_\Omega u_i u_0 \beta z_i \nabla \Phi \cdot \nabla \phi \, dx \, dt = 0, \tag{3.46}$$

$$\lambda^2 \int_0^T \int_\Omega \nabla \Phi \cdot \nabla \phi \, dx \, dt = \int_0^T \int_\Omega \Big(\sum_{i=1}^n z_i u_i + f \Big) \phi \, dx \, dt, \tag{3.47}$$

and the boundary and initial conditions are satisfied in a weak sense.

In contrast to the convergence result Theorem 3.6 for the FV scheme, here we do not need any additional assumptions on the parameters, but obtain convergence for the full ion transport model. The proof is again similar to the continuous case in Section 2.3 and makes strong use of the a priori estimates gained from the discrete entropy inequality (3.45) and the degenerate Aubin–Lions Lemma 5.4 stated in the Appendix.

3.2.4 Existence of Approximate Solutions and Discrete Entropy Inequality

We proof Theorem 3.12. First, we note that the nonlinear Poisson-equation (3.44) with w^k replaced by $y + \overline{w}_h$ with a given function $y \in \mathcal{S}_D(\mathcal{T}_h)$ has a unique solution Φ^k satisfying $\Phi^k - \overline{\Phi}_h \in \mathcal{S}_D(\mathcal{T}_h)$, since the function $\Phi \mapsto u_i(y, \Phi)$ is bounded. Furthermore, the following estimate holds for some constant $C > 0$:

$$\|\Phi^k\|_{H^1(\Omega)} \le C(1 + \|\overline{\Phi}_h\|_{H^1(\Omega)}). \tag{3.48}$$

For the existence of solutions to the full scheme we employ Leray–Schauder's fixed point theorem for the operator $S : \mathcal{S}_D(\mathcal{T}_h) \times [0,1] \to \mathcal{S}_D(\mathcal{T}_h)$, $(y, \delta) \mapsto v$ where v is the solution to the linear problem

$$a(v, \phi) = F(\phi) \quad \text{for all } \phi \in \mathcal{S}_D(\mathcal{T}_h), \tag{3.49}$$

where

$$a(v, \phi) = \int_\Omega \nabla \phi : B(y + \overline{w}_h, \Phi^k) \nabla v \, dx + \varepsilon \int_\Omega v \cdot \phi \, dx,$$

$$F(\phi) = -\frac{\delta}{\tau} \int_\Omega \big(u(y + \overline{w}_h, \Phi^k) - u(w^{k-1}, \Phi^{k-1}) \big) \cdot \phi \, dx$$

$$- \delta \int_\Omega \nabla \phi : B(y + \overline{w}_h, \Phi^k) \nabla \overline{w}_h \, dx,$$

and $\Phi^k - \overline{\Phi}_h \in \mathcal{S}_D(\mathcal{T}_h)$ is the unique solution to

$$\lambda^2 \int_\Omega \nabla \Phi^k \cdot \nabla \theta \, dx = \int_\Omega \Big(\sum_{i=1}^n z_i u_i(y + \overline{w}_h, \Phi^k) + f \Big) \theta \, dx$$

for all $\theta \in \mathcal{S}_D(\mathcal{T}_h)$.

The bilinear form a and the linear form F are continuous on $\mathcal{S}_D(\mathcal{T}_h)$. The equivalence of all norms on the finite-dimensional space $\mathcal{S}_D(\mathcal{T}_h)$ implies the coercivity of a,

$$a(v,v) \geq \varepsilon \|v\|^2_{L^2(\Omega)} \geq \varepsilon C \|v\|^2_{H^1(\Omega)}.$$

Therefore, we can conclude with the lemma of Lax–Milgram that the operator S is well-defined. Furthermore, the unique solution v to the linear problem (3.49) satisfies

$$\varepsilon C \|v\|^2_{H^1(\Omega)} \leq a(v,v) = F(v) \leq C(\tau)\|v\|_{H^1(\Omega)},$$

and thus v is bounded independently of y and δ, which of course implies that the fixed points $v = S(v,\delta)$ are uniformly bounded. It is also clear that $S(y,0) = 0$ for all $y \in \mathcal{S}_D(\mathcal{T}_h)$. The continuity of S follows from standard arguments, and since $\mathcal{S}_D(\mathcal{T}_h)$ is finite-dimensional, S is also compact. From Leray–Schauder's fixed point theorem it follows that there exists $v^k \in \mathcal{S}_D(\mathcal{T}_h)$ such that $S(v^k, 1) = v^k$, and setting $w^k = v^k + \overline{w}_h$ we have found a solution to (3.43)-(3.44).

The discrete entropy inequality (3.45) is proven by using $\tau v^k = \tau(w^k - \overline{w}_h) \in \mathcal{S}_D(\mathcal{T}_h)$ as a test function in (3.43). Just as in the continuous setting, it can be shown by exploiting the convexity of $\mathcal{H}$ that

$$\int_\Omega (u^k - u^{k-1}) \cdot (w^k - \overline{w}_h)\, dx \geq \mathcal{H}(u^k) - \mathcal{H}(u^{k-1}),$$

which concludes the proof. $\qquad\square$

3.2.5 Convergence of the Scheme

The next step in the analysis of the FE scheme is to use the entropy dissipation inequality (3.45) to obtain a priori gradient estimates for the discrete solution. For this purpose, we transform back to the original variables u^k and do similar estimates and calculations as in the continuous setting, paying attention that our estimates are not only uniform with respect to ϵ and τ, but also with respect to the mesh size h.

Lemma 3.14 (A priori estimates for the FE scheme). *For the solution to the FE scheme from Lemma 3.12 the following estimates hold:*

$$\|u_i^k\|_{L^\infty(\Omega)} + \varepsilon\tau \sum_{j=1}^k \|w_i^j - \overline{w}_{i,h}\|^2_{L^2(\Omega)} \leq C, \qquad (3.50)$$

$$\tau \sum_{j=1}^k \left(\|(u_0^j)^{1/2}\|^2_{H^1(\Omega)} + \|u_0^j\|^2_{H^1(\Omega)} + \|(u_0^j)^{1/2}\nabla(u_i^j)^{1/2}\|^2_{L^2(\Omega)} \right) \leq C, \qquad (3.51)$$

for $i = 1,\dots,n$, where here and in the following, $C > 0$ is a generic constant independent of ε, τ and h.

Proof. The proof of this result is done in analogy to the continuous setting. Therefore, we only write down the main steps, more details can be found in the proof of Lemma 2.6.

It follows immediately from the definition of the entropy variables that $0 \leq u_i^k \leq 1$ almost everywhere for $i = 0, \ldots, n$. Using the definition of the entropy variables and some basic estimates for the integral in (3.45), the recursion in (3.45) can be resolved to

$$
\mathcal{H}(u^k) + \tau \frac{D_{\min}}{4} \sum_{j=1}^{k} \int_{\Omega} \sum_{i=1}^{n} u_i^j u_0^j \left| \nabla \log \frac{u_i^j}{u_0^j} \right|^2 dx + \varepsilon \tau \sum_{j=1}^{k} \| w^j - \overline{w}_h \|_{L^2(\Omega)}^2
$$

$$
\leq \mathcal{H}(u^0) + \tau \frac{D_{\min}}{2} \sum_{j=1}^{k} \int_{\Omega} \sum_{i=1}^{n} |\beta z_i \nabla \Phi^j|^2 dx + \tau k \frac{D_{\max}}{2} \int_{\Omega} \sum_{i=1}^{n} |\nabla \overline{w}_{i,h}|^2 dx.
$$

The right-hand side is uniformly bounded because of the $H^1(\Omega)$ estimate (3.48) for the electric potential, $\tau k \leq T$, and the boundedness of the interpolation operator I_h. The estimates follow now by inserting

$$
\sum_{i=1}^{n} u_i^j u_0^j \left| \nabla \log \frac{u_i^j}{u_0^j} \right|^2 = 4 u_0^j \sum_{i=1}^{n} |\nabla (u_i^j)^{1/2}|^2 + |\nabla u_0^j|^2 + 4 |\nabla (u_0^j)^{1/2}|^2.
$$

$\square$

The a priori estimates from the previous lemma allow us to perform the proof of the convergence Theorem 3.13.

Proof. We will not perform the limit in h, ε and τ simultaneously, but only let let $\epsilon, h \to 0$ at first, since after performing this limit we will be exactly in the same situation as in step 4 of the existence proof in the continuous case in Section 2.3.

We fix now $k \in \{1, \ldots, N\}$, let $u_i^{(\varepsilon,h)} = u_i^{(\varepsilon,h,k)}$ and $\Phi^{(\varepsilon,h)} = \Phi^{(\varepsilon,h,k)}$ be the approximate solution from Lemma 3.12, and set $u_0^{(\varepsilon,h)} = 1 - \sum_{i=1}^{n} u_i^{(\varepsilon,h)}$. The a priori estimates from Lemma 3.14 yield (up to a subsequence) as $\varepsilon, h \to 0$:

$$
u_i^{(\varepsilon,h)} \rightharpoonup^* u_i^k \quad \text{weakly* in } L^\infty(\Omega), \ i = 1, \ldots, n, \tag{3.52}
$$

$$
(u_0^{(\varepsilon,h)})^{1/2} \rightharpoonup (u_0^k)^{1/2}, \quad \Phi^{(\varepsilon,h)} \rightharpoonup \Phi^k \quad \text{weakly in } H^1(\Omega), \tag{3.53}
$$

$$
u_0^{(\varepsilon,h)} \to u_0^k, \quad \Phi^{(\varepsilon,h)} \to \Phi^k \quad \text{strongly in } L^2(\Omega), \tag{3.54}
$$

$$
\varepsilon(w_i^{(\varepsilon,h)} - \overline{w}_{i,h}) \to 0 \quad \text{strongly in } L^2(\Omega), \ i = 1, \ldots, n. \tag{3.55}
$$

Combining (3.51) and (3.53), we can show that $u_i^{(\varepsilon,h)}(u_0^{(\varepsilon,h)})^{1/2} \rightharpoonup u_i^k (u_0^k)^{1/2}$ weakly in $H^1(\Omega)$ and thus also strongly in $L^2(\Omega)$. The same holds for $u_i^{(\varepsilon,h)} u_0^{(\varepsilon,h)}$.

Now let $\phi \in (H^2(\Omega) \cap H_{0,D}^1(\Omega))^n$. We cannot use ϕ_i directly as a test function in (3.43), instead we take $I_h \phi \in \mathcal{S}_D(\mathcal{T}_h)^n$. In order to pass to the limit in (3.43), we rewrite

$$
\int_{\Omega} \nabla(I_h \phi) : B(w^{(\varepsilon,h)}, \Phi^{(\varepsilon,h)}) \nabla w^{(\varepsilon,h)} \, dx = \int_{\Omega} \sum_{i=1}^{n} D_i u_i^{(\varepsilon,h)} u_0^{(\varepsilon,h)} \nabla w_i^{(\varepsilon,h)} \cdot \nabla(I_h \phi_i) \, dx
$$

$$
= \int_{\Omega} \sum_{i=1}^{n} D_i \Big((u_0^{(\varepsilon,h)})^{1/2} \nabla \big(u_i^{(\varepsilon,h)} (u_0^{(\varepsilon,h)})^{1/2} \big) - 3 u_i^{(\varepsilon,h)} (u_0^{(\varepsilon,h)})^{1/2} \nabla (u_0^{(\varepsilon,h)})^{1/2}
$$

$$
+ \beta z_i u_i^{(\varepsilon,h)} u_0^{(\varepsilon,h)} \nabla \Phi^{(\varepsilon,h)} \Big) \cdot \nabla(I_h \phi_i) \, dx. \tag{3.56}
$$

We estimate each of the above summands separately. For instance,

$$\left| \int_\Omega u_i^{(\varepsilon,h)} u_0^{(\varepsilon,h)} \nabla \Phi^{(\varepsilon,h)} \cdot \nabla(I_h \phi_i) dx - \int_\Omega u_i^k u_0^k \nabla \Phi^k \cdot \nabla \phi_i dx \right|$$

$$\leq \left| \int_\Omega u_i^{(\varepsilon,h)} u_0^{(\varepsilon,h)} \nabla \Phi^{(\varepsilon,h)} \cdot \nabla(I_h \phi_i - \phi_i) dx \right|$$

$$+ \left| \int_\Omega (u_i^{(\varepsilon,h)} u_0^{(\varepsilon,h)} \nabla \Phi^{(\varepsilon,h)} - u_i^k u_0^k \nabla \Phi^k) \cdot \nabla \phi_i dx \right|$$

$$\leq \| u_i^{(\varepsilon,h)} u_0^{(\varepsilon,h)} \nabla \Phi^{(\varepsilon,h)} \|_{L^2(\Omega)} \| \nabla(I_h \phi_i - \phi_i) \|_{L^2(\Omega)}$$

$$+ \left| \int_\Omega (u_i^{(\varepsilon,h)} u_0^{(\varepsilon,h)} \nabla \Phi^{(\varepsilon,h)} - u_i^k u_0^k \nabla \Phi^k) \cdot \nabla \phi_i dx \right| .$$

The convergence results from above imply that

$$u_i^{(\varepsilon,h)} u_0^{(\varepsilon,h)} \nabla \Phi^{(\varepsilon,h)} \rightharpoonup u_i^k u_0^k \nabla \Phi^k \quad \text{weakly in } L^2(\Omega).$$

Therefore, and because of the approximation property (3.42) of the interpolation operator I_h, we conclude that

$$\int_\Omega u_i^{(\varepsilon,h)} u_0^{(\varepsilon,h)} \nabla \Phi^{(\varepsilon,h)} \cdot \nabla(I_h \phi_i) dx \to \int_\Omega u_i^k u_0^k \nabla \Phi^k \cdot \nabla \phi_i dx.$$

Analogous results hold for the other summands in (3.56), since we have

$$(u_0^{(\varepsilon,h)})^{1/2} \nabla \big(u_i^{(\varepsilon,h)} (u_0^{(\varepsilon,h)})^{1/2} \big) - 3 u_i^{(\varepsilon,h)} (u_0^{(\varepsilon,h)})^{1/2} \nabla \big((u_0^{(\varepsilon,h)})^{1/2} \big)$$

$$\rightharpoonup (u_0^k)^{1/2} \nabla \big(u_0^k (u_0^k)^{1/2} \big) - 3 u_i^k (u_0^k)^{1/2} \nabla((u_0^k)^{1/2}) \quad \text{weakly in } L^2(\Omega).$$

Thus, the limit $(\varepsilon, h) \to 0$ gives

$$\lim_{(\varepsilon,h)\to 0} \int_\Omega \nabla(I_h \phi) : B(w^{(\varepsilon,h)}, \Phi^{(\varepsilon,h)}) \nabla w^{(\varepsilon,h)} dx = \int_\Omega \sum_{i=1}^n D_i \Big((u_0^k)^{1/2} \nabla \big(u_0^k (u_0^k)^{1/2} \big)$$

$$- 3 u_i^k (u_0^k)^{1/2} \nabla((u_0^k)^{1/2}) + \beta z_i u_i^k u_0^k \nabla \Phi^k \Big) \cdot \nabla \phi_i dx.$$

Furthermore, we deduce that

$$\left| \varepsilon \int_\Omega (w_i^{(\varepsilon,h)} - \overline{w}_{i,h})(I_h \phi_i) dx \right| \leq \varepsilon \| w_i^{(\varepsilon,h)} - \overline{w}_{i,h} \|_{L^2(\Omega)} \| I_h \phi_i \|_{L^2(\Omega)} \to 0$$

due to (3.55) and $\| I_h \phi_i \|_{L^2(\Omega)} \leq C$.

Then, performing the limit $h, \varepsilon \to 0$ in (3.43)-(3.44) leads to

$$\frac{1}{\tau} \int_\Omega (u^k - u^{k-1}) \cdot \phi \, dx + \int_\Omega \sum_{i=1}^n D_i (u_0^k)^{1/2} \big(\nabla(u_i^k (u_0^k)^{1/2}) - 3 u_i^k \nabla(u_0^k)^{1/2} \big) \cdot \nabla \phi_i \, dx$$

$$+ \int_\Omega \sum_{i=1}^n D_i u_i^k u_0^k \big(\beta z_i \nabla \Phi^k + \nabla W_i \big) \cdot \nabla \phi_i \, dx = 0,$$

$$\lambda^2 \int_\Omega \nabla \Phi^k \cdot \nabla \theta \, dx = \int_\Omega \Big(\sum_{i=1}^n z_i u_i^k + f \Big) \theta \, dx,$$

for all ϕ_i, $\theta \in H^2(\Omega) \cap H^1_{0,D}(\Omega)$. A density argument shows that we may take test functions ϕ_i, $\theta \in H^1_{0,D}(\Omega)$. The a priori estimates from Lemma 3.14 remain valid in the weak limit.

Now the limit $\tau \to 0$ can be done exactly as in step 4 of the existence proof for the continuous system of Section 2.3, which concludes the proof.

$\square$

4 Numerical Experiments

In this chapter we present two numerical test cases that show how the cross-diffusion system can be applied to simulate ion transport through channels. First, in Section 4.1 we describe the implementation of both numerical methods. In Section 4.2 we simulate a calcium-selective ion channel in two space dimensions. For this test case, we investigate the large-time behavior of the solutions as well as experimental convergence rates and compare the results obtained with both schemes. In Section 4.3 a bipolar ion channel is simulated, again in two space dimensions. The cross-diffusion model has not been applied yet to a test case of this sort, so we focus on the properties of the channel such as rectification of the ion current.

4.1 Implementation of the Numerical Schemes

The finite-volume scheme (3.7)-(3.8) is implemented using MATLAB, version R2017b. The nonlinear system defined by the implicit scheme is solved with a full Newton method in the variables u_0, u_i, Φ for every time step. Note that the simulations are performed with the full set of equations (1.6)-(1.7) without the simplifying assumptions (A1)-(A3) made in section 3.1 for the convergence analysis.

The finite-element discretization defined by equations (3.43)-(3.44) is realized with Python using the C++ based finite-element library NGSolve/Netgen, see [66, 67]. The nonlinear equations in every time step are solved using Newton's method in the variables w_i and Φ. The Jacobi matrix is computed using the NGSolve function `AssembleLinearization`.

The simulations are done with a fixed time step. The computations stop when a stationary state is approximately reached, i.e., when the discrete L^2 norm between the solutions at two consecutive time steps is smaller than 10^{-6}.

We remark that the finite-volume scheme also performs well when we use a simpler semi-implicit scheme, where we compute u from equation (3.7) with Φ taken from the previous time step via Newton's method and subsequently only need to solve a linear equation to compute the update for the potential. For the finite-element discretization, this approach is not feasible. Also, the computationally cheaper implementation used recently in [51] for a similar scheme in one space dimension, where a Newton and Piccard iteration are combined, did not work well in the 2D test cases presented in the following.

Adding the regularization term that is necessary for the existence analysis of the finite-element scheme seemed to make no distinguishable difference in the numerical simulations, therefore it was neglected for the computation of the results presented here.

4.2 Test Case 1: Calcium-Selective Ion Channel

Our first test case models the basic features of an L-type calcium channel (the letter L stands for "long-lasting", referring to the length of activation). This type of channel is of great biological importance, as it is present in the cardiac muscle and responsible for coordinating the contractions of the heart [18]. The selectivity for calcium in this channel protein is caused by the so-called EEEE-locus made up of four glutamate residues. We follow the modeling approach of [59], where the glutamate side chains are each treated as two half charged oxygen ions, accounting for a total of eight $O^{1/2-}$ ions confined to the channel. In contrast to [59], where the oxygen ions are described by hard spheres that are free to move inside the channel region, we make a further reduction and simply consider a constant density of oxygen in the channel that decreases linearly to zero in the baths:

$$u_{\text{ox}}(x,y) = u_{\text{ox,max}} \times \begin{cases} 1 & \text{for } 0.45 \leq x \leq 0.55, \\ 10\,(x-0.35) & \text{for } 0.35 \leq x \leq 0.45, \\ 10\,(0.65-x) & \text{for } 0.55 \leq x \leq 0.65, \\ 0 & \text{else,} \end{cases}$$

where the scaled maximal oxygen concentration equals $u_{\text{ox,max}} = (N_A/\tilde{u}) \cdot 52$ mol/L, where $N_A \approx 6.022 \cdot 10^{23}\,\text{mol}^{-1}$ is the Avogadro constant and $\tilde{u} = 3.7037 \cdot 10^{25} L^{-1}$ the typical concentration (taken from [16, Table 1]). In addition to the immobile oxygen ions, we consider three different species of ions whose concentration evolves according to the continuity equations (1.6): calcium (Ca^{2+}, u_1), sodium (Na^+, u_2), and chloride (Cl^-, u_3). We assume that the oxygen ions not only contribute to the permanent charge density $f = -u_{\text{ox}}/2$ in the Poisson equation (1.7), but also take up space in the channel, so that we have $u_0 = 1 - \sum_{i=1}^{3} u_i - u_{\text{ox}}$ for the solvent concentration.

As a simulation domain we take a simple geometric setup resembling the form of a channel, see Figure 4.1. The boundary conditions are as described in the introduction, with constant values for the ion concentrations and the electric potential in the baths. The physical parameters used in our simulations are taken from [16, Table 1 and Section 5.1] and are summarized in Table 4.2. The simulations are done with a constant time step size $\tau = 2e - 04$. The initial concentrations are simply taken as linear functions connecting the boundary values. An admissible mesh consisting of 74 triangles was created with MATLAB's `initmesh` command, which produces Delauney triangulations. Four finer meshes were obtained by regular refinement, dividing each triangle into four triangles of the same shape.

We remark that the same test case was already used in [17] to illustrate the efficiency of the finite-volume approximation. Furthermore, numerical simulations for a 1D approximation of the calcium channel can be found in [16] for stationary solutions and in [40] for transient solutions.

Figures 4.2 and 4.3 present the (scaled) solution to the ion transport model in the original variables u and Φ at two different times; the first one after only 600 time steps and the second one after 6000 time steps. The results are computed on the finest mesh with 18,944 elements with the finite-volume scheme. The stationary state is approximately reached after 7586 time steps, which corresponds to approximately 48 nanoseconds. The profiles depicted
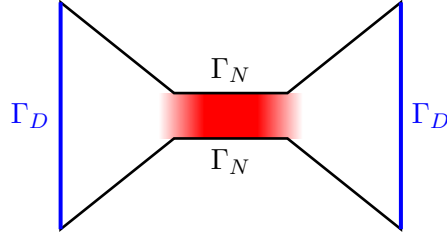
Figure 4.1: Schematic picture of the 2D domain Ω used for the simulations. Dirichlet boundary conditions are prescribed on Γ_D (blue), homogeneous Neumann boundary conditions on Γ_N (black). The red color represents the density of confined $O^{1/2-}$ ions. In scaled quantities, the domain's length equals 1 and its height equals 0.96. The channel's length equals 0.2 and its height 0.16.

Meaning	Value	Unit
Diffusion coefficient D_1	1	
Diffusion coefficient D_2	1.6835	
Diffusion coefficient D_3	2.5696	
Effective permittivity λ^2	4.6793e-4	
Effective mobility β	3.8682	
Bath concentration $\overline{u}_1$ left/right	8.1299e-05/0.0016	
Bath concentration $\overline{u}_2$ left/right	0.0016/0.0016	
Bath concentration $\overline{u}_3$ left/right	0.0016/0.0049	
Applied voltage $\overline{\Phi}$ left/right	-0.5/0	
Typical length $\tilde{L}$	5e-9	m
Typical concentration $\tilde{u}$	3.7037e+28	m^{-3}
Typical voltage $\tilde{\Phi}$	0.1	V
Typical diffusion $\tilde{D}$	7.9000e-10	m^{2}s^{-1}
Boltzmann constant k_B	1.3807e-23	JK^{-1}
Temperature θ	300	K
Avogadros constant N_A	6.0221e+23	mol^{-1}
Vacuum permittivity ϵ_0	8.8542e-12	Fm^{-1}
Relative permittivity ϵ_r	78.4	
Elementary charge e	1.6022e-19	C

Table 4.1: Dimensionless parameters used for the simulation of the calcium-selective ion channel and values used for the scaling (1.4).

in Figure 4.3 are already very close to the stationary state and correspond qualitatively well to the one-dimensional stationary profiles presented in [16]. We observe that during the evolution, sodium inside the channel is replaced by the stronger positively charged calcium ions. For higher initial calcium concentrations, the calcium selectivity of the channel acts immediately.
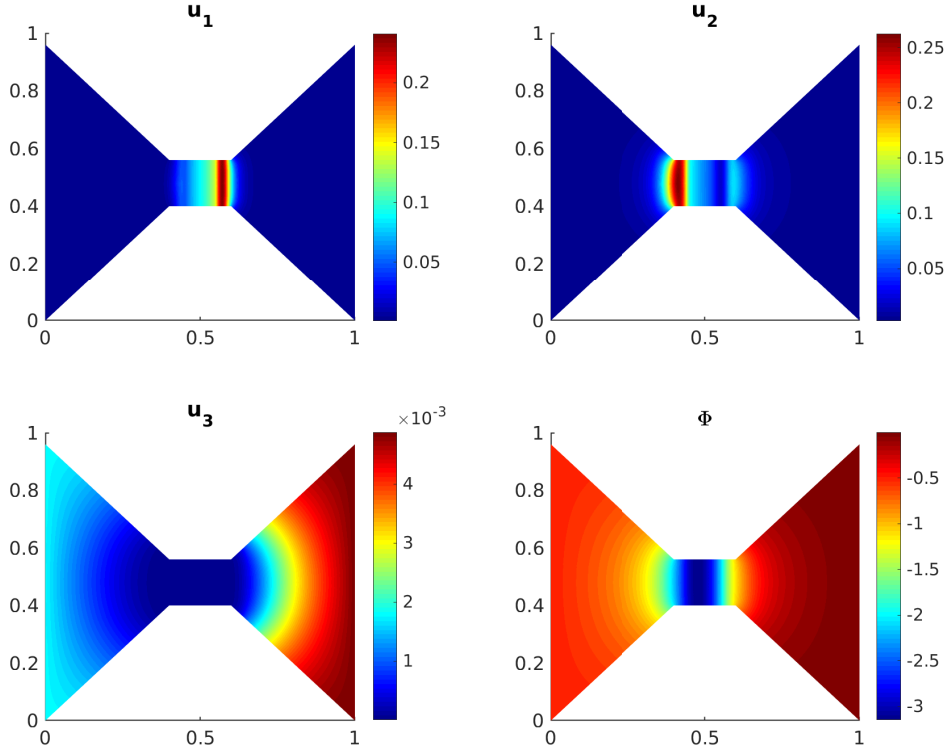

Figure 4.2: Solution after 600 time steps computed from the finite-volume scheme.

For a comparison with the finite-element solution, Figure 4.4 shows the concentration profiles and electric potential as computed with the finite-element scheme in the upper panel. In the lower panel, the difference between the finite-volume and finite-element solutions is plotted. We have omitted the plots for the third ion species (Cl^-), since it vanishes almost immediately from the channel due to its negative charge. While absolute differences are relatively small, we can still observe that the electric potential in the finite-element case is always higher compared to the finite-volume solution, while the peaks of the concentration profiles are more distinctive for the finite-element than for the finite-volume solution.

In order to compare the two numerical methods, we test the convergence of the schemes with respect to the mesh diameter. Since an exact solution to our problem is not available, we compute a reference solution both with the finite-volume and the finite-element scheme on a very fine mesh with 18,944 elements and maximal cell diameter $h \approx 0.01$. The differences between these reference solutions in the discrete L^1 and L^∞ norms are given in
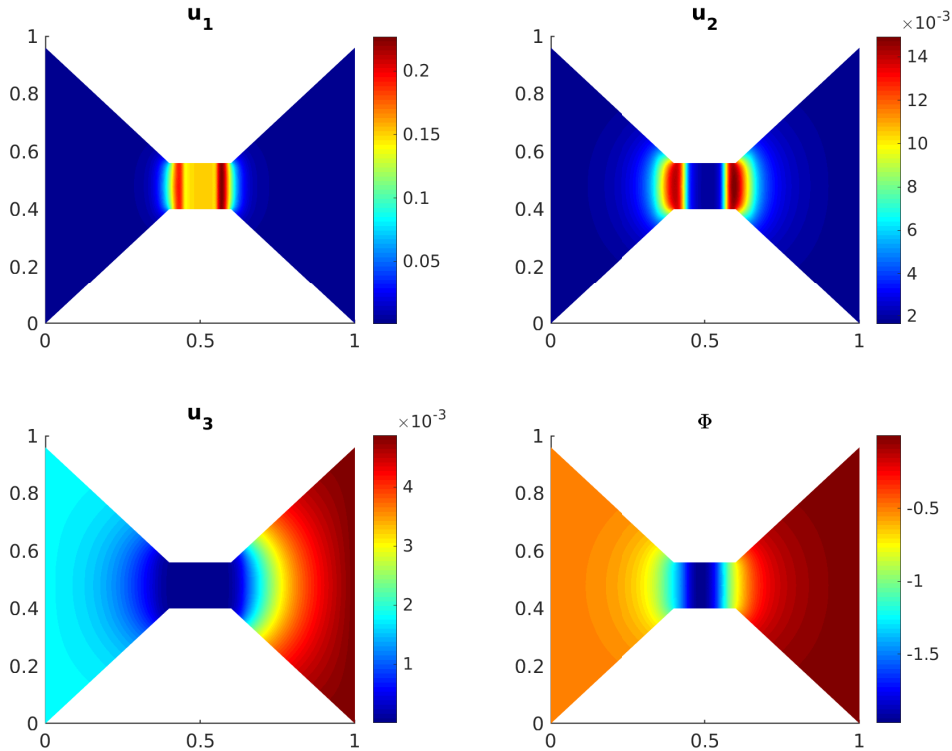
Figure 4.3: Solution after 6000 time steps (close to equilibrium) computed from the finite-volume scheme.

Table 4.2 for the various unknowns. Since the finite-element and finite-volume solutions are found in different function spaces, one has to be careful how to compare them. The values in Table 4.2 are obtained by projecting the finite-element solution onto the finite-volume space of functions that are constant on each cell in NGSolve, thereby introducing an additional error. However, the difference between the reference solutions is still reasonably small, especially when the simulations are already close to the equilibrium state.

To avoid the interpolation error in the convergence plots, we compare the approximate finite-element or finite-volume solutions on coarser nested meshes with the reference solutions computed with the corresponding method. In Figure 4.5, the errors in the discrete L^1 norm between the reference solution and the solutions on the coarser meshes at the two fixed time steps $k = 600$ and $k = 6000$ are plotted. For the finite-volume approximation, we clearly observe the expected first-order convergence in space, whereas for the finite-element method, the error decreases, again as expected, with h^2. These results serve as a validation for the theoretical convergence result proven for the finite-element scheme and show the efficiency of the finite-volume method even in the general case of ion transport, which is not covered by the convergence Theorem 3.13.

In Table 4.3, the average time needed to compute one time step with the finite-element or finite-volume scheme for the five nested meshes is given. Clearly, the finite-volume
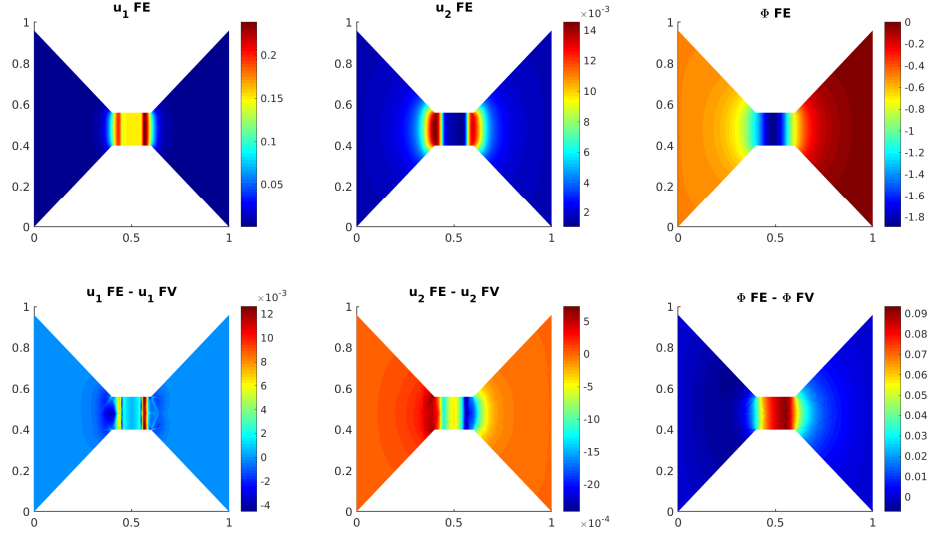
Figure 4.4: Solution after 6000 time steps (close to equilibrium) computed from the finite-element scheme (top) and difference between the finite-volume (FV) and finite-element (FE) solutions (bottom).

	u_1	u_2	u_3	u_0	Φ
L^∞ norm, $k = 600$	2.2405e-02	2.0052e-02	1.0319e-04	1.6695e-02	1.0600e-01
L^1 norm, $k = 600$	2.2642e-04	3.0275e-04	1.3776e-05	2.5983e-04	5.1029e-03
L^∞ norm, $k = 6000$	1.0036e-02	2.3619e-03	1.3677e-04	9.1095e-03	9.5080e-02
L^1 norm, $k = 6000$	1.4161e-04	7.0981e-05	1.5498e-05	1.5615e-04	4.6543e-03

Table 4.2: Difference between the finite-volume and finite-element reference solutions after 600 and after 6000 time steps.

scheme is much faster than the finite-element method. This is mostly due to the computationally expensive assembly of the finite-element matrices. In Figure 4.2, the difference in computational efficiency between the schemes is illustrated by plotting the relative error with respect to the reference solution for the solutions on the four coarser meshes over the average time needed to compute one time step. Even though the finite-element scheme converges with a higher rate, the finite-volume algorithm will reach a given error tolerance faster.

The simulations suggest that the solution tends towards a steady state as $t \to \infty$. The large-time behavior can be quantified by computing the relative entropy with respect to the steady state $(u_i^\infty, \Phi^\infty)$, which is obtained from the corresponding discretizations of the stationary equations with the same parameters and boundary data. In case of the
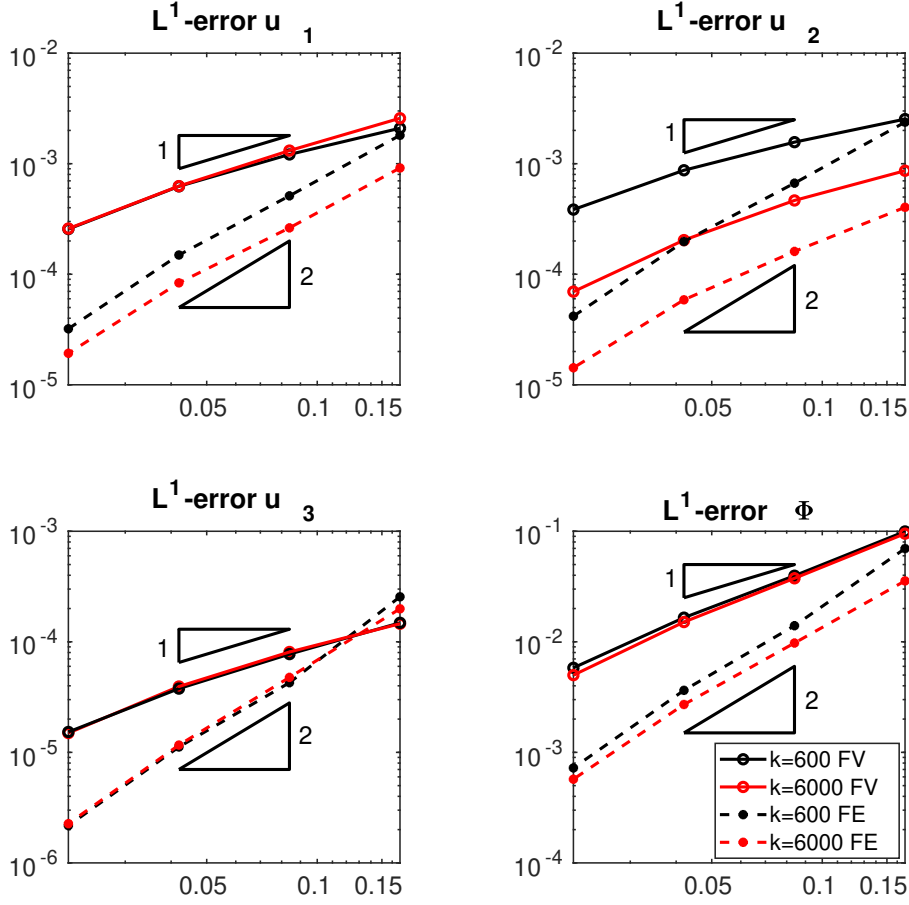
Figure 4.5: L^1-error relative to the reference solution after 600 (black) and after 6000 time steps (red) plotted over the mesh size h. Dashed lines are used for the FE solution, full lines for the FV solution.

finite-volume scheme, the relative entropy is computed for each time step as

$$\mathcal{H}^k = \sum_{K \in \mathcal{T}} \mathrm{m}(K) \sum_{i=0}^{n} u_{i,K}^k \log \left(\frac{u_{i,K}^k}{u_{i,K}^\infty} \right) + \frac{\lambda^2}{2} \sum_{\sigma \in \mathcal{E}} \tau_\sigma \mathrm{D}_{K,\sigma} (\Phi^k - \Phi^\infty)^2.$$

For the finite-element scheme we use the definition (2.1) of the relative entropy with the boundary data replaced by the steady state. The integrals are computed numerically in NGSolve.

Figure 4.7 shows the relative entropy and the L^1 error compared to the equilibrium state for the finite-element and finite-volume solutions on different meshes. Whereas for the coarsest mesh the convergence rates differ notably, we can observe a similar behavior when the mesh is reasonably fine. We note in any case that the relative entropy as well as the discrete L^1 norms of the concentrations and electric potential decay with exponential

	$\mathcal{T}_1$	$\mathcal{T}_2$	$\mathcal{T}_3$	$\mathcal{T}_4$	$\mathcal{T}_5$
FE	2.4065e-01	7.9982e-01	2.1125e+00	4.9844e+00	17.7788e+00
FV	6.7707e-03	2.2042e-02	3.0532e-01	1.7660e+00	2.2418e+00

Table 4.3: Average time needed to compute one time step (in seconds). FE = finite-element scheme, FV = finite-volume scheme.
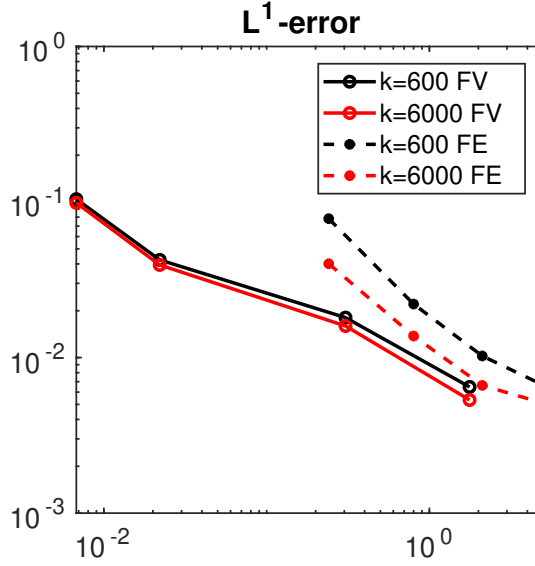

Figure 4.6: Sum of L^1-errors of u and Φ relative to the reference solution after 600 (black) and after 6000 time steps (red) plotted over the average time needed to compute one time step for the meshes $\mathcal{T}_1$-$\mathcal{T}_4$. Dashed lines are used for the FE solution, full lines for the FV solution.

rate. Interestingly, after some initial phase, the convergence is rather slow and increases after this intermediate phase. This phase can be explained by the degeneracy at $u_0 = 0$, which causes a small entropy production slowing down diffusion. Indeed, a small change in the oxygen concentration may prolong the intermediate phase of slow convergence drastically. Figure 4.8 depicts the relative entropy and L^1 error computed with the finite-volume method and a piecewise constant scaled oxygen concentration

$$u_{\text{ox}}(x,y) = \begin{cases} 0.79 & \text{for } 0.35 \leq x \leq 0.65, \\ 0 & \text{else.} \end{cases} \tag{4.1}$$

Compared to Figure 4.7, we observe that the solution needs nearly twice the amount of time to converge to the steady state since there is a long phase of small entropy production.

In Figure 4.9, we investigate the convergence of the relative entropy with respect to the mesh size. As before, we observe second-order convergence for the finite-element scheme and a first-order rate for the finite-volume method.
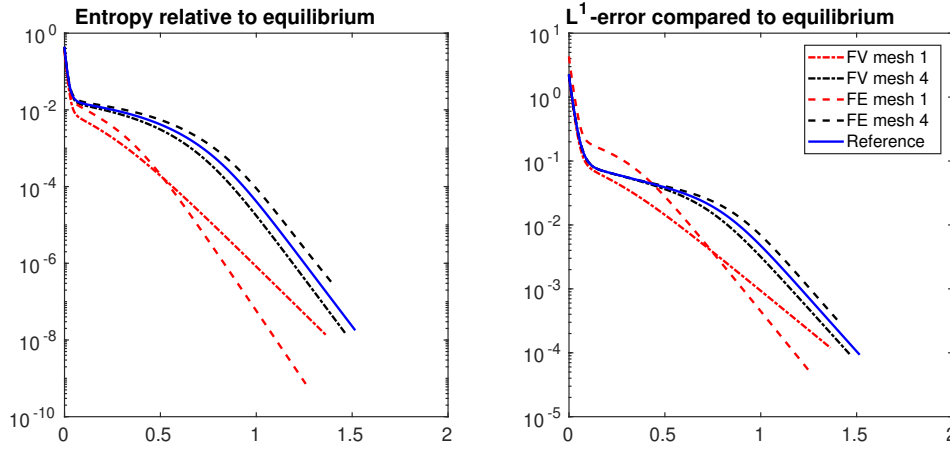
Figure 4.7: Relative entropy (left) and sum of L^1 differences of u and Φ relative to the equilibrium state (right) over time for various meshes. Mesh 1 has 74 triangles, mesh 4 has 18,944 elements.
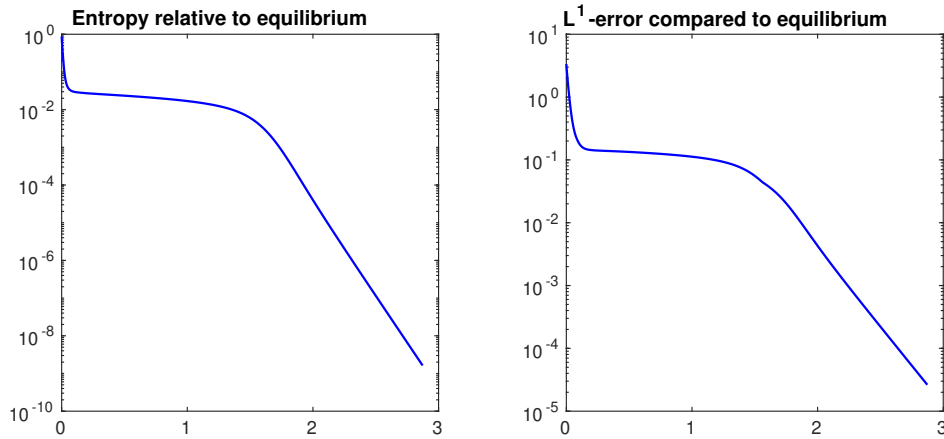

Figure 4.8: Relative entropy (left) and sum of L^1 differences of u and Φ relative to the equilibrium state (right) over time computed with the oxygen density (4.1).
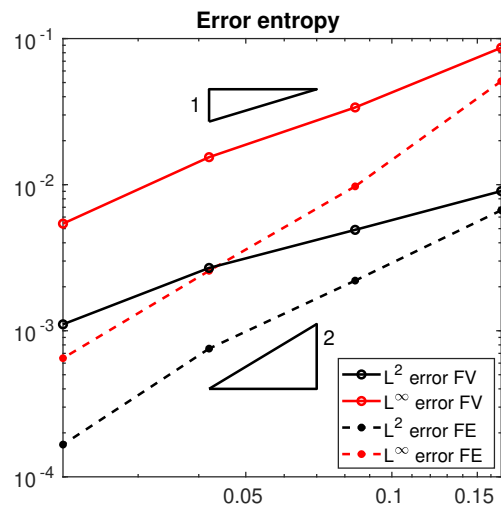
Figure 4.9: Error for the relative entropy with respect to mesh size.

4.3 Test Case 2: Bipolar Ion Channel

The second example models a pore with asymmetric charge distribution, which occurs naturally in biological ion channels but also in synthetic nanopores. Asymmetric pores typically rectify the ion current, meaning that the current measured for applied voltages of positive sign is higher than the current for the same absolute value of voltage with negative sign. The setup is similar to that of an N-P semiconductor diode. The N-region is characterized by the fixed positive charge. The anions are the counter-ions and thus the majority charge carriers, while the cations are the co-ions and minority charge carriers. In the P-region, the situation is exactly the other way around. In the on-state, the current is conducted by the majority carriers, whereas in the off-state, the minority carriers are responsible for the current, which leads to the rectification behavior.

Often, bipolar ion channels are modeled with asymmetric surface charge distributions on the channel walls. However, to fit these channels into the framework of our model, we follow the approach described in [43]. Similar to the first test case, we assume that there are eight confined molecules inside the channel, but this time four molecules are positively charged ($+0.5e$) and the other four molecules are negatively charged ($-0.5e$). The simulation domain $\Omega \subset \mathbb{R}^2$ is depicted in Figure 4.10. The shape of the domain and the parameters used for the simulations are taken from [43] and are summarized in Table 4.4. The mesh (made up of 2080 triangles) was created with NGSolve/Netgen. We consider two mobile species of ions, one cation (Na^+, u_1) and one anion (Cl^-, u_2). The confined ions are modeled as eight fixed circles of radius 1.4, where the concentration $c \equiv c_{max}$ is such that the portion of the channel occupied by these ions is the same as in the simulations in [43]. The solvent concentration then becomes $u_0 = 1 - u_1 - u_2 - c$.
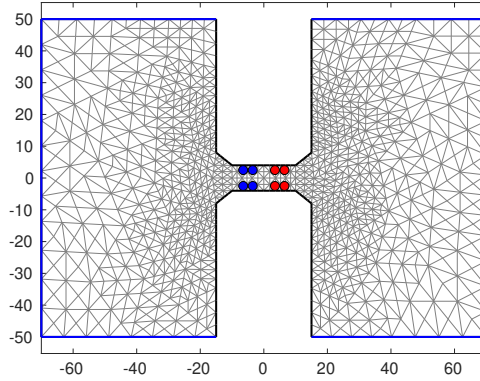

Figure 4.10: Simulation domain with triangulation for the bipolar ion channel. The blue circles represent positively charged confined ions, the red circles negatively charged ions. The black (blue) part of the boundary is equipped with Neumann (Dirichlet) boundary conditions.

By changing the boundary value $\overline{\Phi}_{right}$ for the potential Φ on the right part of the Dirichlet boundary (on the left side, it is fixed to zero), we can apply an electric field in

Meaning	Value	Unit
Diffusion coefficients D_1, D_2	1	
Effective permittivity λ^2	1.1713	
Effective mobility β	3.8922	
Bath concentrations $\overline{u_1}$, $\overline{u_2}$	0.0016	
Confined ion concentration c_{max}	0.2971	
Typical length $\tilde{L}$	1e-10	m
Typical concentration $\tilde{u}$	3.7037e+28	Nm^{-3}
Typical voltage $\tilde{\Phi}$	0.1	V
Typical diffusion $\tilde{D}$	1.3340e-9	m^2s^{-1}

Table 4.4: Dimensionless parameters used for the simulation of the bipolar ion channel and values used for the scaling.

forward bias (on-state, $\overline{\Phi}_{right} = 1$) or reverse bias (off-state, $\overline{\Phi}_{right} = -1$). Figures 4.11 and 4.12 show the stationary state computed with the finite-element method in the on- and off-state, respectively. Evidently, the ion concentrations in the on-state are much higher than in the off-state. In comparison with the results from [43], where the Poisson–Nernst–Planck equations with linear diffusion (referred to as the linear PNP model) were combined with Local Equilibrium Monte–Carlo simulations, we find that with the Poisson–Nernst–Planck equations with cross-diffusion (referred to as the nonlinear PNP model), even in the off-state, the charged ions in the channel attract an amount of ions higher than the bath concentrations.

We remark that the finite-volume scheme produces very similar concentration and potential profiles, therefore the pictures are omitted here. Simulations of the time-dependent equations show, as in the previous section, that the solution tends to the stationary state as $t \to \infty$. We could also observe the exponential decay of the relative entropy and the L^1 distance to the steady state.

From a modeling point of view, it is an important question whether the nonlinear PNP model reproduces the rectification mechanism described above. For this purpose, we need to calculate the electric current I flowing through the pore, given by

$$I = -\sum_i z_i \int_A \mathcal{F}_i \cdot \nu ds, \tag{4.2}$$

where A is the cross-section of the pore and ν the unit normal to A. In the finite-element setting, we can use the representation of the fluxes in entropy variables,

$$\mathcal{F}_i = D_i u_i(w, \Phi) u_0(w, \Phi) \nabla w_i,$$

and compute the integrals in (4.2) using a quadrature formula along the line $x = 10$.
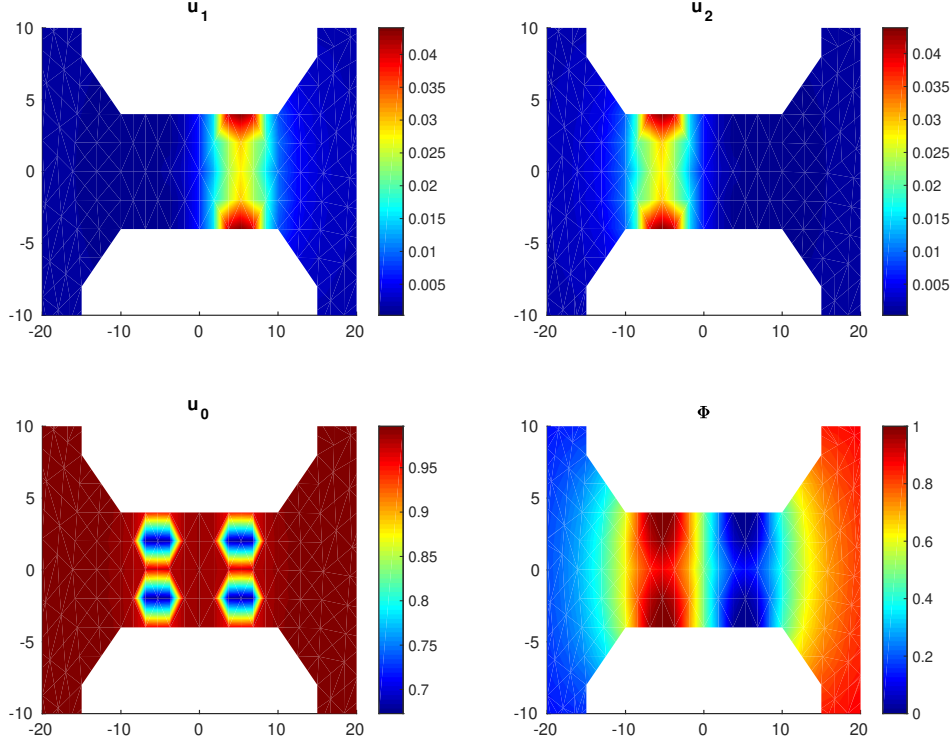
Figure 4.11: Stationary solution in the on-state (channel region).

Figure 4.13 shows the current-voltage curves obtained with the finite-element solutions. In addition, the rectification is depicted, which is calculated for voltages $U \geq 0$ according to

$$r(U) = \left| \frac{I(U)}{I(-U)} \right|.$$

We also compute the current-voltage curve for the linear PNP model, which is obtained from the model equations by setting $u_0 \equiv 1$, such that

$$\partial_t u_i = \operatorname{div} \left(D_i \nabla u_i + D_i \beta z_i u_i \nabla \Phi \right).$$

We expect from the simulations done in [16] for the calcium channel that the current of the nonlinear PNP model is lower than that one from the linear PNP model. This expectation is confirmed also in this case. As Figure 4.13 shows, the rectification is stronger in the nonlinear PNP model. The difference between the two models is even more pronounced when we increase the concentration of the confined ions to $c_{\max} = 0.7$. In that case, the channel gets more crowded and size exclusion has a bigger effect. We observe a significantly lower current and higher rectification for the nonlinear PNP model.
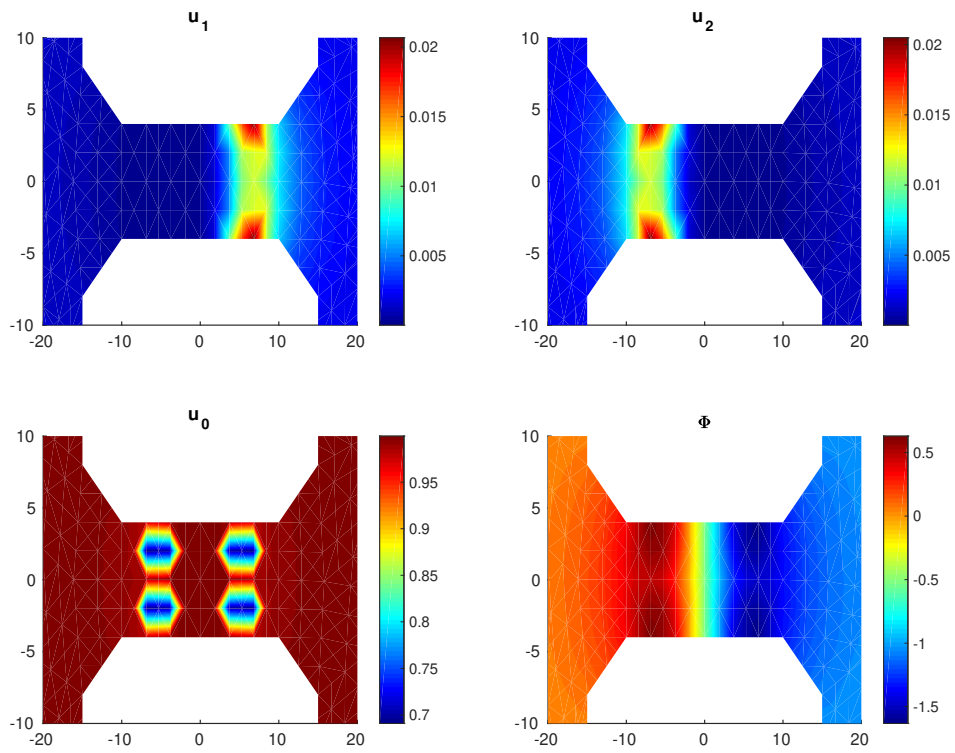
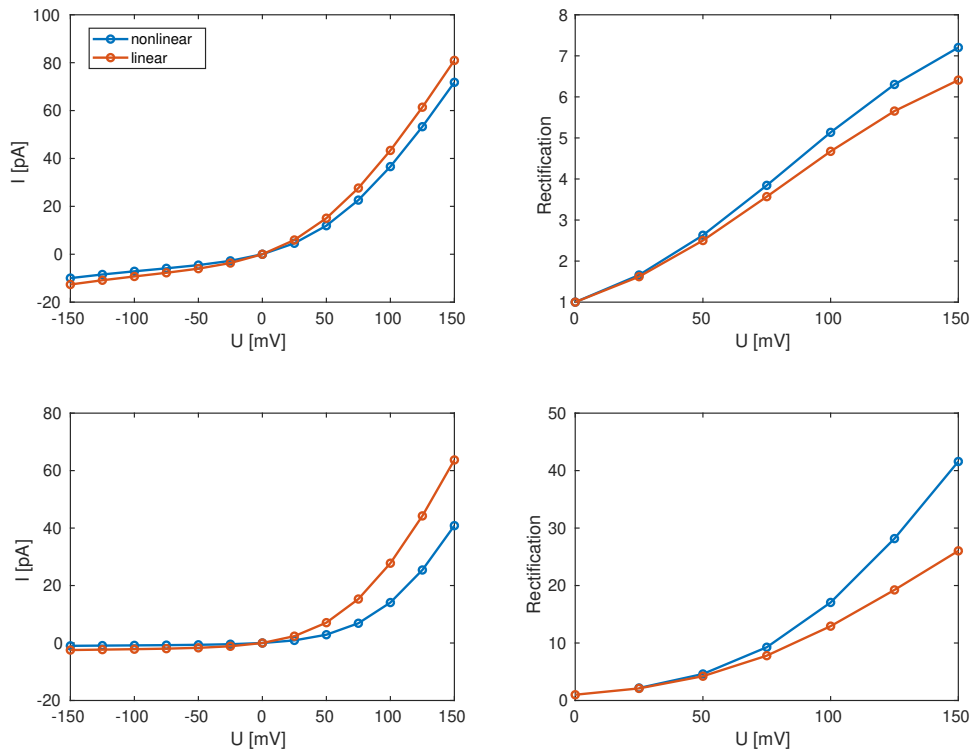Figure 4.12: Stationary solution in the off-state (channel region).

Figure 4.13: Current-voltage curves and rectification for the finite-element solution. First row: The parameters are as in Table 4.4; second row: with $c_{\max} = 0.7$.

5 Discussion and Outlook

Discussion

In this work, we have investigated a degenerate parabolic cross-diffusion model describing ion transport through channels, both from an analytic and numerical point of view. Regarding the existence analysis, we have closed a gap in the existing literature by proving the global-in-time existence of weak solutions to the full model. For this purpose, we have extended the boundedness-by-entropy method to mixed inhomogeneous boundary conditions and the drift term including the electric potential that is coupled via a Poisson equation. Furthermore, we have applied the method of Gajewski to conclude the uniqueness of weak solutions in the case that the ion species are indistinguishable.

Concerning the numerical approximation of the cross-diffusion system, we have presented two new schemes. Both rely on an implicit Euler discretization for the time derivative, but differ with respect to the spatial discretization. The first scheme is based on a finite-volume method, the second one on a finite-element method. In the following, we summarize the differences between both approaches from a theoretical viewpoint and our findings from the numerical experiments.

- **Structure of the scheme:** The finite-element scheme strongly relies on the entropy structure of the system and is formulated in the entropy variables. From a thermodynamic viewpoint, the entropy variables are related to the chemical potentials, which gives a clear connection to nonequilibrium thermodynamics. On the other hand, the finite-volume scheme exploits the drift-diffusion structure that the system displays in the original variables.

- L^∞ **bounds:** Due to the formulation in entropy variables, the L^∞ bounds for the finite-element solutions follow immediately from (2.4) without the use of a maximum principle. In other words, the lower and upper bounds are inherent in the entropy formulation. In the case of the finite-volume scheme, we can apply a discrete maximum principle, but only under the (restrictive) assumption that the diffusion coefficients D_i are the same.

- **Convergence analysis:** The entropy structure used in the finite-element scheme allows us to use the same mathematical techniques for the convergence proof as for the continuous system, but a regularizing term has to be added to ensure the existence of discrete solutions. The convergence for the finite-volume solution requires more restrictive assumptions. As stated above, equal diffusion constants are necessary for proving the L^∞ bounds and the existence of solutions. In addition, we can only obtain the entropy inequality and gradient estimates for vanishing potentials.

- **Initial data:** Since the initial concentrations have to be transformed to entropy variables via (2.3), the finite-element scheme can only be applied for initial data strictly greater than zero. The finite-volume scheme, on the other hand, can handle exactly vanishing initial concentrations.

- **Experimental convergence rate:** In the numerical experiments, both schemes exhibit the expected order of convergence with respect to mesh size (even if we cannot prove any rates analytically): first-order convergence for the finite-volume scheme and second-order convergence for the finite-element scheme.

- **Performance:** The numerical experiments done for this work suggest that the finite-element algorithm needs smaller time steps for the Newton iterations to converge than for the finite-volume scheme, especially when the solvent concentration is close to zero. Furthermore, the assembly of the finite-element matrices is computationally quite expensive resulting in longer running times compared to the finite-volume scheme.

- **Mesh requirements:** A finite-volume mesh needs to satisfy the admissibility condition. This might be a disadvantage for simulations in three space dimensions.

In short, the finite-element scheme allows for structure-preserving properties under natural assumptions, while the finite-volume scheme can be analyzed only under restrictive conditions. On the other hand, the finite-volume scheme allows for vanishing initial concentrations and faster algorithms compared to the finite-element scheme due to the highly nonlinear structure of the latter formulation.

We remark that we have extended the method of Gajewski to prove uniqueness in the finite-volume setting and have proved a new Aubin–Lions lemma of degenerate type, also for this fully discrete setting.

Outlook

We conclude this thesis by stating some open problems connected to this work that could be an inspiration for future research.

Modeling: One big limitation of the ion transport model used in this thesis is that the sizes of all ions are assumed to be equal. Therefore, the model is not able to capture selectivity phenomena that occur due to different ion sizes. The selectivity effects observed in the numerical simulations of the calcium channel are caused only by the different charges of the ions. In [65], a modification of the model that includes different ion sizes is described. The ions are assumed to be spheres of different radii. This leads to additional mathematical difficulties, since for example the explicit inversion of the relation between entropy variables and ion concentrations is lost. However, it is demonstrated that the model still possesses an entropy functional and a formal gradient flow structure, and that the inverse though not explicit still exists. This suggests that the boundedness-by-entropy method could still be applied in this case.

For an even more realistic description of ion channels, the coupling to other equations could be considered. For example, a thermodynamically consistent system of equations as

described in [27] could be used. Since the model used here only describes flow through an open channel, a coupling to equations that model the gating behavior of the channel might be of interest. These modifications however seem to increase the mathematical difficulty of the problem significantly.

Analysis: The longtime behavior of the ion transport system remains an important open question. As already mentioned in [16], if the boundary data is in equilibrium, meaning that $\nabla \overline{w}_i \equiv 0$, or equivalently $\overline{w}_i \equiv k_i$ with $k_i \in \mathbb{R}$, then there is a unique positive equilibrium state (u^∞, Φ^∞) determined by the Fermi-Dirac statistics

$$u_i^\infty = \frac{\exp(k_i - \beta z_i \Phi^\infty - W_i)}{1 + \sum_j \exp(k_j - \beta z_j \Phi^\infty - W_j)},$$

where Φ^∞ is the unique solution of the modified Poisson–Boltzmann equation

$$-\lambda^2 \Delta \Phi^\infty = \sum_{i=1}^n \frac{z_i \exp(k_i - \beta z_i \Phi^\infty - W_i)}{1 + \sum_j \exp(k_j - \beta z_j \Phi^\infty - W_j)} + f.$$

The usual strategy for proving convergence of the solution to the equilibrium is to consider a relative entropy with respect to the equilibrium state (as in (2.1) but with the boundary data replaced by the equilibrium). Then, one tries to show that the relative entropy tends to zero as $t \to \infty$. If now the difference between solution and equilibrium in a suitable norm can be bounded by the entropy, convergence can be concluded.

This strategy has been successfully applied to prove convergence to the equilibrium for the classic PNP model or drift-diffusion system, see for example [48]. For the modified PNP system considered in this thesis, there are only results for considerably reduced versions of the model. In [15], the strong L^1-convergence of the solution to equilibrium is proven, but under the condition that there is no electric potential and homogeneous Neumann boundary conditions only. In this special case, the unique equilibrium state is constant. This result, as it seems, cannot easily be extended to the full ion transport model.

As discussed in chapter 2, the time-discrete solution $(u_i^{(\tau)})$ may not converge strongly, so that we are not able to pass to the limit $\tau \to 0$ in the discrete entropy inequality (2.13). Consequently, we cannot prove that the relative entropy is decreasing along the solution and thus cannot use the strategy explained before. Even if we assume u_0 to be bounded from below uniformly by a positive constant which implies gradient estimates for u_i, there are still difficulties with the coupled potential. Therefore, the asymptotic analysis of the system seems for the moment out of reach. Nevertheless, the numerical simulations suggest interesting phenomena connected to the degeneracy of the diffusion matrix (see Figure 4.8) that call for the development of new techniques.

Numerics: In case of the finite-volume method, of course it would be desirable to find a modification of the scheme such that the analysis can be generalized to arbitrary diffusion coefficients and the coupled potential, which at the moment is not available to us.

For the finite-element scheme, the analysis is already done here for the full model. The main issue that remains is the need for the additional regularizing term. There might be a way to avoid this regularization based on the ideas of [61]. In this paper, a control

volume finite-element scheme for a degenerate nonlinear parabolic equation is proposed that converges without adding regularization. It could be interesting to try whether the technique used in this paper can be applied to the finite-element method proposed in this thesis.

A prospect for future research is to see whether the discretization methods presented here can be applied to similar PDE systems. In the recent preprint [28] an abstract approach for structure preserving schemes for dissipative problems is proposed, however without considering the questions of existence of solutions or convergence, so there is still a lot of work to be done towards a general discretization approach for such problems.

A further open question is whether it is possible to analytically prove the experimental convergence rates that were observed in the numerical experiments (see Figure 4.5).

Appendix A
Computation of the Entropy Variables

The first part of the Appendix is devoted to a (formal) computation of the entropy variables defined in (2.3).

Lemma 5.1. *Let*

$$h(u) = \sum_{i=0}^{n} \int_{\overline{u}_i}^{u_i} \log \frac{s}{\overline{u}_i} ds + \frac{\beta \lambda^2}{2} |\nabla(\Phi - \overline{\Phi})|^2 + \sum_{i=1}^{n} u_i W_i.$$

Then

$$\frac{\partial h}{\partial u_i} = \log \frac{u_i}{u_0} - \log \frac{\overline{u}_i}{\overline{u}_0} + \beta z_i (\Phi - \overline{\Phi}) + W_i, \quad i = 1, \dots, n.$$

Proof. It is clear that

$$\frac{\partial}{\partial u_i} \left(\sum_{i=0}^{n} \int_{\overline{u}_i}^{u_i} \log \frac{s}{\overline{u}_i} ds + \sum_{i=1}^{n} u_i W_i \right) = \log \frac{u_i}{\overline{u}_i} - \log \frac{u_0}{\overline{u}_0} + W_i.$$

Set $H_{\mathrm{el}}(u) = (\beta \lambda^2/2) \int_{\Omega} |\nabla \Psi[u]|^2 dx$, where $\Psi[u] = \Phi - \overline{\Phi}$. Recall that $\overline{\Phi}$ solves $-\lambda^2 \Delta \overline{\Phi} = f$ in Ω, $\nabla \overline{\Phi} \cdot \nu = 0$ on Γ_N. Then $\Psi[u]$ satisfies $-\lambda^2 \Delta \Psi[u] = \sum_{i=1}^{n} z_i u_i$ in Ω together with homogeneous mixed boundary conditions and, by the Poisson equation (1.7),

$$H_{\mathrm{el}}(u) = -\frac{\beta \lambda^2}{2} \int_{\Omega} \Delta \Psi[u] \Psi[u] dx = \frac{\beta}{2} \int_{\Omega} \sum_{i=1}^{n} z_i u_i \Psi[u] dx.$$

Set $h_{\mathrm{el}}(u) = (\beta/2) \sum_{i=1}^{n} z_i u_i \Psi[u]$. It remains to show that $\partial h_{\mathrm{el}}/\partial u_i = \beta z_i \Psi[u]$. For this, we observe that for any (smooth) functions $u = (u_i)$, $v = (v_i)$,

$$\int_{\Omega} \sum_{i=1}^{n} z_i u_i \Psi[v] dx = -\lambda^2 \int_{\Omega} \Delta \Psi[u] \Psi[v] dx = \lambda^2 \int_{\Omega} \nabla \Psi[u] \cdot \nabla \Psi[v] dx$$

$$= \int_{\Omega} \sum_{i=1}^{n} z_i v_i \Psi[u] dx. \tag{5.1}$$

Let e_i be the ith unit vector in $\mathbb{R}^n$ and w be a smooth scalar function. Then, using the

linearity of $u \mapsto \Psi[u]$ and (5.1),

$$\lim_{\varepsilon \to 0} \frac{1}{\varepsilon} \int_\Omega \left(h_{\mathrm{el}}(u + \varepsilon e_i w) - h_{\mathrm{el}}(u) - \varepsilon \beta z_i w \Psi[u] \right) dx$$

$$= \frac{\beta}{2} \int_\Omega \left(\sum_{j=1}^n z_j \delta_{ij} w \Psi[u] + \sum_{j=1}^n z_j u_j \Psi[e_i w] - 2 z_i w \Psi[u] \right)$$

$$= \frac{\beta}{2} \int_\Omega \left(z_i w \Psi[u] + \sum_{j=1}^n z_j \delta_{ij} w \Psi[u] - 2 z_i w \Psi[u] \right) dx = 0,$$

which shows the claim. $\qquad \square$

Appendix B
Some Compactness Results

In this part of the Appendix we summarize some non-standard compactness results that are used throughout this thesis. All of these theorems are generalizations of the Aubin–Lions lemma, that gives a criterion for compactness in Banach-space-valued L^p spaces for functions whose weak derivative is again in some Banach-space-valued L^q space. A basic version of the lemma is formulated as follows.

Theorem 5.2 (Aubin–Lions Lemma). *Let X, B and Y be Banach spaces with $X \subset B \subset Y$ and assume that $X \hookrightarrow B$ is compact and $B \hookrightarrow Y$ is continuous. Let $1 < p < \infty$, $1 < q < \infty$, and let X, Y be reflexive. Define the space*

$$W = \{u \in L^p(0, T; X) : u' \in L^q(0, T; Y)\}.$$

Then the inclusion $W \hookrightarrow L^p(0, T; B)$ is compact.

A proof of this statement can be found for example in [70, Proposition 1.3].

Semi-discrete Setting

We cite here two Aubin–Lions type lemmas that are formulated for the semi-discrete setting of the existence proof in Section 2.3. Recall that we consider functions $u^{(\tau)}(x, t)$ that are piecewise constant in time for a uniform partition of the time interval $(0, T)$ with step size τ, meaning that $u^{(\tau)}(x, t) = u^k(x)$ for $x \in \Omega$ and $t \in ((k-1)\tau, k\tau]$. The shift operator σ_τ is defined as $(\sigma_\tau u^{(\tau)})(\cdot, t) = u^{k-1}$ for $t \in ((k-1)\tau, k\tau]$.

The first result is formulated and proven in [26, Theorem 1].

Theorem 5.3. *Let X, B and Y be Banach spaces with $X \subset B \subset Y$ and assume that $X \hookrightarrow B$ is compact and $B \hookrightarrow Y$ is continuous. Let $1 \le p < \infty$ and let $(u^{(\tau)})$ be a family of piecewise constant in time functions that satisfy*

$$\tau^{-1}\|u^{(\tau)} - \sigma_\tau u^{(\tau)}\|_{L^1(\tau, T; Y)} + \|u^{(\tau)}\|_{L^p(0, T; X)} \le C \quad \text{for all } \tau > 0,$$

where $C > 0$ is a constant independent of τ. Then $(u^{(\tau)})$ is relatively compact in $L^p(0, T; B)$.

The second result is designed especially for situations where only degenerate estimates for the gradient of a function are available. A proof can be found in [49, Lemma 13].

Theorem 5.4. *Let $(y^{(\tau)})$ and $(z^{(\tau)})$ be families of piecewise constant in time functions that are bounded in $L^\infty(0, T; L^\infty(\Omega))$. Assume that (up to non-relabeled subsequences) $y_\tau \to y$*

strongly in $L^2(0, T; L^2(\Omega))$ and $z_\tau \rightharpoonup^* z$ weakly* in $L^\infty(0, T; L^\infty(\Omega))$ as $\tau \to 0$. Assume further that

$$\|y^{(\tau)} z^{(\tau)}\|_{L^2(0,T;H^1(\Omega))} + \|y^{(\tau)}\|_{L^2(0,T;H^1(\Omega))} \leq C,$$
$$\tau^{-1} \|z^{(\tau)} - \sigma_\tau z^{(\tau)}\|_{L^2(\tau,T;(H^1(\Omega))')} \leq C, \quad \text{for all } \tau > 0,$$

where $C > 0$ is a constant independent of τ. Then there exists a subsequence such that $y^{(\tau)} z^{(\tau)} \to yz$ strongly in $L^p(0, T; L^p(\Omega))$ for all $p < \infty$.

Note that if we assume in the previous result that $y^{(\tau)}$ is bounded from below by a positive constant, Theorem 5.4 would immediately follow from Theorem 5.3 since this would imply that $z^{(\tau)}$ is bounded uniformly in $L^2(0, T; H^1(\Omega))$. The strength of Theorem 5.4 lies in the fact that we obtain compactness even though we do not assume to have this gradient estimate for $z^{(\tau)}$.

Fully Discrete Setting

We prove two versions of discrete Aubin–Lions lemmas for the setting of the finite-volume scheme as defined in Section 3.1. The first one is a consequence of [39, Theorem 3.4], the second one extends Theorem 5.4 to the fully discrete case. The latter result is new. Recall that $\Omega_T = \Omega \times (0, T)$, $\nabla_m = \nabla_{\mathcal{T}_m, \triangle t_m}$ is the discrete gradient defined in (3.31), and $\partial_t^{\triangle t}$ is the discrete time derivative defined in (3.28).

Lemma 5.5 (Discrete Aubin–Lions). *Let $\| \cdot \|_{1, \mathcal{T}_m}$ be the norm on $\mathcal{H}_{\mathcal{T}_m}$ defined in (3.3) with the dual norm $\| \cdot \|_{-1, \mathcal{T}_m}$ given by (3.4), and let $(u_m) \subset \mathcal{H}_{\mathcal{T}_m, \triangle t_m}$ be a sequence of piecewise constants in time functions with values in $\mathcal{H}_{\mathcal{T}_m}$ satisfying*

$$\sum_{k=1}^{N_m} \triangle t \big(\|u_m^k\|_{1, \mathcal{T}_m}^2 + \|\partial_t^{\triangle t_m} u_m^k\|_{-1, \mathcal{T}_m}^2 \big) \leq C,$$

where $C > 0$ is independent of the size of the mesh and the time step size. Then there exists a subsequence, which is not relabeled, such that, as $m \to \infty$,

$$u_m \to u \quad \text{strongly in } L^2(\Omega_T),$$
$$\nabla_m u_m \rightharpoonup \nabla u \quad \text{weakly in } L^2(\Omega_T).$$

Proof. The result is a consequence of Theorem 3.4 in [39]. To apply this theorem, we have to show that the discrete norms $\| \cdot \|_{1, \mathcal{T}_m}$ and $\| \cdot \|_{-1, \mathcal{T}_m}$ satisfy the assumptions of Lemma 3.1 in [39]:

1. For any sequence $(v_m) \subset \mathcal{H}_{\mathcal{T}_m}$ such that there exists $C > 0$ with $\|v_m\|_{1, \mathcal{T}_m} \leq C$ for all $m \in \mathbb{N}$, there exists $v \in L^2(\Omega)$ such that, up to a subsequence, $v_m \to v$ in $L^2(\Omega)$.

2. If $v_m \to v$ strongly in $L^2(\Omega)$ and $\|v_m\|_{-1, \mathcal{T}_m} \to 0$ as $m \to \infty$, then $v = 0$.

The first property is proved in, for instance, [34, Lemma 5.6]. Here, we need assumption (3.2) on the mesh. The second property can be replaced, according to [39, Remark 6],

by the condition that $\| \cdot \|_{1,\mathcal{T}_m}$ and $\| \cdot \|_{-1,\mathcal{T}_m}$ are dual norms with respect to the $L^2(\Omega)$ norm, which is the case here. We infer that there exists a subsequence of (u_m), which is not relabeled, such that $u_m \to u$ strongly in $L^2(\Omega_T)$. The weak convergence of the discrete gradients can be proved as in Lemma 4.4 in [20]. Indeed, the boundedness of $(\nabla_m u_m)$ in L^2 implies the convergence to some function $\chi \in L^2(\Omega_T)$ (up to a subsequence). In order to show that $\chi = \nabla u$, it remains to verify that for all test functions $\phi \in C_0^\infty(\Omega_T; \mathbb{R}^d)$,

$$\int_0^T \int_\Omega \nabla_m u_m \cdot \phi \, dx dt + \int_0^T \int_\Omega u_m \operatorname{div} \phi \, dx dt \to 0 \quad \text{as } m \to \infty.$$

This limit follows from the definition of $\nabla_m u_m$ and the regularity of the mesh. We refer to [20, Lemma 4.4] for details. $\qquad\square$

Lemma 5.6 (Discrete Aubin–Lions of "degenerate" type). *Let (y_m) and (z_m) be sequences in $\mathcal{H}_{\mathcal{T}_m, \triangle t_m}$ which are bounded in $L^\infty(\Omega_T)$ and let (y_m) be relatively compact in $L^2(\Omega_T)$, i.e., up to a subsequence, $y_m \to y$ strongly in $L^2(\Omega_T)$ and $z_m \rightharpoonup^* z$ weakly* in $L^\infty(\Omega_T)$. Furthermore, suppose that, for some constant $C > 0$ independent of m,*

$$\sum_{k=1}^{N_m} \triangle t_m \big(\|y_m^k\|_{1,\mathcal{T}_m}^2 + \|y_m^k z_m^k\|_{1,\mathcal{T}_m}^2 + \|\partial_t^{\triangle t_m} z_m^k\|_{-1,\mathcal{T}_m}^2 \big) \leq C.$$

Then there exists a subsequence which is not relabeled such that $y_m z_m \to yz$ strongly in $L^2(\Omega_T)$ as $m \to \infty$.

Proof. The idea of the proof is to use the Kolmogorov–Riesz theorem [12, Theorem 4.26] as in the continuous case; see [15, Section 4.4] or [49, Lemma 13]. The discrete case, however, makes necessary some changes in the calculations. We need to show that

$$\lim_{(\xi,\tau) \to 0} \int_0^{T-\tau} \int_\omega \big((y_m z_m)(x+\xi, t+\tau) - (y_m z_m)(x,t) \big)^2 dx dt = 0 \qquad (5.2)$$

uniformly in m, where $\omega \subset \Omega$ satisfies $x + \xi \in \Omega$ for all $x \in \omega$. First, we separate the space and time translation:

$$\int_0^{T-\tau} \int_\omega \big((y_m z_m)(x+\xi, t+\tau) - (y_m z_m)(x,t) \big)^2 dx dt$$

$$\leq 2 \int_0^{T-\tau} \int_\omega \big((y_m z_m)(x+\xi, t+\tau) - (y_m z_m)(x, t+\tau) \big)^2 dx dt$$

$$+ 2 \int_0^{T-\tau} \int_\omega \big((y_m z_m)(x, t+\tau) - (y_m z_m)(x,t) \big)^2 dx dt =: I_1 + I_2.$$

For the estimate of I_1, we apply a result for space translations of piecewise constant functions v with uniform bounds in the discrete $H^1(\Omega)$ norm, namely

$$\|v(\cdot + \xi) - v\|_{L^2(\Omega)}^2 \leq |\xi| \big(|\xi| + Ch(\mathcal{T}) \big) \|v\|_{1,\mathcal{T}}^2$$

for appropriate ξ, where $C > 0$ only depends on Ω [32, Lemma 4]. This shows that

$$I_1 \leq C_1 |\xi| \big(|\xi| + Ch(\mathcal{T}_m) \big)$$

converges to zero as $\xi \to 0$ uniformly in m.

For the second integral I_2, we write

$$I_2 \leq 4 \int_0^{T-\tau} \int_\omega z_m(x, t+\tau)^2 \big(y_m(x, t+\tau) - y_m(x, t)\big)^2 dxdt$$
$$+ 4 \int_0^{T-\tau} \int_\omega y_m(x, t)^2 \big(z_m(x, t+\tau) - z_m(x, t)\big)^2 dxdt =: I_{21} + I_{22}.$$

The L^∞ bounds on z_m give

$$I_{21} \leq C \int_0^{T-\tau} \int_\omega \big(y_m(x, t+\tau) - y_m(x, t)\big)^2 dxdt.$$

By assumption, the sequence (y_m) is relatively compact in $L^2(\Omega_T)$. Therefore, we can apply the inverse of the Kolmogorov–Riesz theorem [12, Exercise 4.34] to conclude that I_{21} converges to zero as $\tau \to 0$ uniformly in m.

The analysis of I_{22} is more involved. We split the integral in several parts:

$$I_{22} = \int_0^{T-\tau} \int_\omega y_m(x, t)^2 z_m(x, t) \big(z_m(x, t) - z_m(x, t+\tau)\big) dxdt$$
$$+ \int_0^{T-\tau} \int_\omega y_m(x, t+\tau)^2 z_m(x, t+\tau) \big(z_m(x, t+\tau) - z_m(x, t)\big) dxdt$$
$$+ \int_0^{T-\tau} \int_\omega \big(y_m(x, t)^2 - y_m(x, t+\tau)^2\big) z_m(x, t+\tau) \big(z_m(x, t+\tau) - z_m(x, t)\big) dxdt$$
$$=: J_1 + J_2 + J_3.$$

The first two integrals J_1 and J_2 are treated similarly as in [11, Lemma 3.11]. Indeed, let $\lceil s \rceil$ denote the smallest integer larger or equal to s. Defining $n_m(t) := \lceil t/\triangle t_m \rceil$, we can formulate

$$z_m(x, t+\tau) - z_m(x, t) = \sum_{k=n_m(t)+1}^{n_m(t+\tau)} \big(z_{m,K}^k - z_{m,K}^{k-1}\big)$$

for $x \in K$, $0 \leq t \leq T - \tau$. With this formulation, we can bound J_1, using the duality of

$\| \cdot \|_{1,\mathcal{T}_m}$ and $\| \cdot \|_{-1,\mathcal{T}_m}$:

$$J_1 \leq \int_0^{T-\tau} \left(\sum_{K \in \mathcal{T}_m} \mathrm{m}(K) \big(y_{m,K}^{n_m(t)}\big)^2 z_{m,K}^{n_m(t)} \sum_{k=n_m(t)+1}^{n_m(t+\tau)} \big(z_{m,K}^{k-1} - z_{m,K}^k\big) \right) dt$$

$$\leq \int_0^{T-\tau} \left(\sum_{k=n_m(t)+1}^{n_m(t+\tau)} \big\|(y_m^{n_m(t)})^2 z_m^{n_m(t)}\big\|_{1,\mathcal{T}_m} \big\|z_m^k - z_m^{k-1}\big\|_{-1,\mathcal{T}_m} \right) dt$$

$$\leq \frac{1}{2} \int_0^{T-\tau} \sum_{k=n_m(t)+1}^{n_m(t+\tau)} \triangle t_m \big\|(y_m^{n_m(t)})^2 z_m^{n_m(t)}\big\|_{1,\mathcal{T}_m}^2 dt$$

$$+ \frac{1}{2} \int_0^{T-\tau} \sum_{k=n_m(t)+1}^{n_m(t+\tau)} \frac{1}{\triangle t_m} \big\|z_m^k - z_m^{k-1}\big\|_{-1,\mathcal{T}_m}^2 dt$$

$$\leq \frac{\tau}{2} \sum_{k=1}^{N_m} \triangle t_m \big\|(y_m^k)^2 z_m^k\big\|_{1,\mathcal{T}_m}^2 + \frac{\tau}{2} \sum_{k=1}^{N_m} \frac{1}{\triangle t_m} \big\|z_m^k - z_m^{k-1}\big\|_{-1,\mathcal{T}_m}^2,$$

where the last inequality follows from [4, Lemmas 4.1 and 4.2]. Let us remark that, for all $\sigma = K|L \in \mathcal{E}_{\mathrm{int}}$, we can rewrite

$$(y_K)^2 z_K - (y_L)^2 z_L = \frac{y_K + y_L}{2}(y_K z_K - y_L z_L) + \frac{y_K z_K + y_L z_L}{2}(y_K - y_L).$$

Then,

$$\|(y_m^k)^2 z_m^k\|_{1,\mathcal{T}_m}^2 \leq \mathrm{m}(\Omega) \|(y_m^k)^2 z_m^k\|_{L^\infty(\Omega)}^2 + \|y_m^k\|_{L^\infty(\Omega)} \|y_m^k z_m^k\|_{1,\mathcal{T}_m} + \|y_m^k z_m^k\|_{L^\infty(\Omega)} \|y_m^k\|_{1,\mathcal{T}_m}.$$

Hence, $J_1 \leq C\tau$ for some $C > 0$. An analogous estimation leads to $J_2 \leq C\tau$. It remains to estimate the integral J_3. For this, we use, similar to the treatment of I_{21}, the L^∞ bounds on y_m and z_m:

$$J_3 \leq C \int_0^{T-\tau} \int_\omega \big|y_m(x, t+\tau) - y_m(x, t)\big| dx dt.$$

This expression converges to zero uniformly in m because of the relative compactness of (y_m) in $L^2(\Omega_T)$.

We deduce from the previous computations that (5.2) holds true. Therefore, the product $(y_m z_m)$ converges strongly in $L^2(\Omega_T)$, up to some subsequence, and in view of the convergences $y_m \to y$ strongly in $L^2(\Omega_T)$ and $z_m \rightharpoonup^* z$ weakly* in $L^\infty(0,T; L^\infty(\Omega))$, the limit of $(y_m z_m)$ equals yz, which finishes the proof. $\qquad\square$

Bibliography

[1] V. Anaya, M. Bendahmane, M. Langlais, and M. Sepúlveda. A convergent finite volume method for a model of indirectly transmitted diseases with nonlocal cross-diffusion. *Comput. Math. Appl.*, 70(2):132–157, 2015.

[2] V. Anaya, M. Bendahmane, and M. Sepúlveda. Numerical analysis for a three interacting species model with nonlocal and cross diffusion. *ESAIM Math. Model. Numer. Anal.*, 49(1):171–192, 2015.

[3] B. Andreianov, M. Bendahmane, and R. Ruiz-Baier. Analysis of a finite volume method for a cross-diffusion model in population dynamics. *Math. Models Methods Appl. Sci.*, 21(2):307–344, 2011.

[4] O. Angelini, K. Brenner, and D. Hilhorst. A finite volume method on general meshes for a degenerate parabolic convection-reaction-diffusion equation. *Numer. Math.*, 123(2):219–257, 2013.

[5] C. Baiocchi and A. Capelo. *Variational and quasivariational inequalities.* A Wiley-Interscience Publication. John Wiley & Sons, Inc., New York, 1984. Applications to free boundary problems, Translated from the Italian by Lakshmi Jayakar.

[6] J. W. Barrett and J. F. Blowey. Finite element approximation of a nonlinear cross-diffusion population model. *Numer. Math.*, 98(2):195–221, 2004.

[7] J. Berendsen, M. Burger, and J.-F. Pietschmann. On a cross-diffusion model for multiple species with nonlocal interaction and size exclusion. *Nonlinear Analysis*, 159:10–39, 2017.

[8] M. Bessemoulin-Chatard, C. Chainais-Hillairet, and F. Filbet. On discrete functional inequalities for some finite volume schemes. *IMA J. Numer. Anal.*, 35(3):1125–1149, 2015.

[9] M. Bessemoulin-Chatard and A. Jüngel. A finite volume scheme for a Keller-Segel model with additional cross-diffusion. *IMA J. Numer. Anal.*, 34(1):96–122, 2014.

[10] D. Bothe. On the Maxwell-Stefan approach to multicomponent diffusion. In *Parabolic problems*, volume 80 of *Progr. Nonlinear Differential Equations Appl.*, pages 81–93. Birkhäuser/Springer Basel AG, Basel, 2011.

[11] K. Brenner and R. Masson. Convergence of a vertex centered discretization of two-phase Darcy flows on general meshes. *Int. J. Finite Vol.*, 10:1–37, 2013.

[12] H. Brezis. *Functional analysis, Sobolev spaces and partial differential equations*. Universitext. Springer, New York, 2011.

[13] M. Bruna, M. Burger, H. Ranetbauer, and M.-T. Wolfram. Cross-diffusion systems with excluded-volume effects and asymptotic gradient flow structures. *J. Nonlinear Sci.*, 27(2):687–719, 2017.

[14] M. Bruna and S. J. Chapman. Diffusion of multiple species with excluded-volume effects. *The Journal of chemical physics*, 137(20):204116, 2012.

[15] M. Burger, M. Di Francesco, J.-F. Pietschmann, and B. Schlake. Nonlinear cross-diffusion with size exclusion. *SIAM J. Math. Anal.*, 42(6):2842–2871, 2010.

[16] M. Burger, B. Schlake, and M.-T. Wolfram. Nonlinear Poisson-Nernst-Planck equations for ion flux through confined geometries. *Nonlinearity*, 25(4):961–990, 2012.

[17] C. Cancès, C. Chainais-Hillairet, A. Gerstenmayer, and A. Jüngel. Finite-volume scheme for a degenerate cross-diffusion model motivated from ion transport. *Numerical Methods for Partial Differential Equations*.

[18] E. Carafoli, L. Santella, D. Branca, and M. Brini. Generation, control, and processing of cellular calcium signals. *Critical reviews in biochemistry and molecular biology*, 36(2):107–260, 2001.

[19] J. A. Carrillo, F. Filbet, and M. Schmidtchen. Convergence of a finite volume scheme for a system of interacting species with cross-diffusion. *arXiv preprint arXiv:1804.04385*, 2018.

[20] C. Chainais-Hillairet, J.-G. Liu, and Y.-J. Peng. Finite volume scheme for multidimensional drift-diffusion equations and convergence analysis. *M2AN Math. Model. Numer. Anal.*, 37(2):319–338, 2003.

[21] M. Chapwanya, J. M.-S. Lubuma, and R. E. Mickens. Positivity-preserving nonstandard finite difference schemes for cross-diffusion equations in biosciences. *Comput. Math. Appl.*, 68(9):1071–1082, 2014.

[22] P. G. Ciarlet. *The finite element method for elliptic problems*. North-Holland Publishing Co., Amsterdam-New York-Oxford, 1978. Studies in Mathematics and its Applications, Vol. 4.

[23] B. Corry, S. Kuyucak, and S.-H. Chung. Tests of continuum theories as models of ion channels. ii. Poisson–Nernst–Planck theory versus Brownian dynamics. *Biophysical Journal*, 78(5).

[24] P. Degond, S. Génieys, and A. Jüngel. A system of parabolic equations in nonequilibrium thermodynamics including thermal and electrical effects. *Journal de mathématiques pures et appliquées*, 76(10):991–1015, 1997.

[25] K. Deimling. *Nonlinear functional analysis*. Springer-Verlag, Berlin, 1985.

[26] M. Dreher and A. Jüngel. Compact families of piecewise constant functions in $L^p(0, T; B)$. *Nonlinear Anal.*, 75(6):3072–3077, 2012.

[27] W. Dreyer, C. Guhlke, and R. Müller. Overcoming the shortcomings of the Nernst–Planck model. *Physical Chemistry Chemical Physics*, 15(19):7075–7086, 2013.

[28] H. Egger. Structure preserving approximation of dissipative evolution problems. *arXiv preprint arXiv:1804.08648*, 2018.

[29] B. Eisenberg, Y. Hyon, and C. Liu. A mathematical model for the hard sphere repulsion in ionic solutions. *Communications in Mathematical Sciences*, 9(2):459–475, 2011.

[30] R. Eisenberg. Computing the field in proteins and channels. *The Journal of membrane biology*, 150(1):1–25, 1996.

[31] R. Eymard, T. Gallouët, M. Ghilani, and R. Herbin. Error estimates for the approximate solutions of a nonlinear hyperbolic equation given by finite volume schemes. *IMA J. Numer. Anal.*, 18(4):563–594, 1998.

[32] R. Eymard, T. Gallouët, and R. Herbin. Convergence of finite volume schemes for semilinear convection diffusion equations. *Numer. Math.*, 82(1):91–116, 1999.

[33] R. Eymard, T. Gallouët, and R. Herbin. Finite volume methods. In *Handbook of numerical analysis, Vol. VII*, Handb. Numer. Anal., VII, pages 713–1020. North-Holland, Amsterdam, 2000.

[34] R. Eymard, T. Gallouët, and R. Herbin. Finite volume methods. schemes and analysis. course at the university of wroclaw., 2008. URL: `http://www.math.uni.wroc.pl/~olech/courses/skrypt_Roberta_wroclaw.pdf`.

[35] M. Frittelli, A. Madzvamuse, I. Sgura, and C. Venkataraman. Lumped finite elements for reaction–cross-diffusion systems on stationary surfaces. *Comput. Math. Appl.*, 74(12):3008–3023, 2017.

[36] H. Gajewski. On a variant of monotonicity and its application to differential equations. *Nonlinear Anal.*, 22(1):73–80, 1994.

[37] H. Gajewski and I. V. Skrypnik. To the uniqueness problem for nonlinear parabolic equations. *Discrete Contin. Dyn. Syst.*, 10(1-2):315–336, 2004. Partial differential equations and applications.

[38] G. Galiano and V. Selgas. On a cross-diffusion segregation problem arising from a model of interacting particles. *Nonlinear Anal. Real World Appl.*, 18:34–49, 2014.

[39] T. Gallouët and J.-C. Latché. Compactness of discrete approximate solutions to parabolic PDEs—application to a turbulence model. *Commun. Pure Appl. Anal.*, 11(6):2371–2391, 2012.

[40] A. Gerstenmayer and A. Jüngel. Analysis of a degenerate parabolic cross-diffusion system for ion transport. *J. Math. Anal. Appl.*, 461(1):523–543, 2018.

[41] D. Gillespie, W. Nonner, and R. S. Eisenberg. Coupling Poisson–Nernst–Planck and density functional theory to calculate ion flux. *Journal of Physics: Condensed Matter*, 14(46):12129–12145, 2002.

[42] A. Glitzky and R. Hünlich. Global existence result for pair diffusion models. *SIAM J. Math. Anal.*, 36(4):1200–1225, 2005.

[43] Z.Ható, D. Boda, D. Gillespie, J. Vrabec, G. Rutkai, and T. Kristóf. Simulation study of a rectifying bipolar ion channel: Detailed model versus reduced model. *Condens. Matter Phys.*, 19(1):13802, 2016.

[44] B. Hille et al. *Ion channels of excitable membranes*, volume 507. Sinauer Sunderland, MA, 2001.

[45] A. L. Hodgkin and A. F. Huxley. A quantitative description of membrane current and its application to conduction and excitation in nerve. *The Journal of physiology*, 117(4):500–544, 1952.

[46] T.-L. Horng, T.-C. Lin, C. Liu, and B. Eisenberg. PNP equations with steric effects: a model of ion flow through channels. *The Journal of Physical Chemistry B*, 116(37):11422–11441, 2012.

[47] T. L. Jackson and H. M. Byrne. A mechanical model of tumor encapsulation and transcapsular spread. *Math. Biosci.*, 180:307–328, 2002. John A. Jacquez memorial volume.

[48] A. Jüngel. Qualitative behavior of solutions of a degenerate nonlinear drift-diffusion model for semiconductors. *Math. Models Methods Appl. Sci.*, 5(4):497–518, 1995.

[49] A. Jüngel. The boundedness-by-entropy method for cross-diffusion systems. *Nonlinearity*, 28(6):1963–2001, 2015.

[50] A. Jüngel. *Entropy methods for diffusive partial differential equations*. BCAM Springer Briefs. Springer, 2016.

[51] A. Jüngel and O. Leingang. Convergence of an implicit Euler Galerkin scheme for Poisson-Maxwell-Stefan systems. *arXiv preprint arXiv:1809.00413*, 2018.

[52] A. Jüngel and S. Schuchnigg. Entropy-dissipating semi-discrete Runge-Kutta schemes for nonlinear diffusion equations. *Commun. Math. Sci.*, 15(1):27–53, 2017.

[53] B. Lu, M. J. Holst, J. A. McCammon, and Y. C. Zhou. Poisson-Nernst-Planck equations for simulating biomolecular diffusion-reaction processes I: finite element solutions. *J. Comput. Phys.*, 229(19):6979–6994, 2010.

[54] C. Maffeo, S. Bhattacharya, J. Yoo, D. Wells, and A. Aksimentiev. Modeling and simulation of ion channels. *Chemical reviews*, 112(12):6250–6284, 2012.

[55] H. Murakawa. A linear finite volume method for nonlinear cross-diffusion systems. *Numer. Math.*, 136(1):1–26, 2017.

[56] B. Nadler, Z. Schuss, A. Singer, and R. S. Eisenberg. Ionic diffusion through confined geometries: from Langevin equations to partial differential equations. *Journal of Physics: Condensed Matter*, 16(22):S2153, 2004.

[57] E. Neher and B. Sakmann. Single-channel currents recorded from membrane of denervated frog muscle fibres. *Nature*, 260(5554):799, 1976.

[58] W. Nernst. Zur kinetik der in lösung befindlichen körper. *Zeitschrift für physikalische Chemie*, 2(1):613–637, 1888.

[59] W. Nonner, D. Gillespie, D. Henderson, and B. Eisenberg. Ion accumulation in a biological calcium channel: effects of solvent and confining pressure. *The Journal of Physical Chemistry B*, 105(27):6427–6436, 2001.

[60] A. A. H. Oulhaj. Numerical analysis of a finite volume scheme for a seawater intrusion model with cross-diffusion in an unconfined aquifer. *Numer. Methods Partial Differential Equations*, 34(3):857–880, 2018.

[61] A. A. H. Oulhaj, C. Cancès, and C. Chainais-Hillairet. Numerical analysis of a nonlinearly stable and positive control volume finite element scheme for richards equation with anisotropy. 2016.

[62] A. Prohl and M. Schmuck. Convergent discretizations for the Nernst-Planck-Poisson system. *Numer. Math.*, 111(4):591–630, 2009.

[63] K. Rahman and H. J. Eberl. Numerical treatment of a cross-diffusion model of biofilm exposure to antimicrobials. In *Parallel processing and applied mathematics. Part I*, volume 8384 of *Lecture Notes in Comput. Sci.*, pages 134–144. Springer, Heidelberg, 2014.

[64] K. A. Rahman, R. Sudarsan, and H. J. Eberl. A mixed-culture biofilm model with cross-diffusion. *Bull. Math. Biol.*, 77(11):2086–2124, 2015.

[65] B. A. Schlake. Mathematical models for particle transport: Crowded motion. *Westfälische Wilhelms-Universität Münster*, 2011.

[66] J. Schöberl. NETGEN An advancing front 2D/3D-mesh generator based on abstract rules. *Computing and Visualization in Science*, 1(1):41–52, 1997.

[67] J. Schöberl. C++11 implementation of finite elements in NGSolve. Technical Report ASC-2014-30, Institute for Analysis and Scientific Computing, September 2014.

[68] E. Shamir. Regularization of mixed second-order elliptic problems. *Israel J. Math.*, 6:150–168, 1968.

[69] N. Shigesada, K. Kawasaki, and E. Teramoto. Spatial segregation of interacting species. *J. Theoret. Biol.*, 79(1):83–99, 1979.

[70] R. E. Showalter. *Monotone operators in Banach space and nonlinear partial differential equations*, volume 49 of *Mathematical Surveys and Monographs*. American Mathematical Society, Providence, RI, 1997.

[71] M. J. Simpson, K. A. Landman, and B. D. Hughes. Multi-species simple exclusion processes. *Physica A: Statistical Mechanics and its Applications*, 388(4):399–406, 2009.

[72] R. Temam. *Infinite-dimensional dynamical systems in mechanics and physics*, volume 68 of *Applied Mathematical Sciences*. Springer-Verlag, New York, second edition, 1997.

[73] G. M. Troianiello. *Elliptic differential equations and obstacle problems*. The University Series in Mathematics. Plenum Press, New York, 1987.

[74] W. Van Roosbroeck. Theory of the flow of electrons and holes in germanium and other semiconductors. *Bell System Technical Journal*, 29(4):560–607, 1950.

[75] V. K. Vanag and I. R. Epstein. Cross-diffusion and pattern formation in reaction–diffusion systems. *Physical Chemistry Chemical Physics*, 11(6):897–912, 2009.

[76] N. Zamponi and A. Jüngel. Analysis of degenerate cross-diffusion population models with volume filling. *Ann. Inst. H. Poincaré Anal. Non Linéaire*, 34(1):1–29, 2017.

[77] Q. Zheng, D. Chen, and G.-W. Wei. Second-order Poisson–Nernst–Planck solver for ion transport. *Journal of computational physics*, 230(13):5239–5262, 2011.

Curriculum Vitae

Personal Data

Name	**Anita Gerstenmayer**
Date of birth	02.01.1991
Place of birth	Tulln an der Donau, Austria
Nationality	Austrian
Email	`anita.gerstenmayer@asc.tuwien.ac.at`

Qualifications

07/2015–current	PhD in Technical Mathematics, TU Wien. Supervisor: Prof. Ansgar Jüngel.
11/2013–06/2015	MSc in Technical Mathematics, TU Wien, with distinction. Supervisor: Prof. Felix Breitenecker.
10/2009–11/2013	BSc in Technical Mathematics, TU Wien, with distinction.
06/2009	Matura exam, BRG Tulln, with distinction.

Employment

07/2015–current	University assistant, Institute for Analysis and Scientific Computing, TU Wien.
09/2014–02/2015	Internship at Austrian Institute of Technology, Health & Environment Department, Vienna.
10/2013–02/2015	Tutor at TU Wien.
2007–2013	Employee of Gerstenmayer GmbH, Tulln, Austria.

Scholarships

2010, 2011, 2014	Merit-based scholarship, TU Wien.
09/2011–07/2012	Erasmus outgoing scholarship, Università degli Studi di Pisa, Italy.

Publications, Preprints & Work in Progress

A. Gerstenmayer and A. Jüngel. Comparison of a finite-element and finite-volume scheme for a degenerate cross-diffusion system for ion transport. *Submitted for publication.*

C. Cancès, C. Chainais-Hillairet, A. Gerstenmayer and A. Jüngel. Finite-volume scheme for a degenerate cross-diffusion model motivated from ion transport. *To appear in: Numerical Methods for Partial Differential Equations.*

A. Gerstenmayer and A. Jüngel. Analysis of a degenerate parabolic cross-diffusion system for ion transport. *J. Math. Anal. Appl.*, 461(1):523-543, 2018.

Scientific Talks & Posters

10/2018	Poster at workshop "Applied Mathematics and Simulation for Semiconductors", Berlin, Germany.
08/2018	Contributed talk at workshop "Asymptotic Behavior of systems of PDE arising in physics and biology", Lille, France.
10/2017	Contributed talk at workshop "Analysis and Advanced Numerical Methods for Partial Differential Equations", Crete, Greece.
07/2017	Contributed talk at Equadiff conference, Bratislava, Slovakia.

Teaching Experience

Exercise classes at TU Wien for the following subjects:

2015, 2017, 2018	Partial differential equations.
2016, 2018	Nonlinear partial differential equations.
2017	Variational calculus.
2014	Analysis for physicists.
2013, 2014	Preparatory course mathematics.
2013, 2014	Analysis for computer scientists.

Additional Information

- Languages: German (mother tongue), English (fluent), Italian (fluent), Spanish (intermediate), French (basic).

- Software proficiency: C, Java, LaTeX, Maple, Matlab, Microsoft Office, Python.